

Preparation of natural rubber powder modified with
bis(triethoxysilylpropyl)tetrasulfide treated silica by spray drying process



A Thesis Submitted in Partial Fulfillment of the Requirements
for the Degree of Master of Engineering in Chemical Engineering

Department of Chemical Engineering

FACULTY OF ENGINEERING

Chulalongkorn University

Academic Year 2019

Copyright of Chulalongkorn University

การเตรียมพยางค์ธรรมชาติที่ปรับปรุงด้วยไทรเอทอกซีไซลิลโพรพิลเททระซิลไฟด์ที่ใช้ปรับสภาพซิลิกา
โดยกระบวนการอบแห้งแบบพ่นฝอย



วิทยานิพนธ์นี้เป็นส่วนหนึ่งของการศึกษาตามหลักสูตรปริญญาวิศวกรรมศาสตรมหาบัณฑิต
สาขาวิชาวิศวกรรมเคมี ภาควิชาวิศวกรรมเคมี
คณะวิศวกรรมศาสตร์ จุฬาลงกรณ์มหาวิทยาลัย
ปีการศึกษา 2562
ลิขสิทธิ์ของจุฬาลงกรณ์มหาวิทยาลัย

Thesis Title	Preparation of natural rubber powder modified with bis(triethoxysilylpropyl)tetrasulfide treated silica by spray drying process
By	Miss Intira Boonvisood
Field of Study	Chemical Engineering
Thesis Advisor	Assistant Professor APINAN SOOTTITANTAWAT, D.Eng.
Thesis Co Advisor	Patrick Tang Siah Ying, Ph.D.

Accepted by the FACULTY OF ENGINEERING, Chulalongkorn University in
Partial Fulfillment of the Requirement for the Master of Engineering

..... Dean of the FACULTY OF
ENGINEERING
(Professor SUPOT TEACHAVORASINSKUN, D.Eng.)

THESIS COMMITTEE

..... Chairman
(Assistant Professor Pattaraporn Kim, Ph.D.)

..... Thesis Advisor
(Assistant Professor APINAN SOOTTITANTAWAT, D.Eng.)

..... Thesis Co-Advisor
(Patrick Tang Siah Ying, Ph.D.)

..... Examiner
(Professor SARAWUT RIMDUSIT, Ph.D.)

..... External Examiner
(Wiyong Kangwansupamonkon, Ph.D.)

อินทิดา บุญวิสูตร : การเตรียมผงยางธรรมชาติที่ปรับปรุงด้วยไตรเอทอกซีซิลิลโพรพิล เททระซัลไฟด์ที่ใช้ปรับสภาพซิลิกาโดยกระบวนการอบแห้งแบบพ่นฝอย. (Preparation of natural rubber powder modified with bis(triethoxysilylpropyl)tetrasulfide treated silica by spray drying process)
 อ.ที่ปรึกษาหลัก : ผศ. ดร.อภิรักษ์ สุทธิธรรวษ, อ.ที่ปรึกษาร่วม : ดร.แพทริก แทงค์ เซีย ยิง

ในอุตสาหกรรมพอลิเมอร์มีการนำผงยางธรรมชาติมาใช้อย่างกว้างขวางเนื่องจากความมีเสถียรภาพและความสะดวกในการใช้งาน แต่อย่างไรก็ตามผงยางธรรมชาติมีความยุ่งยากในการผลิตเนื่องจากยางมีการยึดติดกัน ดังนั้นจึงนำซิลิกามาใช้ในการห่อหุ้มอนุภาคยางเพื่อหลีกเลี่ยงการยึดเกาะกันของอนุภาคยาง แต่ซิลิกาและยางธรรมชาติมีความไม่เข้ากัน ซึ่งซิลิกาสามารถปรับปรุงให้มีความไม่ชอบน้ำมากขึ้นได้โดยการใช้สารคู่ควบไฮโดรเจนไตรเอทอกซีซิลิลโพรพิล เททระซัลไฟด์ งานวิจัยนี้มีวัตถุประสงค์เพื่อเตรียมผงยางธรรมชาติที่ถูกปกคลุมด้วยซิลิกาโดยการใช้วิธีผสมผสานระหว่างการปรับปรุงด้วยไฮโดรเจนไตรเอทอกซีซิลิลโพรพิลและกระบวนการอบแห้งแบบพ่นฝอย ผลของอัตราส่วนโดยมวลระหว่างไฮโดรเจนไตรเอทอกซีซิลิลโพรพิลและซิลิกาที่ 1%, 5%, 8%, 10%, และ 12% ได้รับการศึกษาในขั้นตอนการปรับปรุงซิลิกา ผลการศึกษาพบว่าอัตราส่วนที่ 8% ของไฮโดรเจนไตรเอทอกซีซิลิลโพรพิลมีความเหมาะสมที่สุดในการปรับปรุงพื้นผิวของซิลิกาเนื่องจากให้ประสิทธิภาพการต่องิ่งสูงที่สุด ส่วนขั้นตอนที่สองคือการเตรียมผงยางธรรมชาติโดยเครื่องอบแห้งแบบพ่นฝอย โดยในส่วนนี้ได้มีการศึกษาผลของไฮโดรเจนไตรเอทอกซีซิลิลโพรพิลต่อคุณสมบัติของผงยางธรรมชาติ ผลที่ได้จากงานวิจัยนี้แสดงให้เห็นถึงความประสบความสำเร็จในการผลิตผงยางธรรมชาติที่มีรูปร่างทรงกลมสม่ำเสมอ นอกจากนี้ผลการทดลองบ่งชี้ให้เห็นว่าไฮโดรเจนไตรเอทอกซีซิลิลโพรพิลสามารถปรับปรุงความเข้ากันได้ระหว่างซิลิกาและยางธรรมชาติได้โดยแสดงให้เห็นถึงการเพิ่มขึ้นของปริมาณยางบาวนด์และพบว่าอัตราส่วนโดยมวลระหว่างซิลิกาและยางธรรมชาติในช่วง 3:1 ถึง 2:1 สามารถทำให้อนุภาคยางส่วนใหญ่ถูกห่อหุ้มโดยอนุภาคซิลิกาได้อย่างเพียงพอ

สาขาวิชา วิศวกรรมเคมี
 ปีการศึกษา 2562

ลายมือชื่อนิสิต
 ลายมือชื่อ อ.ที่ปรึกษาหลัก
 ลายมือชื่อ อ.ที่ปรึกษาร่วม

6170342921 : MAJOR CHEMICAL ENGINEERING

KEYWORD: Natural rubber powder, Spray dry, Modified silica, Encapsulation

Intira Boonvisood : Preparation of natural rubber powder modified with bis(triethoxysilylpropyl)tetrasulfide treated silica by spray drying process.

Advisor: Asst. Prof. APINAN SOOTTITANTAWAT, D.Eng. Co-advisor: Patrick Tang Siah Ying, Ph.D.

In polymer industry, Natural rubber powder (NRP) is broadly used because of its stability and useability. Although, NRP is difficult to be produced due to the rubber adhered together. Consequently, silica was used to encapsulated the rubber particle to avoid adhesion of rubber. However, there is a polarity difference between silica and rubber. Silica can be made hydrophobic via surface modification with silane coupling agent, bis[3-(triethoxysilyl)propyl]tetrasulfide (TESPT). This research study aimed to prepare uniform silica-coated NRP via a combination of silane modification and spray drying technique. The effect of the mass ratio of TESPT and silica is 1%, 5%, 8%, 10%, and 12% were investigated in the modification of silica step. The results found that 8% of TESPT is most suitable for modifying silica as evidenced by its highest grafting efficiency. The second step is the preparation of NRP. The effect of TESPT and the mass ratio of silica to natural rubber at 3:1, 2:1, 1:1 and 0.5:1 to the properties of NRP were investigated in this step. The findings of this study demonstrated the feasibility of the production of uniformly spherical NRP. Moreover, the results indicated that TESPT can improve the compatibility between NR and silica resulting in higher bound rubber content and the mass ratio of silica to NR ranging from 3:1 to 1:1 the most of NR particles were sufficiency encapsulated in silica particle.

Field of Study: Chemical Engineering

Student's Signature

Academic Year: 2019

Advisor's Signature

Co-advisor's Signature

ACKNOWLEDGEMENTS

Firstly, I would like to express my sincere gratitude to my thesis advisor, Asst. Prof. Dr. Apinan Soottitantawat and my co-advisor, Dr. Patrick Tang Siah Ying for encouragement, valuable suggestions and motivation that made my thesis completed. This thesis would not have been completed if without their support.

Moreover, I also would like to special thanks to Asst. Prof. Dr. Pattaraporn Kim as a chairman, Professor Dr. Sarawut Rimdusit and Dr. Wiyong Kangwansupamonkon as the members of my thesis committee for their encouragement, insightful comments and useful suggestions.

I am really thankful to all members of center of Excellence in Particle and Material Processing Technology, Department of Chemical Engineering, Chulalongkorn University. Further thanks to all staffs in Department of Chemical Engineering, Chulalongkorn University.

Finally, I gratefully thank my family and my friends for providing me for encouragement and supporting me throughout my study year and my life.

Intira Boonvisood

TABLE OF CONTENTS

	Page
ABSTRACT (THAI).....	iii
ABSTRACT (ENGLISH).....	iv
ACKNOWLEDGEMENTS	v
TABLE OF CONTENTS	vi
LIST OF TABLES	ix
LIST OF FIGURES	x
CHAPTER 1 INTRODUCTION.....	1
1.1 Background and Problem statement.....	1
1.2 Research objectives	3
1.3 Contribution of study	4
1.4 Scope of research	4
CHAPTER 2 FUDAMENTAL THEORY AND LITERATURE REVIEWS.....	6
2.1 Fundamentals.....	6
2.1.1 Natural rubber	6
2.1.2 Silicon dioxide	8
2.1.3 Silane coupling agent.....	9
2.1.4 Microencapsulation technology.....	11
2.1.5 Spray drying method.....	12
2.2 Literature reviews.....	14
2.2.1 Surface modification of silica with silane coupling agents.....	14
2.2.2 Preparation of rubber powder	21

CHAPTER 3 EXPERIMENTAL	26
3.1 Materials.....	26
3.2 Experimental procedure	26
3.2.1 Preparation of modified silica step	26
3.2.2 Preparation of Natural rubber powder step.....	27
3.3 Hydrolysis of TESPT	27
3.3 Preparation of modified silica.....	27
3.4 Preparation of natural rubber powder.....	28
3.5 Characterizations	29
3.5.1 The morphology and elemental composition	29
3.5.2 The particle size and size distribution.....	30
3.5.2 The functional group and the grafting degree (K).....	30
3.5.3 The thermal stability.....	30
3.5.4 The bound rubber content.....	31
CHAPTER 4 RESULTS AND DISCUSSION.....	32
4.1 The preparation of modified silica (m-SiO ₂) with TESPT	32
4.1.1 Hydrolysis of TESPT	32
4.1.1.1 The functional group of TESPT hydrolysate	32
4.1.2 Surface modification of silica	35
4.1.2.1 The morphology of modified silica colloidal	35
4.1.2.2 The morphology of m-SiO ₂	37
4.1.2.3 The particle size and size distribution of modified silica.....	39
4.1.2.4 The grafting degree of modified silica.....	41
4.1.2.5 The thermal stability and composition of modified silica.....	48

4.2 The preparation of natural rubber powder	50
4.2.1 The effect of TESPT in natural rubber powder	51
4.2.1.1 The morphology of mixture before spray dry.....	51
4.2.1.2 The functional group of NRP.....	53
4.2.1.3 The morphology of NRP.....	55
4.2.1.4 The elemental composition of NRP	62
4.2.1.5 The particle size and size distribution of NRP	65
4.2.1.6 The thermal stability of NRP.....	67
4.2.1.7 The bound rubber content of NRP.....	68
4.2.2 The effect of the mass ratio of silica to natural rubber	70
4.2.2.1 The morphology of mixture before spray dry.....	70
4.2.2.2 The functional group of NRP.....	71
4.2.1.3 The morphology of NRP.....	72
4.2.1.4 The elemental composition of NRP	75
4.2.1.5 The particle size and size distribution of NRP.....	77
4.2.1.6 The thermal stability of NRP.....	78
CHAPTER 5 CONCLUSION	80
5.1 Conclusion	80
5.2 Recommendation.....	80
REFERENCES	81
VITA.....	86

LIST OF TABLES

	Page
Table 1 Physical Properties of Natural Rubber [16].	8
Table 2 Physical Properties of silica [17].	9
Table 3 Values of grafting degree (K) of modified silica with different amount of TESPT [20].	18
Table 4 Values of grafting degree (K) of modified silica with different temperature [29].	18
Table 5 The FTIR functional group of TESPT, TESPT hydrolysate and ethanol [33]. ...	34
Table 6 The FTIR functional group of TESPT, pure and modified silica [33, 36].	42
Table 7 The grafting degree value of m-SiO ₂	46
Table 8 The weight loss in first and second region of dried pure silica and modified silica powder with different amount of TESPT.	49
Table 9 Elemental composition of modified silica/NR powder obtained by EDS.	63
Table 10 The elemental composition on surface of pure silica and NRP.	64
Table 11 The elemental composition inside the particle of NRP	65
Table 12 The Mean Diameter of NRP with and without TESPT.	66
Table 13 The composition of NRP 3:1 with TESPT.	68
Table 14 Bound rubber content of NRP with and without TESPT	69
Table 15 the elemental composition on surface of NRP particle	76
Table 16 the elemental composition inside the NRP particle.	77
Table 17 The Mean Diameter of NRP prepared at different mass ratio of silica to NR77	
Table 18 The Compositions and weight loss of NRP prepared at different mass ratio of silica to NR	79

LIST OF FIGURES

	Page
Figure 1 Natural rubber from <i>Hevea brasiliens</i> [12].....	6
Figure 2 Chemical structure of natural rubber [13].....	7
Figure 3 Two possible models for the structure of the natural rubber latex particle surface [14].....	7
Figure 4 General formula of silane coupling agents.....	10
Figure 5 chemical structure of TESPT [19].....	10
Figure 6 six types of microcapsules [25].....	12
Figure 7 flow diagram of a traditional spray dryer [28].....	13
Figure 8 Silica-silane-rubber coupling [21].....	15
Figure 9 Surface modification mechanism of silica with silane coupling agent TESPT [20].....	16
Figure 10 The FTIR spectra of pure silica and modified silica by TSM [20].....	17
Figure 11 Schematic diagram showing the synthesis of Si-Sx by in-situ surface modification method [31].....	19
Figure 12 FTIR spectra of pure silica (Si-Sx-0) and functionalized nano silica (Si-Sx-6.5) [31].....	20
Figure 13 TEM images of (a) Si-Sx-0 and (b) Si-Sx-6.5 as well as (c) size distribution of Si-Sx-0 and Si-Sx-6.5 [31].....	20
Figure 14 TEM image of SBR latex particles (a) and SEM photograph of NPSBR particles (b) [6].	21
Figure 15 SEM micrographs of the NRP at different magnifications (a) x1,000 and (b) x10,000 [7].....	22

Figure 16 Relationship between the NRP yield (%) obtained and the (a) SDS (phr) and the (b) DRC (%) content [3].	24
Figure 17 SEM micrographs of the NRP synthesized under the optimum condition (a) without SDS, (b) with 12 phr SDS and (c) the SDS particles [3].	24
Figure 18 The mechanism of TESPT hydrolysis and surface modification of silica with TESPT.	28
Figure 19 Schematic of a spray dryer.	29
Figure 20 FTIR spectra of TESPT, TESPT hydrolysate and ethanol.	33
Figure 21 FTIR spectra of TESPT, TESPT hydrolysate and ethanol.	35
Figure 22 TEM image of modified silica colloidal at A) low magnitude and B) high magnitude.	36
Figure 23 The size distribution curve of modified silica colloidal.	37
Figure 24 SEM images of A) pure silica, B) m-SiO ₂ -1, C) m-SiO ₂ -5, D) m-SiO ₂ -8, E) m-SiO ₂ -10 and F) m-SiO ₂ -12.	38
Figure 25 The Mean Diameter of spray dried pure silica and m-SiO ₂ powders prepared at different amount of TESPT.	39
Figure 26 The size distribution curve of spray dried pure silica and m-SiO ₂ powders prepared at different amount of TESPT.	40
Figure 27 FTIR spectra of TESPT, pure silica and m-SiO ₂ -12.	42
Figure 28 FTIR spectra of pure silica and m-SiO ₂ -12 at wave number 2800 to 3000 cm ⁻¹	43
Figure 29 FTIR spectra of dried modified silica powder with different amount of TESPT.	44
Figure 30 FTIR spectra of dried modified silica powder with different amount of TESPT at wave number 2800-3000 cm ⁻¹	45
Figure 31 The grafting degree of m-SiO ₂ with different amount of TESPT	47

Figure 32 The generally reaction scheme of TESPT over the surface of silica [37].	47
Figure 33 The TGA curve of dried pure silica and modified silica powder with different amount of TESPT.	49
Figure 34 The relationship between the weight loss in the second region and the weight ratio of TESPT to silica.	50
Figure 35 TEM micrographs of NRL particle at A) low magnitude and B) high magnitude	52
Figure 36 TEM micrographs of NRL particle after mixed with (A) modified silica, (B) unmodified silica with the mass ratio of silica to NR at 3:1, (C) modified silica, (D) unmodified silica with the mass ratio of silica to NR at 1:1.	53
Figure 37 The FTIR spectra of TESPT, NR, pure silica, NRP with TESPT and NRP without TESPT with the mass ratio of silica to NR at 3:1.	55
Figure 38 SEM micrographs of A) pristine NR and B) modified silica/NR powder.	56
Figure 39 the visible images of A) NRP 3:1 with TESPT, B) NRP 3:1 without TESPT, C) NRP 1:1 with TESPT and D) NRP 1:1 without TESPT.	57
Figure 40 the SEM images of A), B) NRP 3:1 with TESPT and C), D) NRP 3:1 without TESPT.	57
Figure 41 the SEM images of A), B) NRP 1:1 with TESPT and C), D) NRP 1:1 without TESPT.	58
Figure 42 the SEM image of cross-section microcapsule particle of NRP 1:1 with TESPT A) dense and B) hollow particle.	59
Figure 43 the SEM images of hollow microcapsule particle of A) NRP 3:1 with TESPT, B) NRP 3:1 without TESPT, C) NRP 1:1 with TESPT and D) NRP 1:1 without TESPT.	60
Figure 44 The mechanism of the many types of particle formation[34].	60
Figure 45 the FE-SEM images at the surface of microcapsule particle of NRP 3:1 with TESPT A) low magnitude and B) high magnitude.	61

Figure 46 A) and B) SEM images of modified silica/NR powder and EDS mapping of C) carbon D) silicon E) oxygen.	62
Figure 47 the sample position for EDS analysis on the particle surface.....	63
Figure 48 the sample position for EDS analysis inside the particle	65
Figure 49 The size distribution curve of NRP with and without TESPT	66
Figure 50 the TGA curves of silica, NR, TESPT and NRP.....	67
Figure 51 Bound rubber content of NRP with and without TESPT	69
Figure 52 TEM micrographs of natural rubber latex particle after mixed modified silica with the mass ratio of silica to natural rubber at 3:1(A), 2:1(B), 1:1(C) and 0.5:1(D).	71
Figure 53 The FTIR spectra of NRP prepared at different mass ratio of silica to NR. ...	72
Figure 54 The image of NRP with the mass ratio of silica to natural rubber at 3:1(A), 2:1(B), 1:1(C) and 0.5:1(D).	73
Figure 55 SEM micrographs of NRP with the mass ratio of silica:natural rubber at 3:1(A), 2:1(B), 1:1(C) and 0.5:1(D).	74
Figure 56 SEM micrographs of NRP with the mass ratio of silica:natural rubber at 3:1(A), 2:1(B), 1:1(C) and 0.5:1(D).	75
Figure 57 The size distribution curve of NRP prepared at different mass ratio of silica to NR	78
Figure 58 The TGA curve of NRP prepared at different mass ratio of silica to NR.....	79

CHAPTER 1

INTRODUCTION

1.1 Background and Problem statement

Natural rubber is both an indispensable and renewable natural resource. It is used in many industrial and consumer products for example tires, gloves, elastics, shoes, sports equipment and engineering product [1]. In rubber industry, natural rubber was used in two main forms, which are concentrated latex and dry rubber and dry rubber. Fresh natural rubber latex from rubber tree were added chemicals and centrifuged to obtain concentrated latex of 60% DRC (dry rubber contents) and it contains of water about 40%. For this reason, transportation of latex is difficult and expensive because the required volume of packaging is also greater and special handling is needed, since the concentrated latex consist of ammonia as an anticoagulant [2]. Therefore, the decreasing of water content in concentrated latex has benefits for rubber industry. For dry rubber such as rubber sheet and rubber block, the transportation is can be easier and the required volume of packaging is lower than latex, but the process to produce dried rubber from latex take long time. The conventional method to produce dried rubber has many steps. To begin with, add some chemical such as formic acid and acetic acid to natural rubber latex to remove water and from the coagulated latex. After that, use a roller to make a rubber sheet. Nonetheless, drying a rubber sheet takes a long time and uses the high energy to form a smoked rubber sheet or rubber block [3].

Moreover, natural rubber often uses as an additive in polymer industry such as nylon, polypropylene, epoxy, and polyethylene [4] to improve mechanical properties of polymer because of its mechanical properties with high tensile modulus. It will improve ductility, elongation at break, impact strength and also increased the crystallization of polymer blended with natural rubber powder [5]. Natural rubber is used as an additive or filler in form of natural rubber powder because the size of the filler should be in the micrometer scale and uniformly and

rubber in powder form can direct to blending process in the polymer industry, so it is necessary to make the natural rubber in powder form.

In decade years, the powder technology of rubber was interested because of its stability, easy to transport and comfortable for blending process in production of many products. The synthesis of rubber powder could not be directly produced because natural rubber has the ability to stick to itself. Therefore, many research requires the use of chemicals or various methods before the drying process to obtain the rubber powder. For instance, Daishuang Li et al. reported the synthesis of nano-powdered styrene-butadiene rubber (NPSBR) by gamma radiation for promote crosslinking density of the latex and followed by drying with spray dryer and use the obtained NPSBR as toughening agent for polystyrene and high-impact polystyrene [6]. Moreover, many research demonstrated that they have been successfully prepared the rubber powder via irradiation and spray drying process but this method has negative effects because of the high cost and the safety problems of irradiation step [6]. Lucilene B. et al. prepared the rubber powder by modified styrene-butadiene latex with a colloidal silica and some chemical agents such as methyl methacrylate and sodium 4-styrene sulfonate before spray drying process to avoid irradiation process [4].

Sea-Oui P. et al. (2010) reported the method of natural rubber powder from high ammonia rubber latex via modified the latex with chemicals such as potassium hydroxide, zinc oxide, sulfur and the other ingredients and followed by spray drying [7]. Jaiphuephae T. (2010) prepared natural rubber powder from natural rubber latex via spray drying and used sodium dodecyl sulfate to solve the problem of blockages at the atomizer of spray dryer by rubber. Furthermore, He found that the obtained natural rubber powder has a spherical shape and small size but the rubber powder has agglomeration [8]. Moreover, Sapanon P. (2010) synthesized the natural/silica composite powder by encapsulation of natural rubber latex particles with silica before spray drying process and used the synthesized composite powder as a filler in polylactide but it has a limit for usage [9]. Sangthongyingdee N. (2015) successfully prepared natural rubber powder by graft polymethyl methacrylate monomer onto

natural rubber particle via interfacial polymerization method and followed by spray drying process to prevent adhesion of natural rubber particles [10].

Natural rubber powder was successfully prepared by spray drying method. This method is very popular because it's could control the particle size and easy to scale up to the industrial scale. However, natural rubber has a limited to use due to the physical characteristics are unstable depend on temperature that the natural rubber is soft and sticky when heated but it will be hard and brittle when the temperature is low [11] and natural rubber has inherit properties that were adhered together for this reason, it should be encapsulation to prevent the natural rubber from heat and prevent the rubber stick to itself and other materials.

This research prepares the natural rubber powder by spray drying method and uses the encapsulation technique to encapsulate the natural rubber particle with a silica particle. Moreover, the silica particle is modified by two step method modification due to the poor compatibility and interaction between highly polar silica particles and non-polar natural rubber particles [8]. Furthermore, both are negative charge so that difficult to interact with each other that is unfavorable for achieving the desired natural rubber powder. This is why silica particles need to modify surface with silane coupling agent such as bis[3-(triethoxysilyl)propyl]tetrasulfide (TESPT), which is most commonly used to modify the silica to improve compatibility and interaction between silica particle and natural rubber particle.

1.2 Research objectives

1.2.1 To study and characterize natural rubber powder using silica modified with TESPT by spray drying method.

1.3 Contribution of study

This research demonstrates experimental factors that have effects in morphology and properties of the synthesized natural rubber powder in laboratory scale that indicate the optimum parameter for the synthesis of natural rubber silica powder to control the size and properties of this powder and can be used the results of this research for scale up the production from laboratory scale to industrial scale.

1.4 Scope of research

1.4.1 Study the effect of time of TESTP hydrolysis reaction.

1.4.2 Study the effect of content of TESPT at 1, 5, 8 and 10% by mass of silica at the conditions of spray dry are inlet temperature at 120°C, feed rate at 10 ml/min, nozzle flow rate at 400 L/h and solid content of mixture before spray drying at 10% by mass.

1.4.3 Study the effect of TESPT-treated silica in natural rubber powder at the conditions of spray dry are inlet temperature at 120°C, feed rate at 10 ml/min, nozzle flow rate at 400 L/h and solid content of mixture before spray drying at 10% by mass.

1.4.4 Study the mass ratio of silica:natural rubber at 0.5:1, 1:1, 2:1 and 3:1 at the conditions of spray dry are inlet temperature at 120°C, feed rate at 10 ml/min, nozzle flow rate at 400 L/h and solid content of mixture before spray drying at 10% by mass.

Investigate variables of modified silica powder were :

- Morphology
- Particle size and size distribution
- Functional group
- Grafting degree

- Thermal properties

Investigate variables of natural rubber powder were :

- Morphology and elemental composition
- Particle size and size distribution
- Functional group
- Thermal properties
- Encapsulation of natural rubber particle
- Bound rubber content



CHAPTER 2

FUDAMENTAL THEORY AND LITERATURE REVIEWS

2.1 Fundamentals

2.1.1 Natural rubber

Natural rubber (NR) from *Hevea brasiliensis*, which is a species of rubber tree originated from Amazon, South America as shows in Fig.1 Natural rubber latex (NRL) that obtained from *Hevea brasiliensis* is white color and has 30% DRC (dry rubber content). After the NRL was centrifuge process, which is obtained concentrated latex that is 60% DRC. For long time storage, ammonia is added into the NRL [11]. The chemical structure of NR is nearly 100% cis-1,4 polyisoprene shows in Fig.2 with molecular weight in rang 1 to 2.5×10^6 .

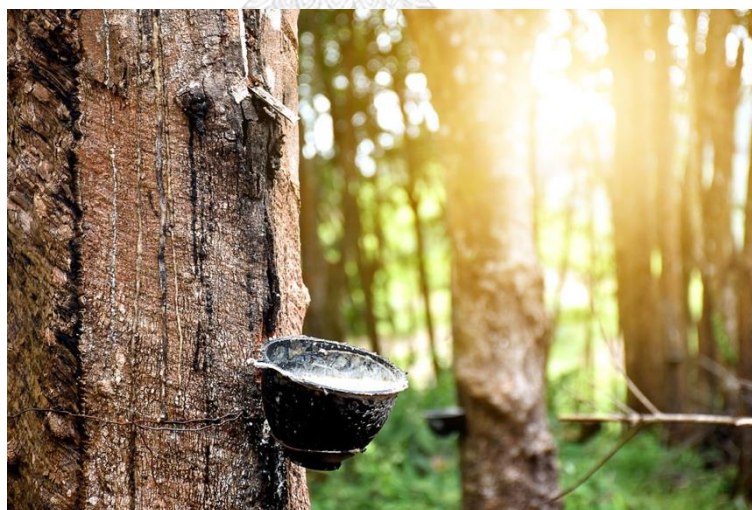


Figure 1 Natural rubber from *Hevea brasiliensis* [12].

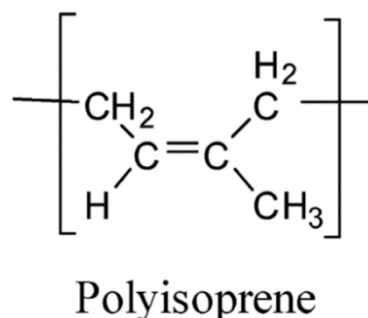


Figure 2 Chemical structure of natural rubber [13].

The surface nanostructure of natural rubber particles latex from *Hevea brasiliensis* shows in Fig.3 There are two possible models for the structure of the natural rubber latex particle surface. First model is the NRL particle surface was surrounded by double layers such as proteins layer and phospholipids layer show as Fig.3A. On the other hand, second model presented that the NRL particle surface was surrounded by a single layer, which mixed domains of phospholipids and proteins shows as Fig.3B The molecule of NR linked with phospholipids and proteins. Moreover, the α - and ω - terminal ends could be orientated themselves, the surface of NR has hydrophilic ends as a thin layer and then the polyisoprene molecules could form the hydrophobic core [14].

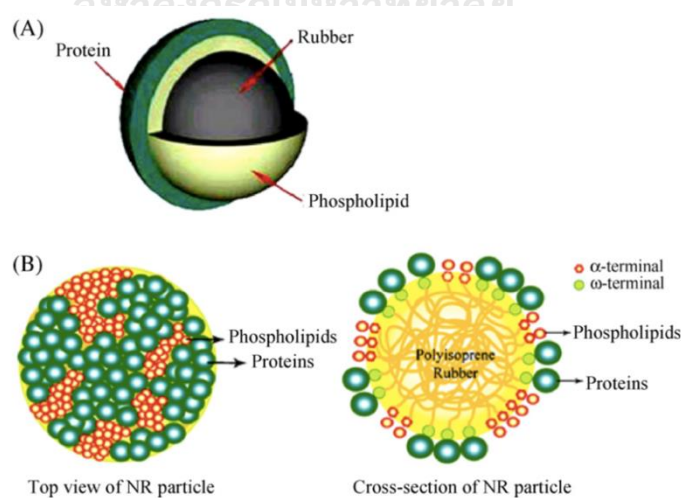


Figure 3 Two possible models for the structure of the natural rubber latex particle surface [14].

The physical properties of NR present in Table 1. Furthermore, the NR has chemical properties including [15]:

- Elasticity: NR has the ability to be stretched without destruction of its structure. It returns to its original shape when the strain is removed.
- Oxidation: The double bonds of rubber can be oxidized by oxygen and ozone but oxidation can be prevented by adding antioxidants.
- Effect of solvents: NR does not react with water and does not allow water to pass through. It is resistant to alkalis and weak acids. Moreover, it is soluble in some organic solvents such as benzene and toluene.
- Effect of heat: NR is not resistant to heat. At high temperature it becomes soft and sticky.

Table 1 Physical Properties of Natural Rubber [16].

Parameter	Value
Density at 20°C	0.906 – 0.916 g/cm ³
Specific Heat	1.905 KJg ⁻¹ K ⁻¹
Refractive Index	1.5191
Heat of Combustion	45.2 KJ/Kg

2.1.2 Silicon dioxide

Silicon dioxide, also known as silica, which is another name for the chemical compound composed of silicon atom and oxygen atom with the chemical formula SiO₂. The important physical properties of silica exhibit in Table 2.

Table 2 Physical Properties of silica [17].

Parameter	Value
Crystal structure	Amorphous
Atomic weight	60.08 g/mole
Density (thermal, dry/wet)	2.27/2.18 g/cm ³
Molecules	2.3x10 ²² / cm ³
Specific heat	1.0 J/g-K
Melting point	1700°C
Young's modulus	6.6x10 ¹⁰ N/m ²
Thermal expansion coefficient	5.6x10 ⁻⁷ /K
Poisson's ratio	0.17
Thermal conductivity	1.1 W/m-K - 1.4 W/m-K
Relative dielectric constant	3.7 - 3.9
Dielectric strength	10 V/cm
Energy bandgap	8.9 eV
DC resistivity	10 ¹⁷ Ωcm

2.1.3 Silane coupling agent

Silane coupling agents are inorganic-organic compounds, which also used to improve adhesion between two materials that are dissimilar such as organic and inorganic materials. So, silane coupling agents are important for polymer industry to improve the mechanical properties of composite material, to improve adhesion between two materials and to modify the surface of material. General formula of silane coupling agents consist of two main groups shows in Fig.4 [18].

- X group such as vinyl groups, epoxy groups, methacryloxy groups, and amino groups, which can form chemical bond with organic materials such as natural rubber, synthetic rubber and synthetic resins.

- OR group such as methoxy groups and ethoxy groups, which can generate chemical bound with inorganic materials for instant metal, glass, inorganic fiber.

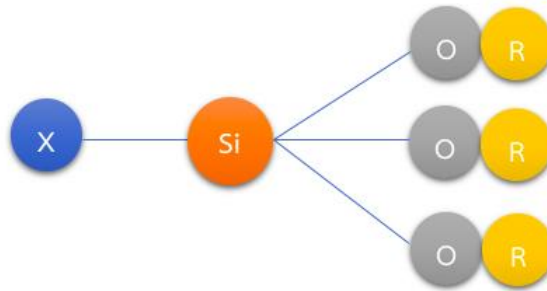


Figure 4 General formula of silane coupling agents.

There are many type of silane coupling agents, which wildly use for surface modification of silica particles to prepare rubber/silica composites including [19]:

- mercaptopropyltriethoxysilane (MEPTS)
- bis[3-(triethoxysilyl) propyl] tetrasulfide (TESPT)
- bis[γ -triethoxysilylpropyl] disulfide (TESPD).

Nevertheless, TESPT is the most popular use for modify the surface of silica because many researches reported that TESPT has efficiency to improve compatibility between silica and rubber and improve dispersion of silica in rubber matrix [20-22]. The chemical structure of TESPT shows in Fig.5.

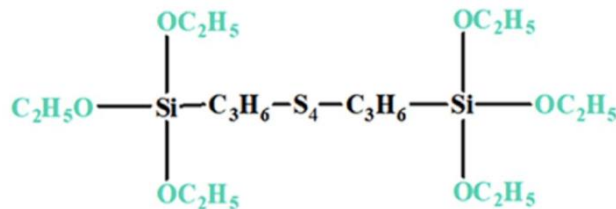


Figure 5 chemical structure of TESPT [19].

2.1.4 Microencapsulation technology

Microencapsulation is a process in which small particles or droplets are surrounded by a coating or embedded in a homogeneous or heterogeneous matrix, to give small capsules with many useful properties. This technique can provide a physical barrier between core compound and the other components of the product [23]. Microencapsulation is widely used in many industries such as food, cosmetic and pharmaceutical because of microencapsulation has many benefits include [24]:

- Microencapsulation technique can be protected materials from conditions such as heat, moisture, oxygen and will prolong shelf-life.
- Microencapsulation technique can be controlled or sustained release to help develop new deliver mechanisms of drug.
- To enable the encapsulated material to act as extraction aides for product removal.
- Microencapsulation technique can improve flow properties by converting a liquid into a solid particle which improves handling, usage and storage.
- Microencapsulation technique can improve organoleptic properties to mask its unpleasant taste and/or small and improve its visual appearance as well as its texture.

Microencapsulation is provided many types of microcapsules shows in Fig.6.

There are six types of microcapsules such as [25]:

- (i) Simple microcapsule (core shell)
- (ii) Matrix (microsphere)
- (iii) Irregular microcapsule
- (iv) Multicore microcapsule
- (v) Multiwall microcapsule
- (vi) Assembly of microcapsule.

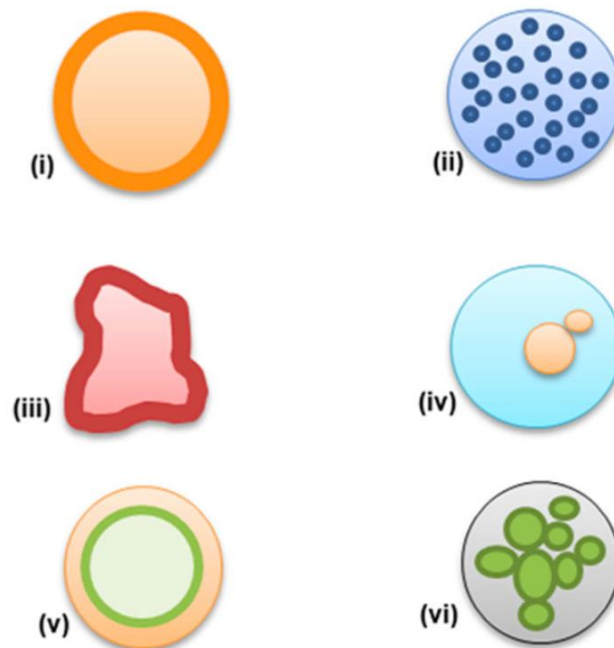


Figure 6 six types of microcapsules [25].

Moreover, microencapsulation technique can be categorized into three main groups [26]:

- (i) Physical methods including spray drying, supercritical fluid precipitation, lyophilization and solvent evaporation
- (ii) Chemical methods such as molecular inclusion complexation and interfacial polymerization
- (iii) Physico-chemical methods for example liposomes, coacervation and ionic gelation.

2.1.5 Spray drying method

Spray drying is defined as the transformation of a fluid from a liquid state into a dried particulate form by spraying the fluid into a hot drying medium [27]. Spray drying method is commonly used because it is easy to use, fast, reproducible and easy to scale up. This method is well established in many industries such as chemical, food and pharmaceutical industries. There are many benefits of spray drying method such as:

- Spray drying method can control a particle size, morphology and shape of product.
- This is one step process, which can directly convert various liquid feeds into dry powders.
- Spray drying method is fast process, low operating cost and low energy consumption.
- This process is scale up capability.
- Spray drying method can provided high encapsulation efficiency and extended shelf life.
- This is a versatile technique for the formulation of nanocapsules with various encapsulating excipients.

Spray drying method involve of four steps shows in Fig.7 such as (i) heating of the drying gas, (ii) droplet generation, (iii) drying of the droplets, and (iv) particle collection [28].

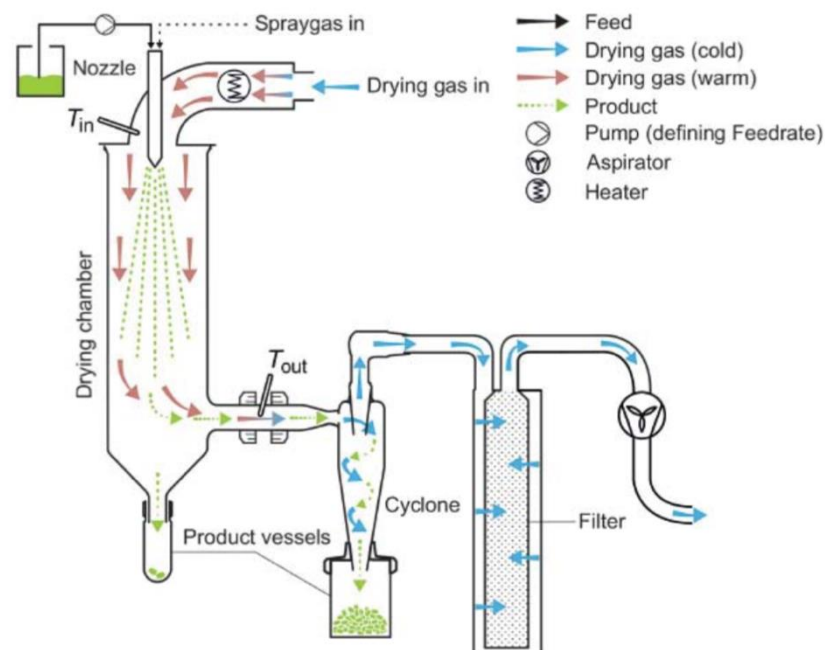


Figure 7 flow diagram of a traditional spray dryer [28].

2.2 Literature reviews

2.2.1 Surface modification of silica with silane coupling agents

Silica is broadly used as a filler in rubber industry to improve the dynamic and static mechanical properties of rubber industry, such as wet skid resistance and rolling resistance. Although, silica has poor compatibility with rubber matrix because of the surface of silica nanoparticle has a large number of hydroxyl groups and high surface energy, as a result to severe agglomeration of silica particles and weak rubber-filler interaction. Therefore, surface modification of silica was introduced to improve the compatibility between silica and rubber. Many researches were successfully modified the surface modification of silica with silane coupling agents [29].

The surface modification of silica has two methods, first method is one step method (OSM). In this method silica, rubber matrix and silane coupling agents are blended in a two-roll mill or an internal mixer at the same time. After mixing silane coupling agents react with hydroxyl groups on the surface of silica particles and sulfur atom of TESPT reacts with the unsaturated bounds of the rubber while the curing process [20] shows in Fig.8. In 2010, Sea-Oui et al. modified the surface of silica with two types of silane coupling agents such as bis-(3-triethoxysilylpropyl) tetrasulfane (Si-69) and 3-thiocyanatopropyl triethoxy silane (Si-264) by this method and used the silica as a filler in polychloroprene (CR). They found that both Si-69 and Si-264 improved the manufacturability of the rubber compounds by reduced the energy of mixing process and increased crosslinking density of the vulcanizates. Moreover, both silane coupling agents could improve the mechanical properties of the vulcanizates and the dispersion of silica particles in the vulcanizates [30].

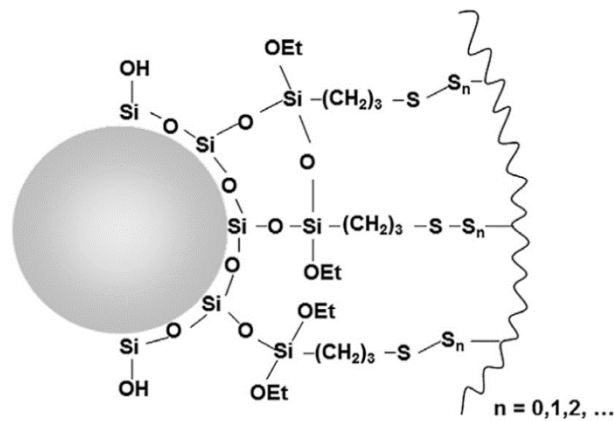


Figure 8 Silica-silane-rubber coupling [21].

In 2013, Yan Li et al. reported that the surface modification of silica by OSM is not clear about interaction between silica and silane coupling agents is chemical bonding during condensation reaction between hydrolyzed hydroxyl of silane coupling agents and hydroxyl group of silica surface or it is simple physical absorption. Consequently, they studied the surface modification of silica by two-step method (TSM), which is a second method of surface modification of silica. Firstly, TESPT was hydrolyzed by added absolute ethanol and deionized water into a beaker and used acetic acid to adjust the pH value. After 10 h, they obtained “TESPT hydrolysates”, which the ethoxyl group transformed to hydroxyl group and used it for prepared the modified silica by mixed the obtained TESPT hydrolysates with silica and stirred for 16 h. The mass ratio of TESPT and silica is 8%, 12% and 15% were investigated and they used modified silica that were prepared by both method as a filler in styrene butadiene rubber (SSBR) composite to improve the mechanical properties.

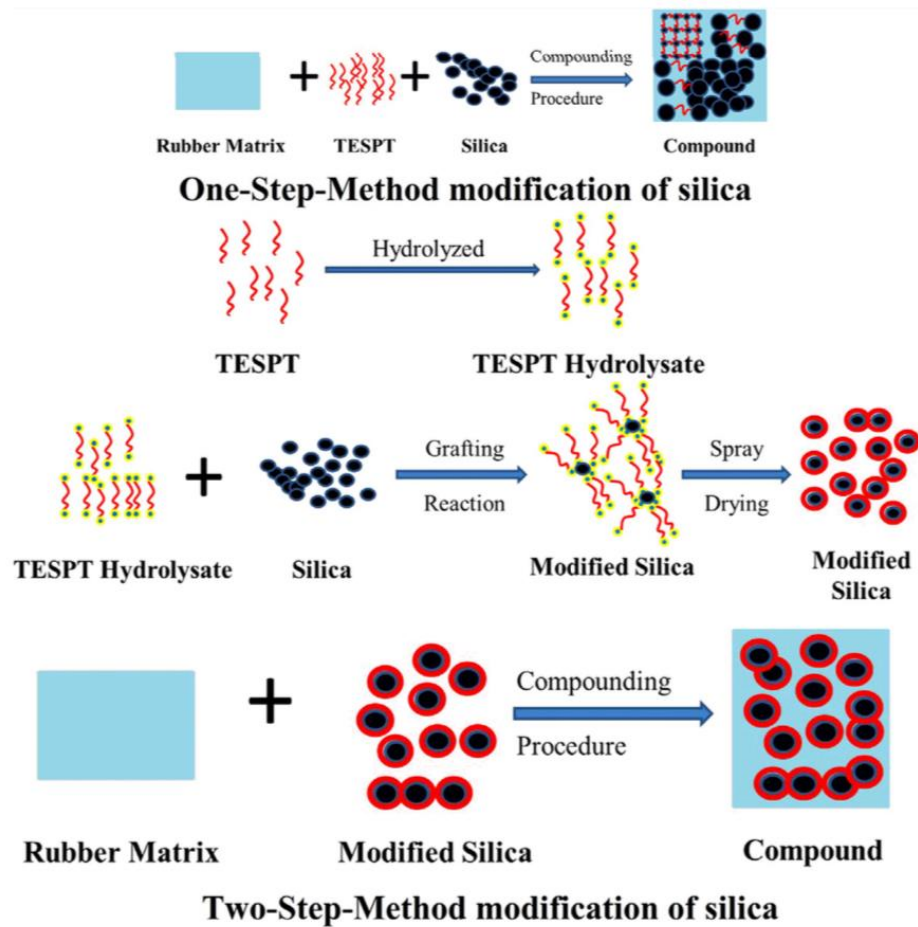


Figure 9 Surface modification mechanism of silica with silane coupling agent TESPT [20].

The mechanism of OSM and TSM modification of silica shows in Fig.9 In the novel TSM modification, The TESPT was first hydrolyzed to obtained TESPT hydrolysate, and then TESPT hydrolysate is grafted on the surface of silica during spray drying process and the chemical bonds occurred at the interface between TESPT hydrolysate and silica. This method preferred a small sized pre-distribution of silica and improved the compatibility between silica and rubber matrix, resulting the homogeneously disperse silica nanoparticles in the rubber matrix. Nevertheless, In the traditional OSM modification, silica nanoparticles are dispersed by shear force so that the TESPT has limited to contact the surface of the silica due to silica aggregates to bigger particles and parts of them dissolve in the rubber matrix.

Yan Li et al. (2013) found that the modified silica was successfully prepared by a novel two-step method (TSM), which confirmed by FTIR spectra. Fig.10 shows FTIR spectra of pure silica and modified silica with different content of TESPT by TSM, resulting there is strong absorbance peak at 1117 cm^{-1} and 3400 cm^{-1} in Fig.10A, which corresponded to Si-O-Si groups of silica and stretching vibration peak of hydroxyl groups of silica surface respectively. As shown in Fig.10B, the modified silica has absorbance peak at 2700 cm^{-1} to 3000 cm^{-1} attributed to inorganic group (the CH_2 vibration) of TESPT, but pure silica not found this peak indicated that TESPT could be successfully grafted on silica particles.

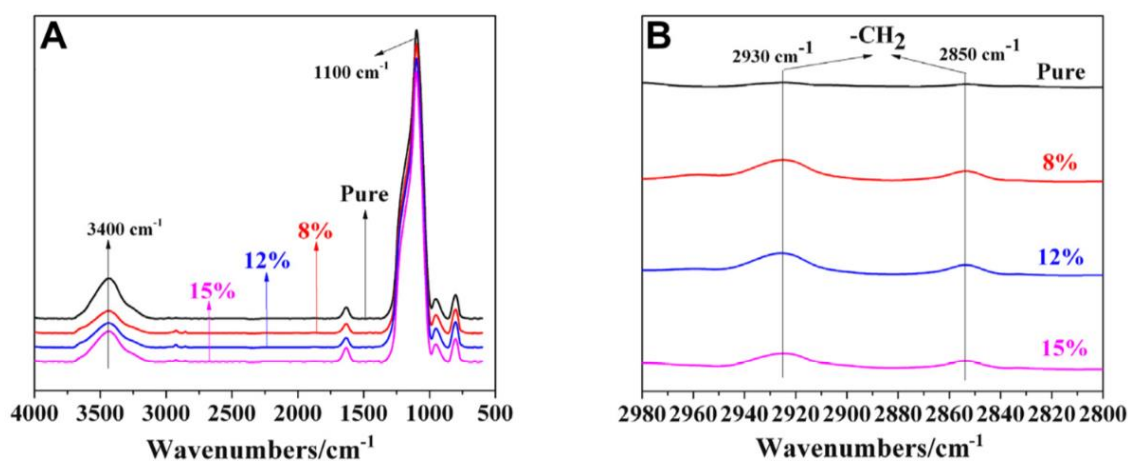


Figure 10 The FTIR spectra of pure silica and modified silica by TSM [20].

The effect of mass ratio of TESPT and silica at 8%, 12% and 15% were studied by FTIR. The grafting degree (K) that demonstrates to the organic degree on SiO_2 was calculated from Eq. 1 and FTIR spectra in Fig.10A. The K values of modified silica shows in Table 3, resulting the value of K with 8% of TESPT is highest and followed by 12% and 15% respectively. The decreasing of the grafting degree with increasing TESPT amount indicated that an oligomer was formed via inter-reaction or hydrogen bonds by hydroxyl of TESPT hydrolysates, the appearance of oligomer could obstruct the grafting of the other TESPT on the surface of silica lead to the lower succession of the surface modification of silica when the amount of TESPT increase in the system.

$$K = (R - r)/R \times 100\% \quad (1)$$

Where K is the grafting degree of the hydroxyl, R is the ratio of the hydroxyl peak at 3447 cm^{-1} to Si-O-Si peak at 1108 cm^{-1} of FTIR spectra of pure silica, r is the ratio of the hydroxyl peak at 3447 cm^{-1} to Si-O-Si peak at 1108 cm^{-1} of FTIR spectra of modified silica.

Table 3 Values of grafting degree (K) of modified silica with different amount of TESPT [20].

Sample	8%	12%	15%
K (%)	45.2	41.6	32.4

Moreover, Yan Li et al. (2013) discovered that the novel TSM could be decreased the processing energy consumption of blending process to produce the SSBR composite with modified silica about 25.7% compare with the OSM and TSM could improve the wet skid resistance of the SSBR composite with modified silica [20].

In 2014, Yan Li et al. have more studied about the surface modification of silica with TESPT by TSM and they focused on the effect of the temperature in process of TSM modification. In this research the temperature at $30-70^\circ\text{C}$ were investigated and the result presents in Table 4, which demonstrated that the grafting degree of modified silica at 50°C is higher than the others. Form the results they consider that the grafting reaction activity is low at low temperature lead to low reaction possibility between silica and TESPT hydrolysate [29].

Table 4 Values of grafting degree (K) of modified silica with different temperature [29].

Modification temperature / $^\circ\text{C}$	30	40	50	60	70
K/%	40.3	58.4	62.2	41.2	34.8

In 2018, Qingfeng Tian et al. prepared the modified silica by similar method with Yan Li et al. they called “in-situ surface modification method” to obtain surface functionalized nano silica (Si-Sx) and used the similar type of silane coupling agent, Bis[3-(triethoxysilyl)propyl]tetrasulfide (Si69, denoted as TESPT). The functionalized nano silica (Si-sx) was produced by hydrolyzed TESPT. After that, nano-silica was added and stirred at 80 °C to obtain a solid, followed by cleaned with distilled water and spray dry to afford a powder. The schematic route of the synthesis of Si-Sx shows in Fig.11. They found that TESPT is successfully grafted on the surface of silica nanoparticles, which confirms by FTIR spectra in Fig.12, resulting the functionalized nano silica has transmittance peak in the wavenumber range of 2850-2900 cm^{-1} corresponded to methylene characteristic peaks that is the component of TESPT.

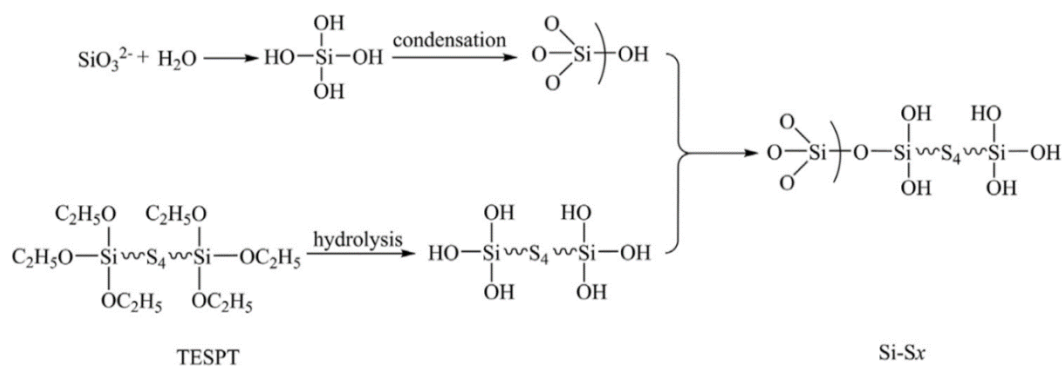


Figure 11 Schematic diagram showing the synthesis of Si-Sx by in-situ surface modification method [31].

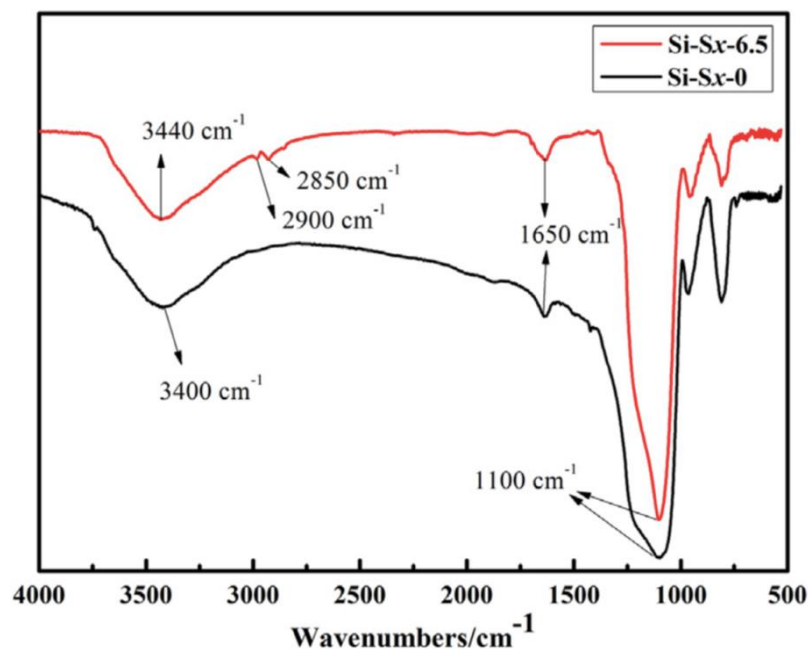


Figure 12 FTIR spectra of pure silica (Si-Sx-0) and functionalized nano silica (Si-Sx-6.5) [31].

Moreover, the researcher reported that could decrease the agglomeration of silica nanoparticles that shows in Fig.13, which found that the size of the functionalized nano silica smaller than pure silica indicated that TESPT could improve compatibility between silica and the organic medium [31].

จุฬาลงกรณ์มหาวิทยาลัย

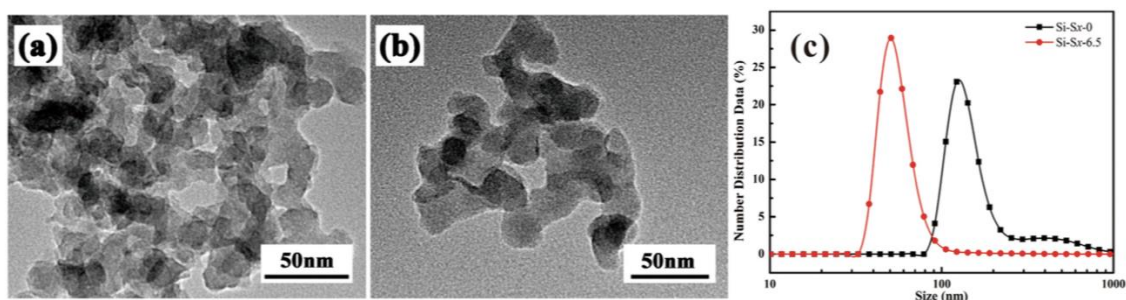


Figure 13 TEM images of (a) Si-Sx-0 and (b) Si-Sx-6.5 as well as (c) size distribution of Si-Sx-0 and Si-Sx-6.5 [31].

2.2.2 Preparation of rubber powder

Due to many advantages of the powder technology of rubber such as stability, easy to transport and comfortable for blending process in production of many products. So, many research have been studied to preparation of rubber powder, which both of natural rubber and synthesized rubber but, the synthesis of rubber powder could not be directly produced because natural rubber has the ability to stick to itself. Therefore, many research requires the use of chemicals or various methods before the drying process to obtain the rubber powder.

In 2007, Daishuang Li et al. reported the synthesized nano-powdered styrene-butadiene rubber (NPSBR) was successfully prepared by gamma radiation for promote crosslinking density of the styrene-butadiene (SBR) latex, which used the functional monomers 2-ethyl hexyl acrylate (2-EHA) and trimethylolpropane triacrylate (TMPTA) as crosslinking agents and followed by drying with spray dryer to obtained NPSBR. The particles size of the synthesized NPSBR is approximately 100 nm, that is the same as SBR latex particles shows in Fig.14. The obtained NPSBR was used as a toughening agent for polystyrene (PS) and high-impact polystyrene (HIPS). Form the results shown that the synthesized NPSBR could be toughening both PS and HIPS [6]. Afterward, Rezaei Abadchi, M. at el. (2014) Successfully prepared polybutadiene rubber (BR) powder by similar method with Daishuang Li et al., which used ^{60}CO radiation and spray drying to get BR powder [32].

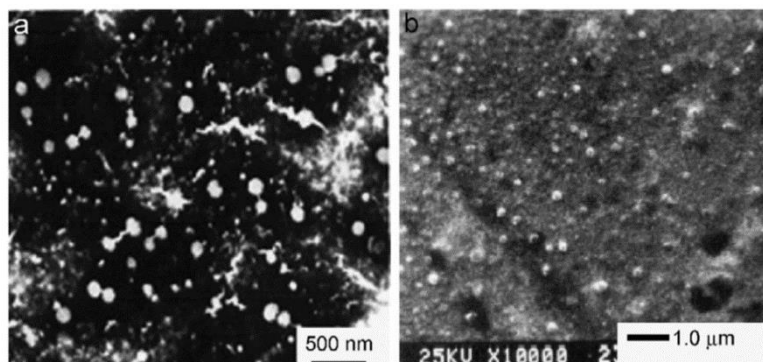


Figure 14 TEM image of SBR latex particles (a) and SEM photograph of NPSBR particles (b) [6].

Moreover, There are several researches demonstrated that they have been successfully prepared the rubber powder via irradiation and spray drying process but this method has negative effects because of the high cost and the safety problems of the irradiation step [4]. To avoid the irradiation process, Paiva L. et al. (2014) prepared the rubber powder by modified styrene-butadiene latex with colloidal silica and some chemical agents such as methyl methacrylate, sodium 4-styrene sulfonate and sodium persulfate as a polymerization initiator. This method consists of two steps such as chemical modification of rubber latex and spray drying process [4].

In 2010, Sea-Oui P. et al. reported the method of natural rubber powder from high ammonia rubber latex via modified the latex with chemicals such as potassium hydroxide, zinc oxide, sulfur and the other ingredients and followed by spray drying. The obtained NRP from spray drying process is a fine powder and the color of powder is light yellowish. Figure 15 shows the morphology of obtained NRP, which found that the NRP was a spherical shape and have large particle size distribution in range 1 to 100 μm [7].

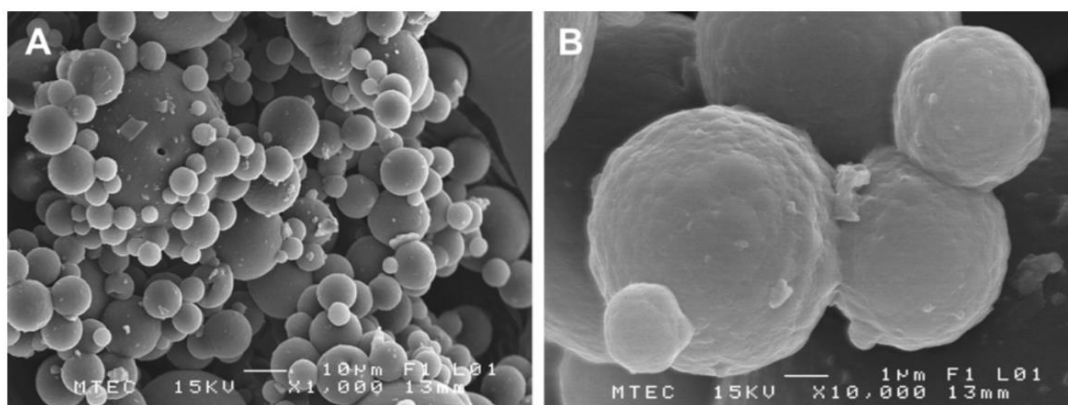
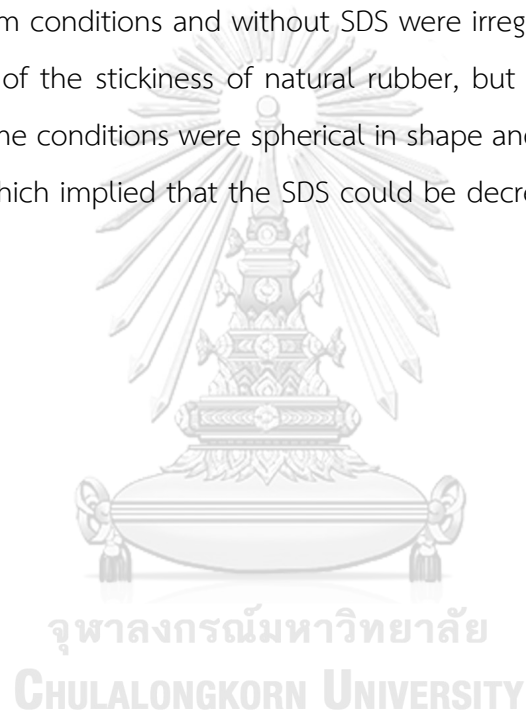


Figure 15 SEM micrographs of the NRP at different magnifications (a) x1,000 and (b) x10,000 [7].

In 2010, Jaiphuephae T. prepared natural rubber powder from natural rubber latex via spray drying and used sodium dodecyl sulfate to solve the problem of blockages at the atomizer of spray dryer by rubber. Furthermore, He found that the obtained natural rubber powder has a spherical shape and small size but the rubber

powder has agglomeration [8]. Afterwards, Jaiphuephae T. et al (2014) have been studied yield optimization of natural rubber powder (NRP) by spray drying process. The results demonstrated that the yield of NRP depended on the amount of sodium dodecyl sulfate (SDS) and the percentage of dry rubber content (DRC) of natural rubber latex shows in Fig.16, which indicated that the optimum conditions were 12 phr of SDS and 15% DRC that could obtained the NRP yield of 44.9%. The optimum conditions of spray drying step were inlet air temperature of 130°C, nozzle flow rate of 600 L h⁻¹ and feed rate of 4 mL min⁻¹. Further, They found that the obtained NRP under the optimum conditions and without SDS were irregular in shape and adhered together because of the stickiness of natural rubber, but the obtained NRP with 12 phr SDS at the same conditions were spherical in shape and not found agglomeration shows in Fig.17 ,which implied that the SDS could be decreased the stickiness of the natural rubber [3].



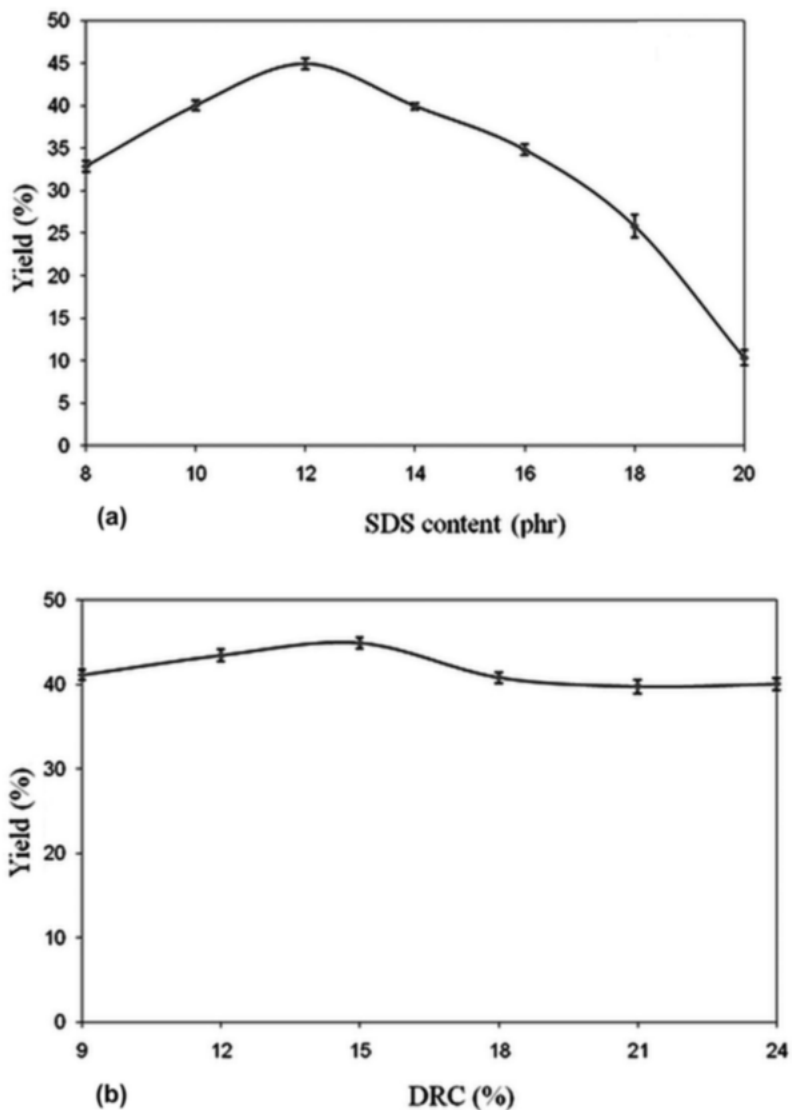


Figure 16 Relationship between the NRP yield (%) obtained and the (a) SDS (phr) and the (b) DRC (%) content [3].

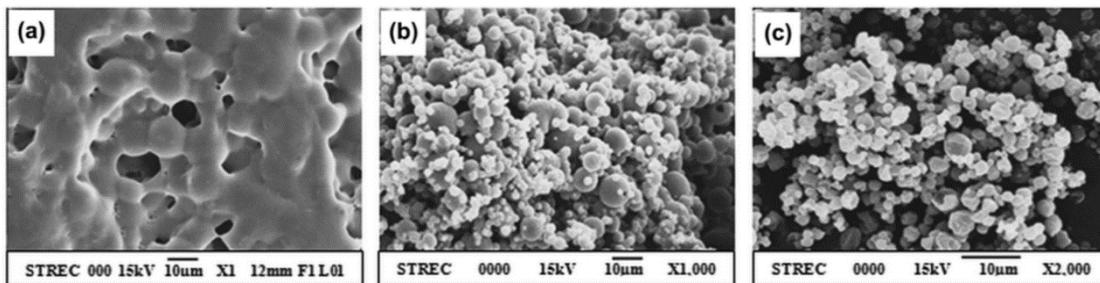


Figure 17 SEM micrographs of the NRP synthesized under the optimum condition (a) without SDS, (b) with 12 phr SDS and (c) the SDS particles [3].

in 2011, Sopanon P. synthesized the natural/ silica composite powder by encapsulation of natural rubber latex particles with silica before spray drying process and used the synthesized composite powder as a filler in polylactide but it has a limit for usage [9]. Moreover, in 2015 Sangthongyingdee N. successfully prepared natural rubber powder by graft polymethyl methacrylate monomer onto natural rubber particle via interfacial polymerization method and followed by spray drying process to prevent adhesion of natural rubber particles [10].



CHAPTER 3

EXPERIMENTAL

3.1 Materials

3.1.1 Natural rubber latex 60% DRC (Dry rubber content), which high ammonia was obtained from Rubber Research Institute, Thailand.

3.1.2 The colloidal silica 50 wt% (LUDOX TM-50) suspension in H₂O, the surface area is 110-150 m²/g was purchased from Sigma-Aldrich, USA.

3.1.3 Acetic acid glacial and was procured from Qrec, New Zealand.

3.1.4 Ethanol was procured from Qrec, New Zealand.

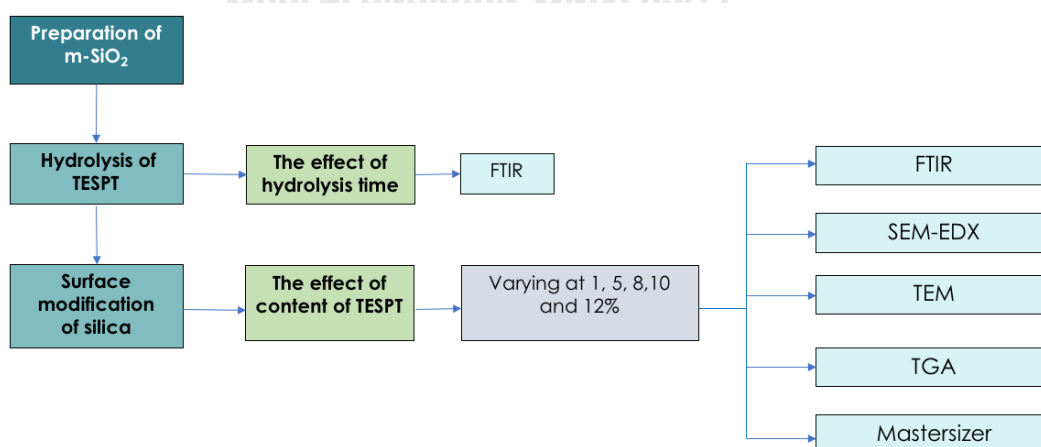
3.1.5 Silane coupling agent bis[3-(triethoxysilyl)propyl]tetrasulfide (TESPT) was obtained from Ecopower chemical Co., Limited, China.

3.1.6 Toluene was purchased from Qrec, New Zealand.

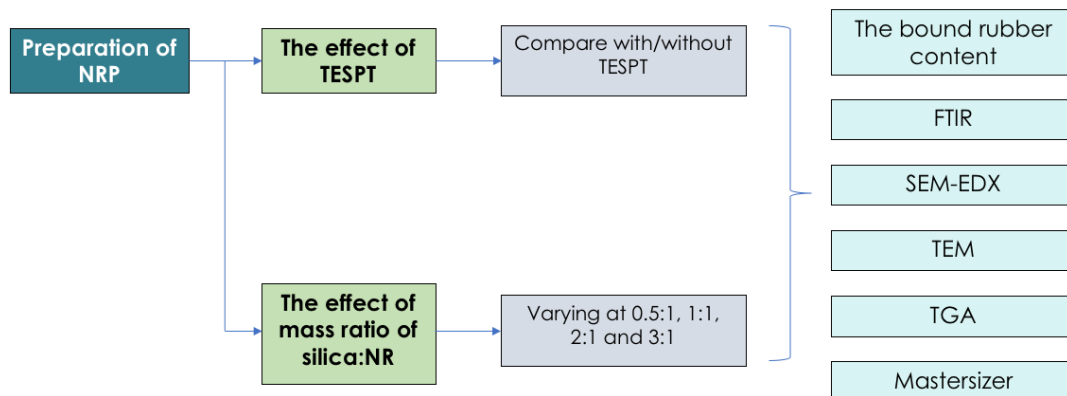
3.1.7 Sodium lauryl sulfate was purchased Univar solutions, USA.

3.2 Experimental procedure

3.2.1 Preparation of modified silica step



3.2.2 Preparation of Natural rubber powder step



3.3 Hydrolysis of TESPT

The hydrolysis of TESPT was studied the effect of hydrolysis time. To begin with, Ethanol 200 ml was mixed with deionized water 6 ml. After that, acetic acid was added into a beaker to adjust the pH of the solution to approximately 4.5 and added 20 ml of TESPT into the beaker. Then, the sample were characterized by FTIR at 1, 2, 3, 4, 5, 6, 7, 8, 9, 10, 24 and 48 h. After complete hydrolysis reaction, the TESPT hydrolysates were obtained. TESPT hydrolysates are TESPT that ethoxyl group transforms into a hydroxyl group shows in Fig.18.

3.3 Preparation of modified silica

The preparation of modified silica ($m\text{-SiO}_2$) using silane coupling agent, TESPT involves two steps: (1) hydrolysis of TESPT; (2) surface modification of silica via silane condensation reaction. Figure 1 shows the synthesis route of $m\text{-SiO}_2$. First, 200 ml of ethanol was mixed with 6 ml of deionized water. Acetic acid was then added into a beaker for pH adjustment to approximately 4.5 followed by the addition of 20 ml of TESPT into the beaker to obtain a silane hydrolysates. TESPT hydrolysates forms as a

results of hydrolysis of ethoxyl groups into a hydroxyl groups. Next, colloidal silica was added into the TESPT hydrolysates and stirred at room temperature for 16 h, followed by drying with spray dryer (BUCHI B-190, Switzerland) to produce m-SiO₂ powder for characterization and the schematic of the spray drying process was shown in Figure 2. The spray drying process was performed at an inlet temperature of 120°C, feed rate of 10 ml/min, nozzle flow rate of 400 L/h and at inlet solid content of mixture of 10%. The mass ratio of TESPT and silica were varied at 1%, 5%, 8%, 10% and 12%, and the samples of modified silica with TESPT:silica mass ratio of 1%, 5%, 8%, 10% and 12% were respectively labeled as m-SiO₂-1, m-SiO₂-5, m-SiO₂-8, m-SiO₂-10 and m-SiO₂-12.

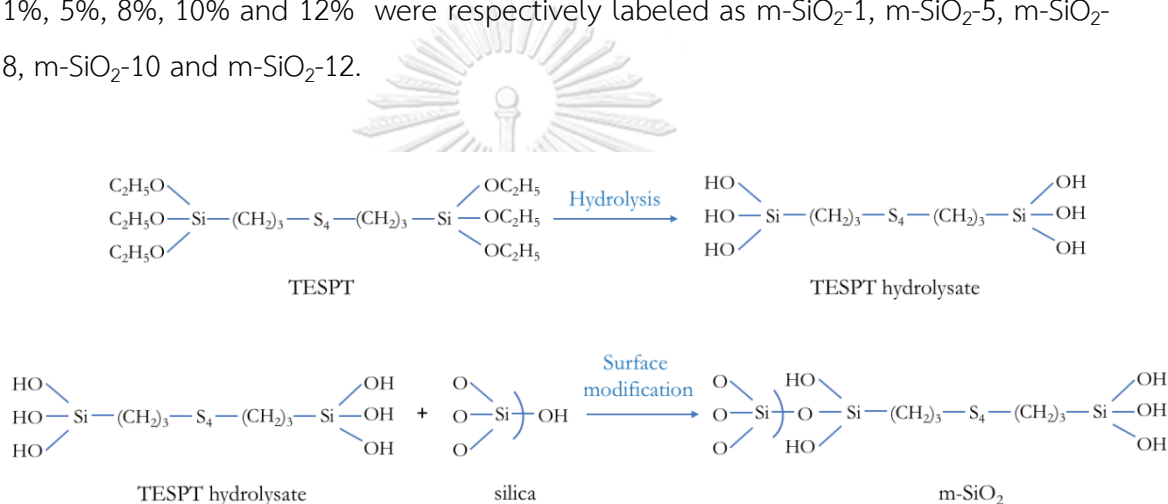


Figure 18 The mechanism of TESPT hydrolysis and surface modification of silica with TESPT.

3.4 Preparation of natural rubber powder

Natural rubber powder (NRP) was prepared by adding colloidal silica into the TESPT hydrolysates that prepared by the same method with topic 3.3. Then, the solution was stirred at for 16 h. After that, pre-vulcanized natural rubber latex 60% was added into a beaker and followed by stirring with magnetic stirrer for 10 min. Finally, drying the solution with spray dryer to obtain NRP for characterization later. The mass ratio of silica to rubber were studied at 0.5:1, 1:1, 2:1 and 3:1 respectively. The conditions of spray drying process is inlet temperature at 120°C, feed rate at 10

ml/min, nozzle flow rate at 400 L/h and solid content of mixture before spray drying at 10%.

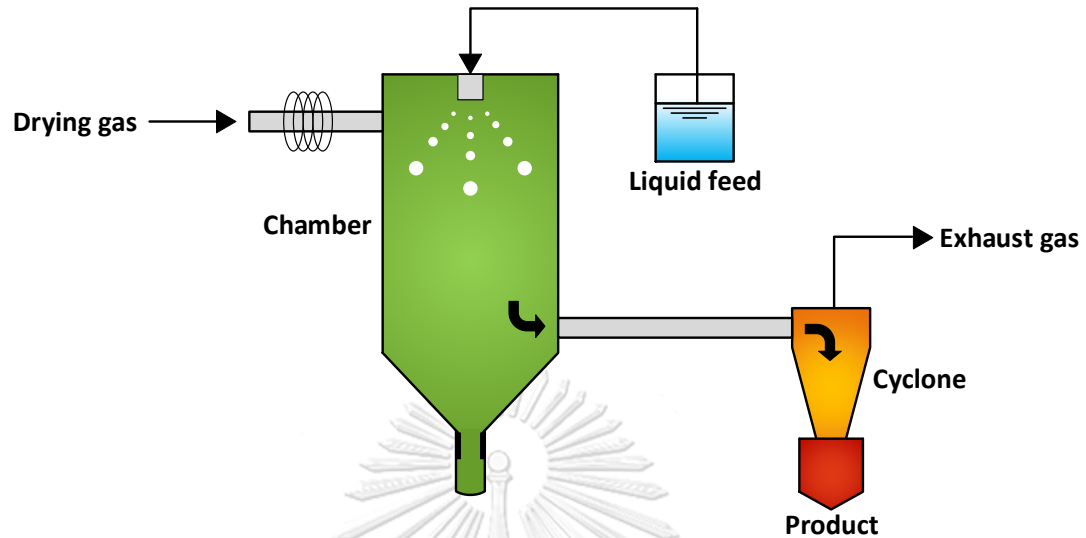


Figure 19 Schematic of a spray dryer.

3.5 Characterizations

3.5.1 The morphology and elemental composition

The morphology of natural rubber latex particle and silica particle colloidal before spray drying process were characterized by transmission electron microscope (TEM, jem-1400, JEOL Ltd., Tokyo, Japan). The NRL particle was fumed with Osmium tetroxide (OsO_4) vapor, which used as staining agent to provide contrast to the TEM image.

The morphology and elemental composition of m- SiO_2 and NRP, which obtained from spray drying process were studied using scanning electron microscope and energy dispersive X-ray spectrometer (SEM-EDS, IT500HR and IT300, JEOL Ltd., Tokyo, Japan). The sample was coated with gold for 3 mins using sputter coater.

The surface morphology of NRP, which obtained from spray drying process were studied by Field Emission Scanning Electron Microscope and Energy Dispersive X-ray Spectrometer (JEOL JSM-7610F, Oxford X-Max 20, JEOL Ltd., Tokyo, Japan). The sample was coated with platinum for 3 mins using sputter coater.

3.5.2 The particle size and size distribution

The particle size and size distribution of modified silica colloidal, modified silica powder and natural rubber were characterized using laser diffraction analyzer (mastersizer2000, Malvern, United Kingdom). The modified silica colloidal and modified silica powder were determined using water as mobile phase. The NRP samples were dispersed with water and used SDS as surfactant. Moreover, it was dispersed using sonicated for 10 mins before input into the instrument.

3.5.2 The functional group and the grafting degree (K)

The functional group of pure silica, TESPT, TESPT hydrolysate and m-SiO₂ were determined by Fourier transform infrared spectrometry (FTIR, Perkin Elmer, USA) in the range 400-4000 cm⁻¹. The grafting degree (K) that demonstrates to the organic degree on-SiO₂ was calculated from Eq. 1 [9].

$$K = (R - r)/R * 100\% \quad (1)$$

Where K is the grafting degree of the hydroxyl, R is the ratio of the hydroxyl peak at 3447 cm⁻¹ to Si-O-Si peak at 1108 cm⁻¹ of FTIR spectra of pure silica, r is the ratio of the hydroxyl peak at 3447 cm⁻¹ to Si-O-Si peak at 1108 cm⁻¹ of FTIR spectra of m-SiO₂.

3.5.3 The thermal stability

The thermal stability of NRP measured by thermogravimetric analysis (TGA/DSC1, METTLER TOLEDO, Thailand) under nitrogen atmosphere. The sample were heated at heating rate of 20°C/min in range 25-800°C.

3.5.4 The bound rubber content

The bound rubber content (BRC) of the synthesized NRP were determined by added 0.25g of the NRP into toluene 50 ml and placed in room temperature for 7 days and dispersed the particle using vortex mixer everyday. After that, the sample was filtered with filter paper, and then dried in air at room temperature for 1 day. Finally, the remained sample was dried in an oven at 70°C until the weight of sample is constant. The bound rubber content calculated from Eq. 2.

$$\text{BRC} = \frac{m_{fg} - m_f}{m_r} \times 100\% \quad (2)$$

Where BRC is bonded rubber content

m_{fg} is the weight of filler (silica) gel

m_f is the weight of filler in the compound

m_r is the weight of rubber in the compound

CHAPTER 4

RESULTS AND DISCUSSION

This research studies the preparation of natural rubber powder modified with bis(triethoxysilylpropyl)tetrasulfide (TESPT) treated silica by spray drying method. There are two main steps to synthesis natural rubber powder involves the preparation of modified silica with TESPT and the preparation of natural rubber powder with modified silica. This chapter describes results and discussion of the preparation of modified silica step and the preparation of natural rubber powder step respectively.

4.1 The preparation of modified silica (m-SiO₂) with TESPT

The preparation of modified silica (m-SiO₂) using silane coupling agent, TESPT involves two steps: (1) hydrolysis of TESPT; (2) surface modification of silica via silane condensation reaction.

4.1.1 Hydrolysis of TESPT

4.1.1.1 The functional group of TESPT hydrolysate

The hydrolysed silane, TESPT hydrolysate were characterized by FTIR to studied the functional group. Figure 20 shows the FTIR spectra of TESPT, TESPT hydrolysate and ethanol. The FTIR spectrum of TESPT hydrolysate has the broad absorption peak of the hydroxyl stretching vibration peak that is located at approximately 3400 cm⁻¹, similarly to the FTIR spectrum of ethanol. Moreover, the

spectrum of TESPT hydrolysate and ethanol present the absorption peak around 1640 cm^{-1} , attributed to the stretching vibration mode of the H-O-H bond of absorbed water. On the other hand, the FTIR spectrum of pristine TESPT not found the absorption peak of the hydroxyl group and the absorption peak of absorbed water. This results according to the report of Li, Y. et al (2013), which indicated that some ethoxyl ($-\text{CH}_2$) groups of TESPT transform into a hydroxyl groups($-\text{OH}$) after hydrolysis with water under acidic condition that offers the necessary condition for silica and silane grafting reaction [29]. In addition, The absorption peak of the C-H stretching of CH_3 and CH_2 at $2800\text{--}3000\text{ cm}^{-1}$ and the absorption peak of the Si-O asymmetric and symmetric stretching at $1300\text{--}1000$ and 793 cm^{-1} [33] respectively are found at the FTIR spectra of TESPT and TESPT hydrolysate due to they are the components of TESPT. The FTIR functional group of TESPT, TESPT hydrolysate and ethanol were summarized in Table 5.

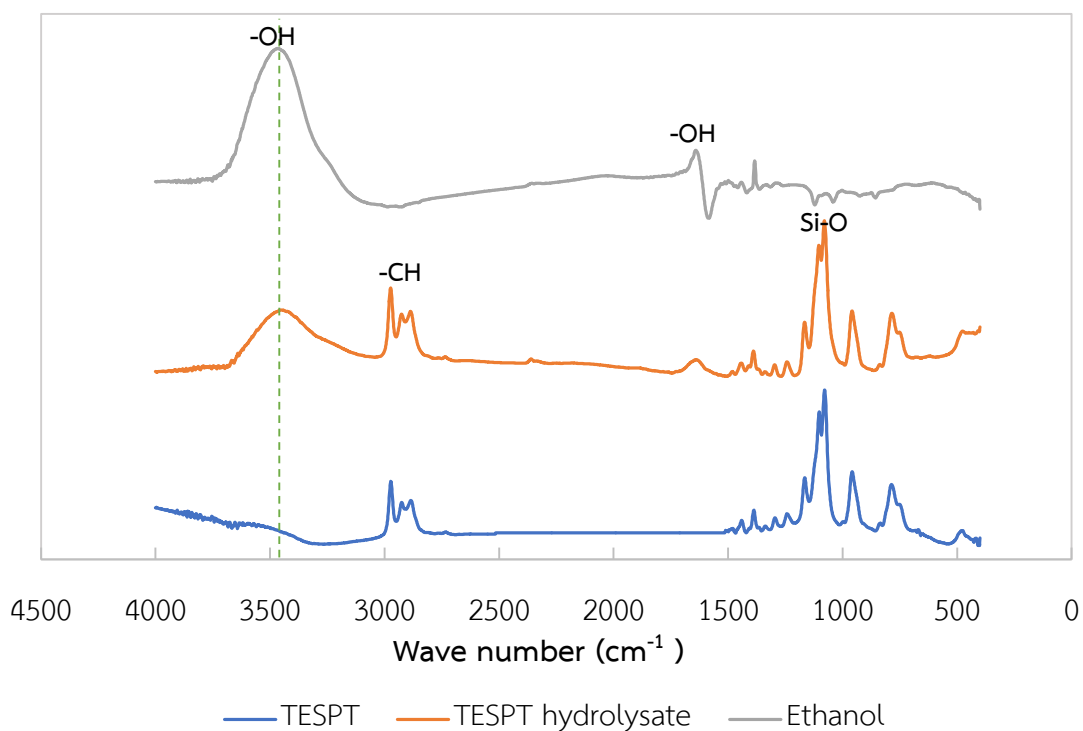


Figure 20 FTIR spectra of TESPT, TESPT hydrolysate and ethanol.

Table 5 The FTIR functional group of TESPT, TESPT hydrolysate and ethanol [33].

Wave number (cm ⁻¹)	Functional group
3600-3000	O-H stretching
3000-2800	C-H stretching
1650	O-H bending
1300-1000	Si-O asymmetric stretching
960	C-H rocking
793	Si-O symmetric stretching

4.1.1.2 Effect of time to TESPT hydrolysate.

The step of hydrolysis of TESPT was studied the effect of time to TESPT hydrolysate by using the result of the FTIR spectra of TESPT hydrolysate at different times for optimizing the reaction time to occur the complete hydrolysis reaction of TESPT. Figure 21 presents the FTIR peak ratio of the hydroxyl stretching vibration peak at approximately 3400 cm⁻¹ to the FTIR peak of C-H bond of organic group at 2974 cm⁻¹, which is the component of TESPT. From this figure shown that the peak ratio of hydroxyl with different hydrolysis time were a significant increase throughout the period from the beginning to 10 h, and there were remained constant at approximately 1.6 after 10 h later. This indicates that the hydrolysis reaction of TESPT has completely occur after 10 h later.

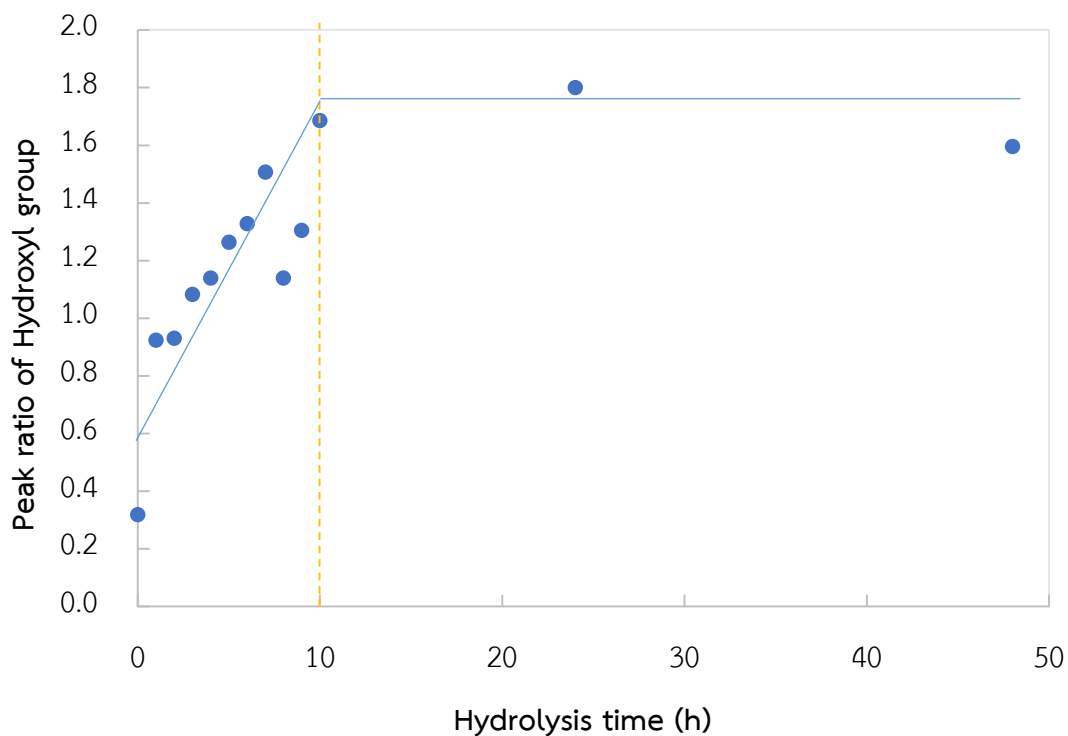


Figure 21 FTIR spectra of TESPT, TESPT hydrolysate and ethanol.

4.1.2 Surface modification of silica

After TESPT was hydrolyzed to transform into TESPT hydrolysate, they reacted with the surface of silica particle via a condensation reaction to form modified silica ($m\text{-SiO}_2$). Both $m\text{-SiO}_2$ colloidal before spray dry and dried $m\text{-SiO}_2$ powder were characterized by TEM, SEM, FTIR and TGA analysis to determine the suitable concentration of TESPT to modify the surface of the silica particle.

4.1.2.1 The morphology of modified silica colloidal

The modified silica colloidal with a TESPT amount of 8 wt.% by mass of silica was measured the morphology and particle size before drying via TEM analysis. The TEM image of modified silica colloidal shows in fig. 22 that it was in spherical form

and uniform particle distribution. The average particle size of m-SiO₂ colloidal from TEM image was approximately 10 nm. This size of m-SiO₂ colloidal is a suitable size to coat the natural rubber latex particle because the particle size of natural latex particle was found in average diameter at 318 nm [10], which the particle size of modified silica is much less than the particle size of natural rubber latex. There is suitable size according to the report of Nandiyanto, A.B.D. and K. Okuyama reported that when the particle size of two component are different, the unique particle can be formed by a spray drying process. A coating or surrounding of one component by the others can be produced that is called as the microencapsulation phenomena. Moreover, the size of one component should be less than the others 3 times ($d_{p1} < 3d_{p2}$) [34]. The size distribution of modified colloidal silica shows in Fig. 23. The figure demonstrated that the average particle size of m-SiO₂ colloidal was approximately 10 nm, which similar to the results of TEM analysis. The size distribution of modified colloidal silica is a unimodal distribution, which is only a single highest peak. The results shown that the particle size of m-SiO₂ colloidal is uniformly.

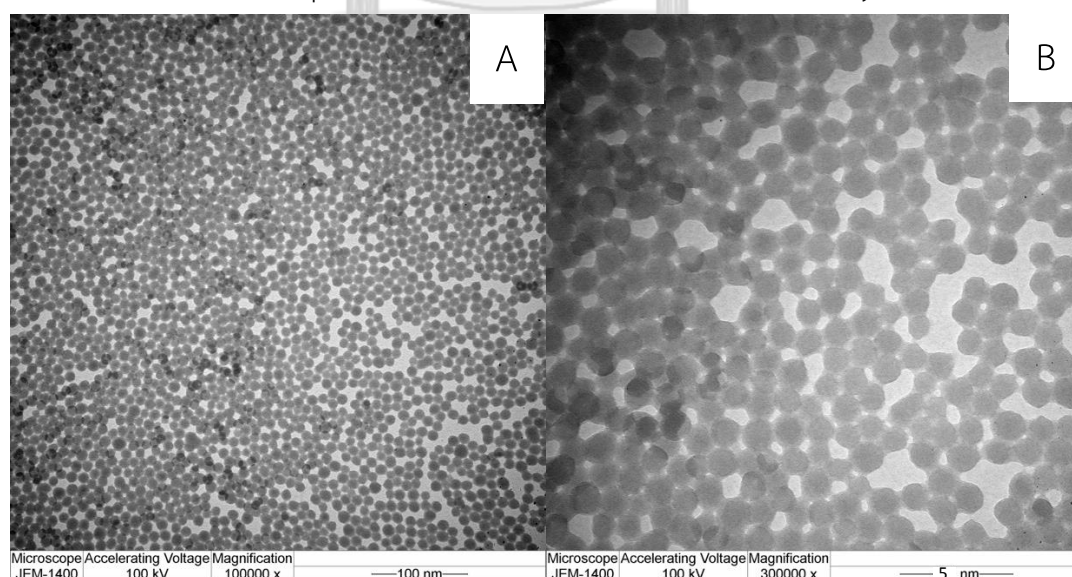


Figure 22 TEM image of modified silica colloidal at A) low magnitude and B) high magnitude.

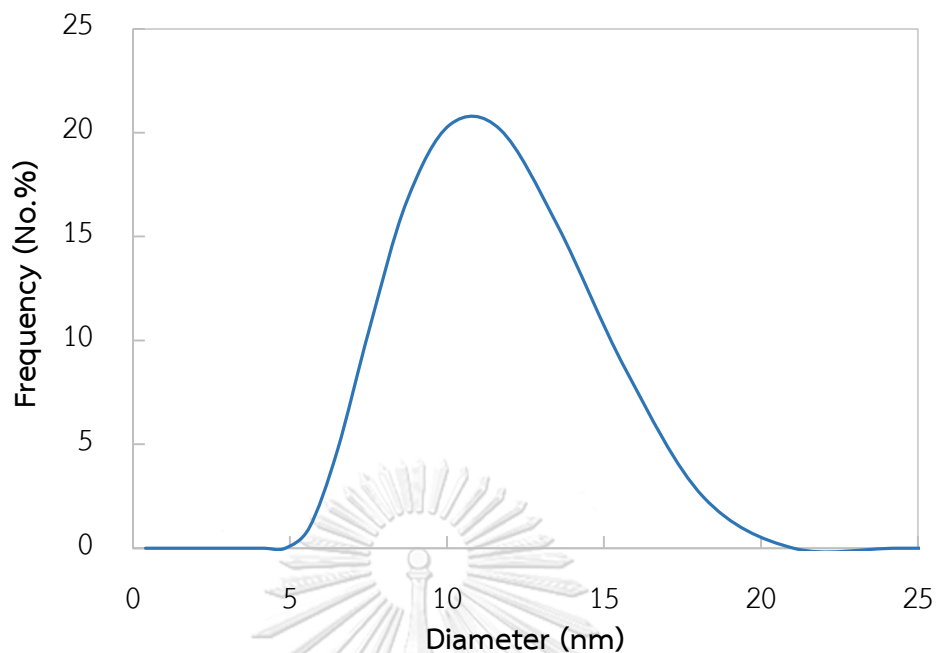


Figure 23 The size distribution curve of modified silica colloidal.

4.1.2.2 The morphology of m-SiO₂

The morphology of spray dried pure silica and m-SiO₂ powders prepared at different amount of TESPT were characterized using SEM, and the micrographs were shown in Fig. 24. SEM images illustrated that the pure silica (Fig. 24A) and m-SiO₂ (Fig. 24B-F) were of spherical shapes and uniform particle distribution. No morphological changes were detected in silica particles before and after surface medication with TESPT.

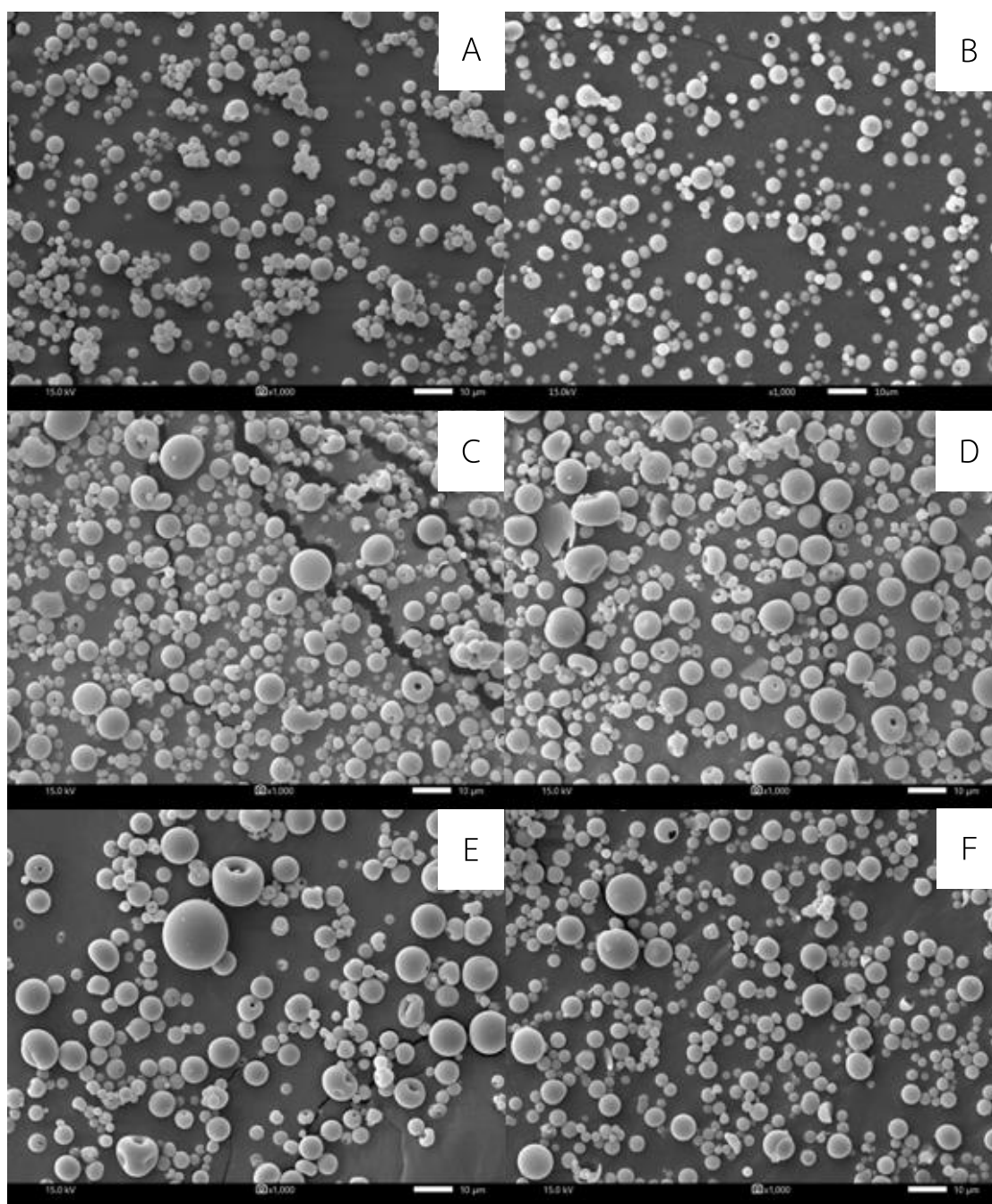


Figure 24 SEM images of A) pure silica, B) m-SiO₂-1, C) m-SiO₂-5, D) m-SiO₂-8, E) m-SiO₂-10 and F) m-SiO₂-12.

4.1.2.3 The particle size and size distribution of modified silica.

The particle size of spray dried pure silica and m-SiO₂ powders prepared at different amount of TESPT were characterized using laser diffraction analyzer (mastersizer2000), and the values were shown in Fig. 25. The results exhibited that the geometric mean diameter of pure silica is larger than modified silica, which indicated that TESPT can prevent the agglomeration of silica due to the hydroxyl groups on the surface silica particle decrease after modification [20]. In other word, m-SiO₂ can demonstrate better compatibility between silica and natural rubber than unmodified silica [31]. The spray dried m-SiO₂ powders with amount of TESPT at 1 and 5 wt.% presented the larger geometric mean diameter than the m-SiO₂ powders with amount of TESPT at 8 to 12 wt.%, which show the quite similar geometric mean diameter and m-SiO₂-8 has smallest particle size. The result exhibited that the amount of TESPT

Less than 8 %wt. of silica is not enough to modified the surface of silica.

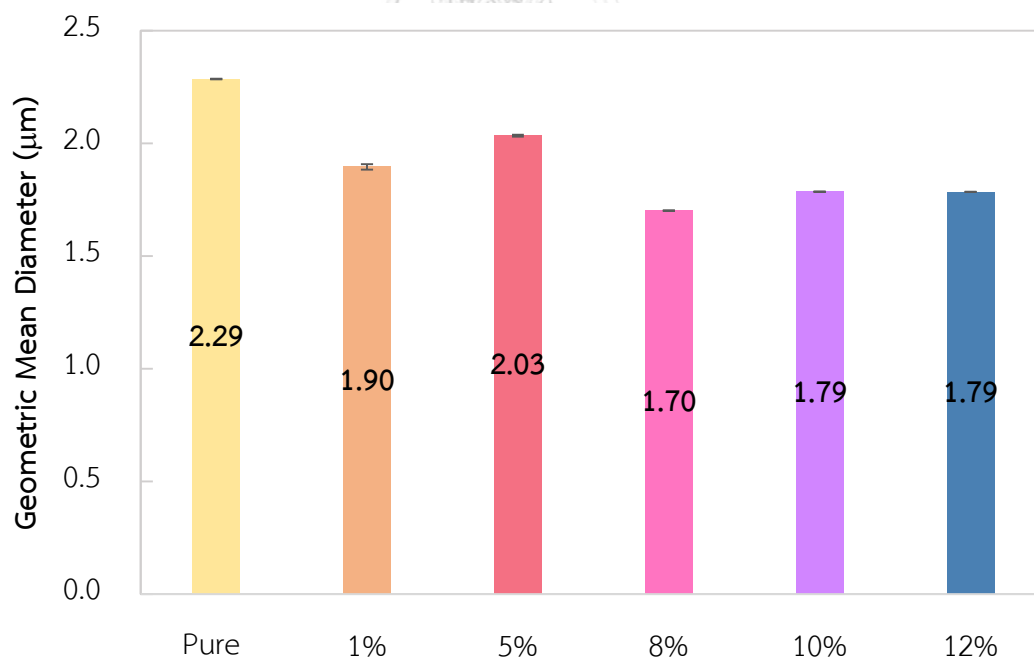


Figure 25 The Mean Diameter of spray dried pure silica and m-SiO₂ powders prepared at different amount of TESPT.

Figure 26 shows the size distribution curve of spray dried pure silica and m-SiO₂ powders prepared at different amount of TESPT. The size distribution of both pure silica and m-SiO₂ are a bimodal distribution. The narrow first particle size peak of pure silica has lower intensity than modified silica. On the other hand, the broad second particle size peak of pure silica has higher intensity than modified silica. The result showing pure silica has agglomeration with each other indicated TESPT can decrease that agglomeration. After modification, the second particle size peak of the m-SiO₂ powders with increasing amount of TESPT from 8 to 12 wt.% shift into smaller size region, showing a good modification effect of TESPT on the surface of silica.

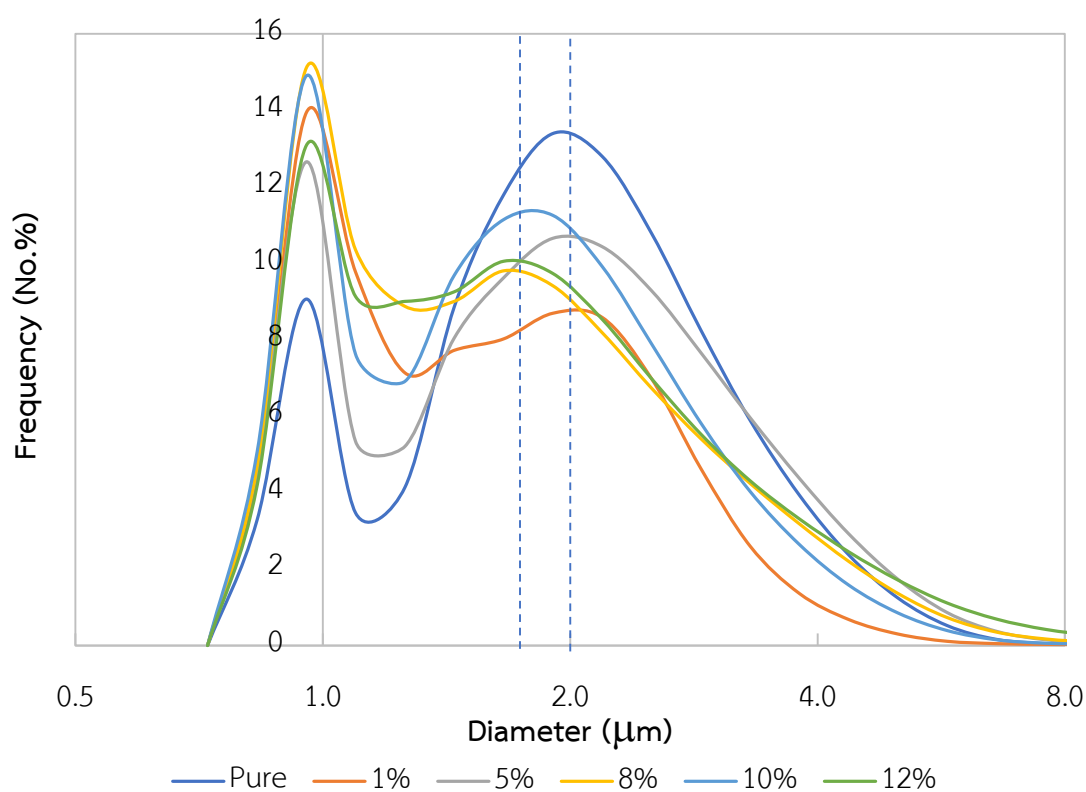


Figure 26 The size distribution curve of spray dried pure silica and m-SiO₂ powders prepared at different amount of TESPT.

4.1.2.4 The grafting degree of modified silica

The functional group of m-SiO₂

Pure silica, modified silica and TESPT were determined the chemical structure and functional group via FTIR analysis. Figure 27 shows the FTIR spectra of TESPT, pure silica and m-SiO₂-12. From Fig. 27, it is apparent that FTIR spectra of pure silica and m-SiO₂ have absorption peaks at 1100 cm⁻¹, which was attributed to the Si-O-Si asymmetric stretching vibration. The absorption peaks observed at 1650 cm⁻¹ and 3400 cm⁻¹ were assigned to deforming and stretching vibration modes of the hydroxyl groups present on silica particle surface [35]. After modification with TESPT, the characteristic absorption peak of hydroxyl group become weaker. This is because the amount of hydroxyl groups on the surface of silica gradually decreases mainly due to a chemical reaction between hydroxyl groups of silica and silanol groups of TESPT, as described in Fig. 18. The absorption peak detected in the wavenumber range of 2800-2900 cm⁻¹ corresponds to the methylene (-CH₂-) characteristic peaks [31]. The FTIR functional group of TESPT, pure and modified silica were summarized in Table 6.

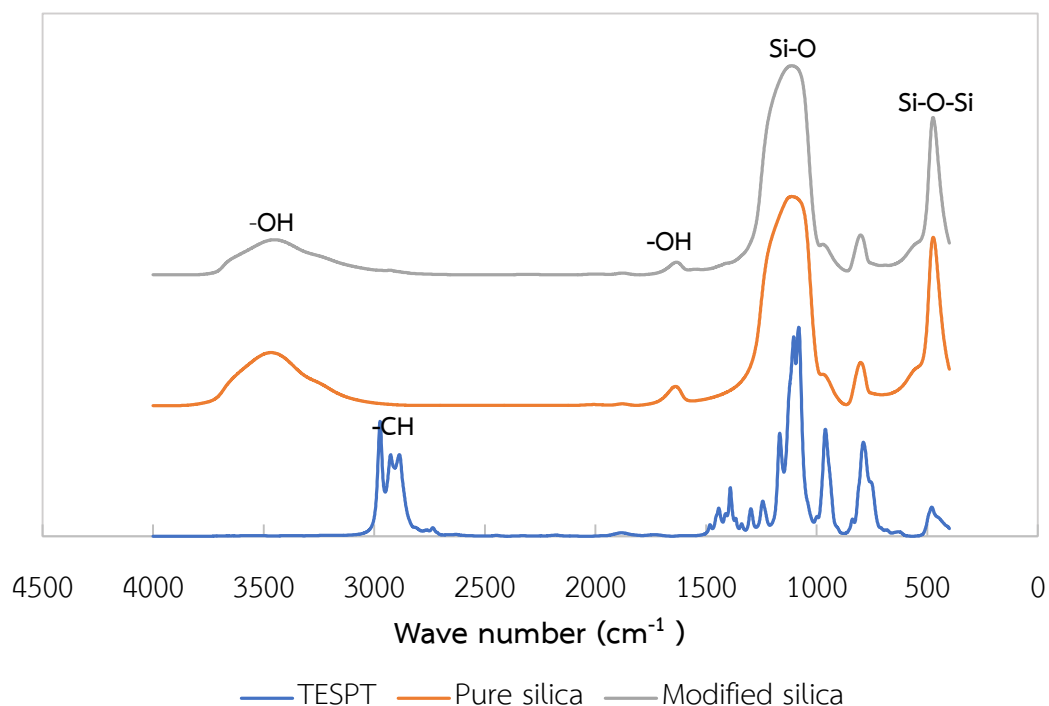


Figure 27 FTIR spectra of TESPT, pure silica and m-SiO₂-12.

Table 6 The FTIR functional group of TESPT, pure and modified silica [33, 36].

Wavenumbers (cm ⁻¹)	Functional Groups
3400	-OH Stretching from Si-OH
2800-3000	C-H stretching from CH ₂ and CH ₃
1680	-OH Bending from water molecules
1300-1000	Si-O asymmetric stretching
1100	-Si-O Asymmetric stretching on -Si-O-Si-
964	Si-O Stretching from Si-OH
800	-Si-O Symmetric stretching from -Si-O-Si-
480	Si-O-Si Bending

Figure 28 shows the comparative FTIR spectra of both pure silica and m-SiO₂-12 in the wavenumber range of 2800-3000 cm⁻¹. Based on Figure 28, it is noticeable that the spectra of modified silica with a strong absorption peak at 2928 cm⁻¹, which corresponds to the organic groups of TESPT, namely methylene (-CH₂-). The close-up comparison indicated that silane groups have been successfully grafted on the surface of silica particles via a chemical bond established between silicon atom of silica and oxygen atom of TESPT [20, 31].

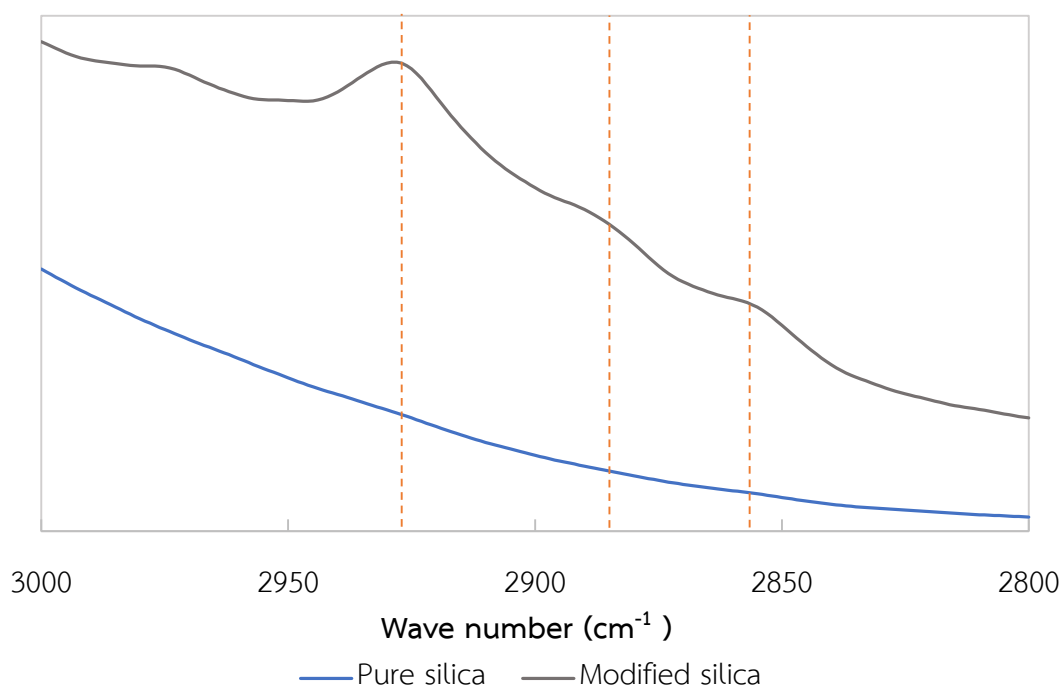


Figure 28 FTIR spectra of pure silica and m-SiO₂-12 at wave number 2800 to 3000 cm⁻¹.

The grafting degree of m-SiO₂

The m-SiO₂ powders prepared at different amount of TESPT via spray drying were characterized using FTIR and the resultant spectra was shown in Fig. 29. Based on Fig. 5, All sample have the same absorption peak at approximately 3400, 1600, 1100, 800 and 480 cm⁻¹, which corresponds to -OH Stretching, -OH Bending, -Si-O Asymmetric stretching, -Si-O Symmetric stretching and Si-O-Si Bending respectively. All aforementioned absorption peaks are the components of silica particle. From Fig.

29, we could not observe the absorption peak of organic groups of TESPT because the amount of TESPT is less when compared to silica. Figure 30 shows the FTIR spectra of dried modified silica powder with different amount of TESPT. Based on Figure 30, it is noticeable that the spectra of modified silica prepared with amount of TESPT 8 to 12 wt.% present a strong absorption peak approximately 2900 cm^{-1} , which corresponds to the organic groups of TESPT. An addition, the spectra of modified silica prepared with amount of TESPT 5 wt.% shows a weak absorption peak approximately 2900 cm^{-1} but it can't observe on the spectra of modified silica prepared with amount of TESPT 1 wt.%. from the result indicated that the amount of TESPT at 1 %wt. of silica is not enough to detect with this technique.

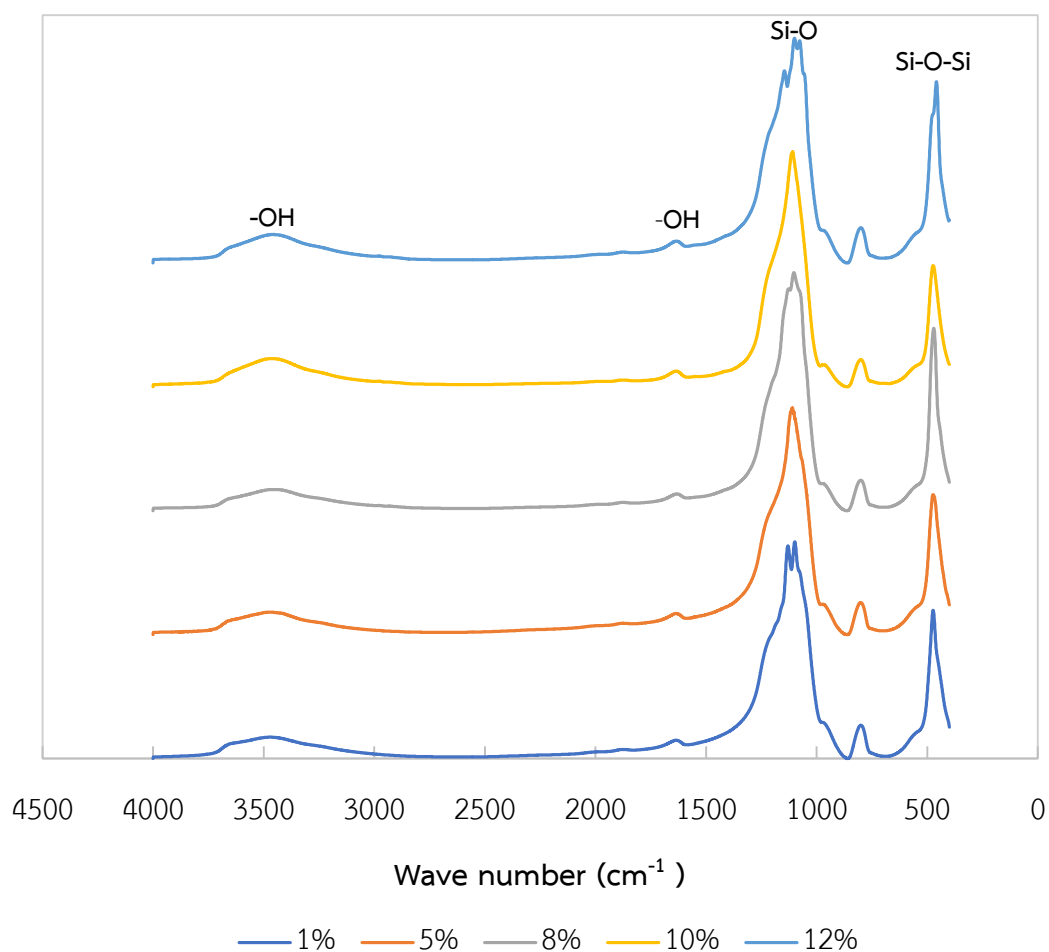


Figure 29 FTIR spectra of dried modified silica powder with different amount of TESPT.

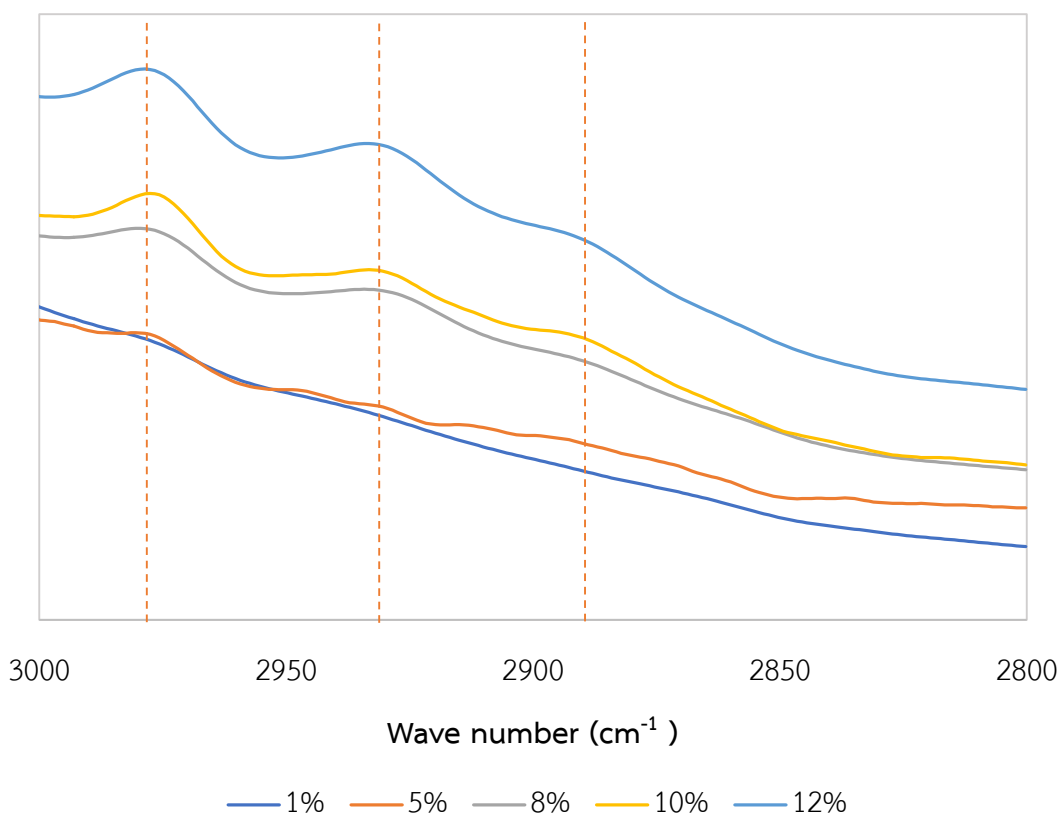


Figure 30 FTIR spectra of dried modified silica powder with different amount of TESPT at wave number 2800-3000 cm⁻¹

จุฬาลงกรณ์มหาวิทยาลัย

The grafting degree (K) of the as-prepared m-SiO₂ was determined based on FTIR results. Figure 31 presents the grafting degree of m-SiO₂ with different amount of TESPT. It was found that the modified silica with 8% of TESPT (m-SiO₂-8) exhibited highest K value followed by the samples modified respectively by 5% and 1% of silane. The K values of m-SiO₂-5 and m-SiO₂-1 decreasing due to decreasing TESPT concentration, resulting lower grafting efficiencies. On the contrary, the k values of m-SiO₂-10 and m-SiO₂-12 are lower than m-SiO₂-8 respectively. The decreasing of K values with increasing TESPT concentration implied that siloxane oligomers were formed via inter-reaction or hydrogen bonds by hydroxyl of TESPT hydrolysates. As the TESPT content increases, the presence of oligomers attached to first layer of reacted silane on silica surface could hinder the further silane grafting and reduce

energy absorption of silica thus lead to the lower grafting efficiencies [9]. The generally reaction scheme of TESPT over the surface of silica was initially proposed by Hunsche et al which presents in Fig. 32. From fig.32 reported that the mechanism consists of reactions in which water plays an significant role as promotor through the hydrolysis reaction of TESPT ethoxy groups, leading to a group of silanol (scheme A) which can the undergo a condensation reaction with a group of silanol resulting in grafted silane species (scheme B). Moreover, the grafted silane species can reacts with other grafted silane species or vicinal silane species via oligomerization or co-condensation, which through nucleophilic substitution and formation of ethanol (scheme C) or water (scheme D), resulting to polycondensed species that called siloxane oligomers [37]. The formation of siloxane oligomers from the literature, which is in good agreement with the decreasing of K values with increasing TESPT concentration in our results.

Table 7 The grafting degree value of m-SiO₂

Sample	Mass ratio of TESPT(%)	K (%)
m-SiO ₂ -1	1	59.23
m-SiO ₂ -5	5	64.78
m-SiO ₂ -8	8	74.22
m-SiO ₂ -10	10	52.02
m-SiO ₂ -12	12	49.06

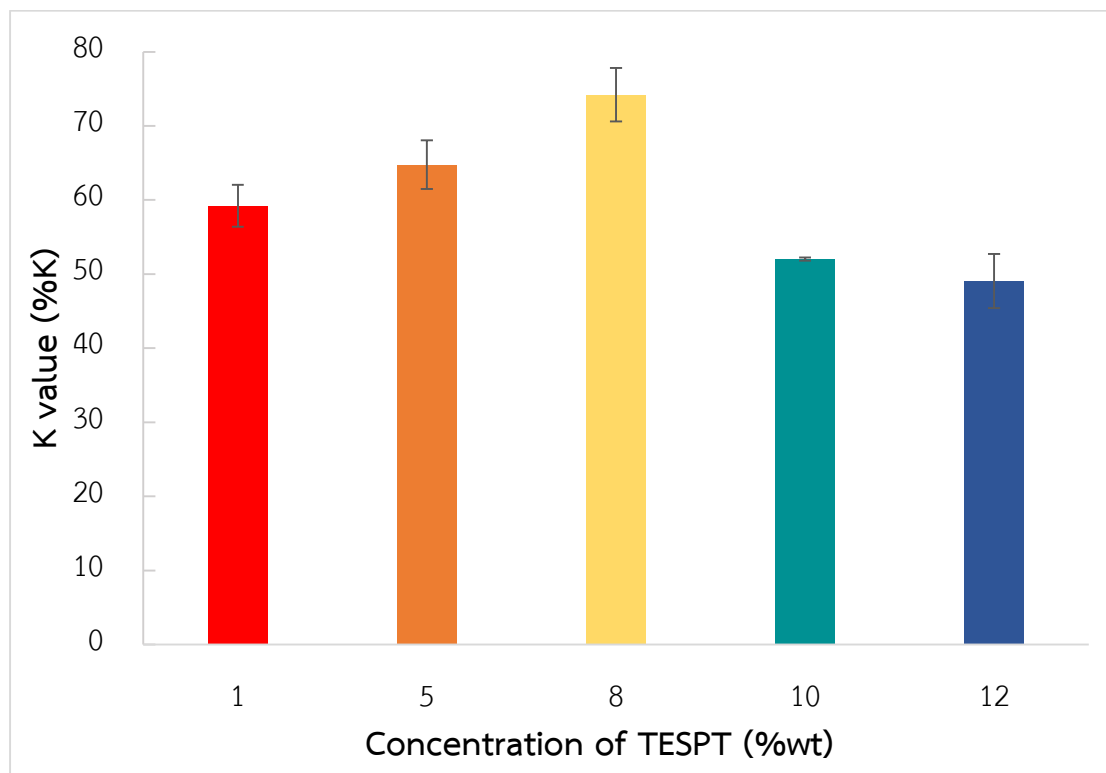


Figure 31 The grafting degree of m-SiO₂ with different amount of TESPT

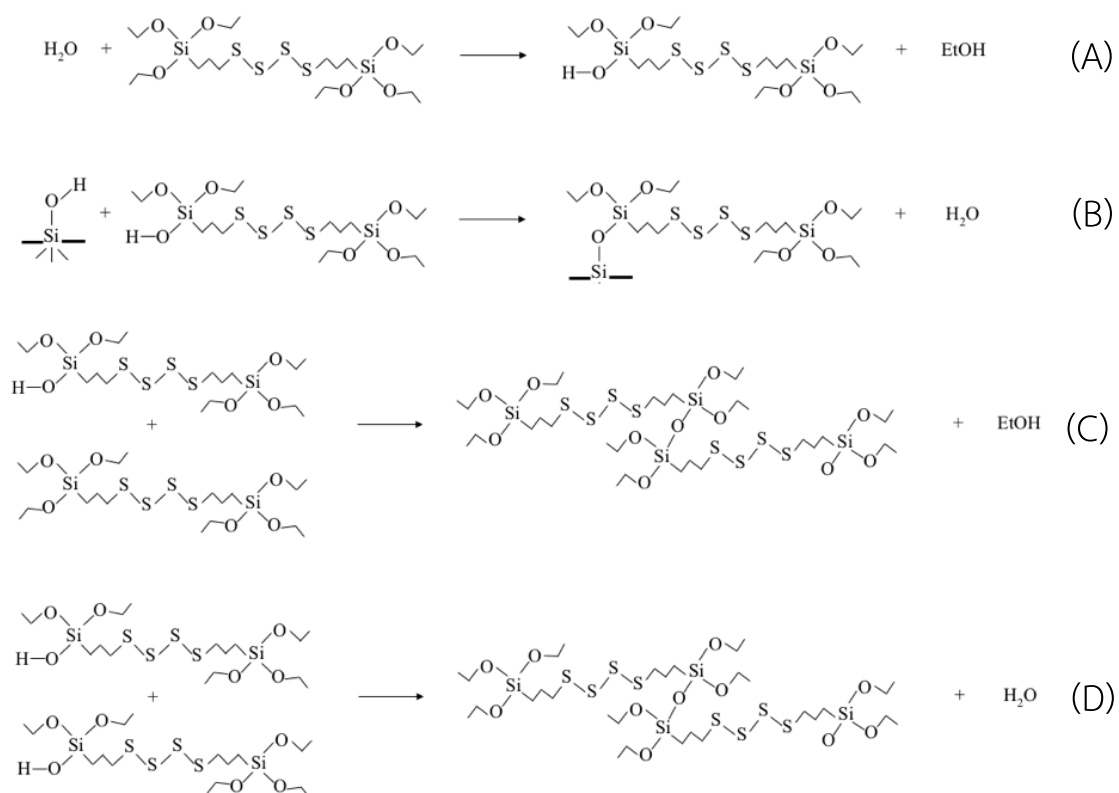


Figure 32 The generally reaction scheme of TESPT over the surface of silica [37].

4.1.2.5 The thermal stability and composition of modified silica

The dried pure silica and modified silica powder with different amount of TESPT were investigated the thermal stability and composition by TGA analysis that shows in Fig. 33. From this figure, Both pure and modified silica show large weight loss in the region of temperature between 25°C and 120°C (first region). The weight loss in this region was because of to the removal of the adsorbed water on the surface of silica. Table 8 present the weight loss in first region of the modified silica with 8% to 12% of TESPT are lower than pure silica due to the chemical bonding of the TESPT hydrolysate with the hydroxyl group of silica surface [29, 35]. Moreover, this is reasonable as the grafted TESPT increases the hydrophobicity of silica and thus prevents the absorption of water [22]. In the region between 120°C and 800°C (second region), all of modified silica present a large weight loss more than pure silica. The weight loss of modified silica in the second region was owing to the degradation of TESPT on the surface of silica, and the weight loss of pure silica was because of the dehydroxylation of hydroxyl groups on the surface of silica [35]. In Table 8 and Fig. 34 show the weight loss in the second region of all modified silica has the same trend with the weight ratio of TESPT to silica, which the weight loss is increase when increasing the weight ratio of TESPT to silica.

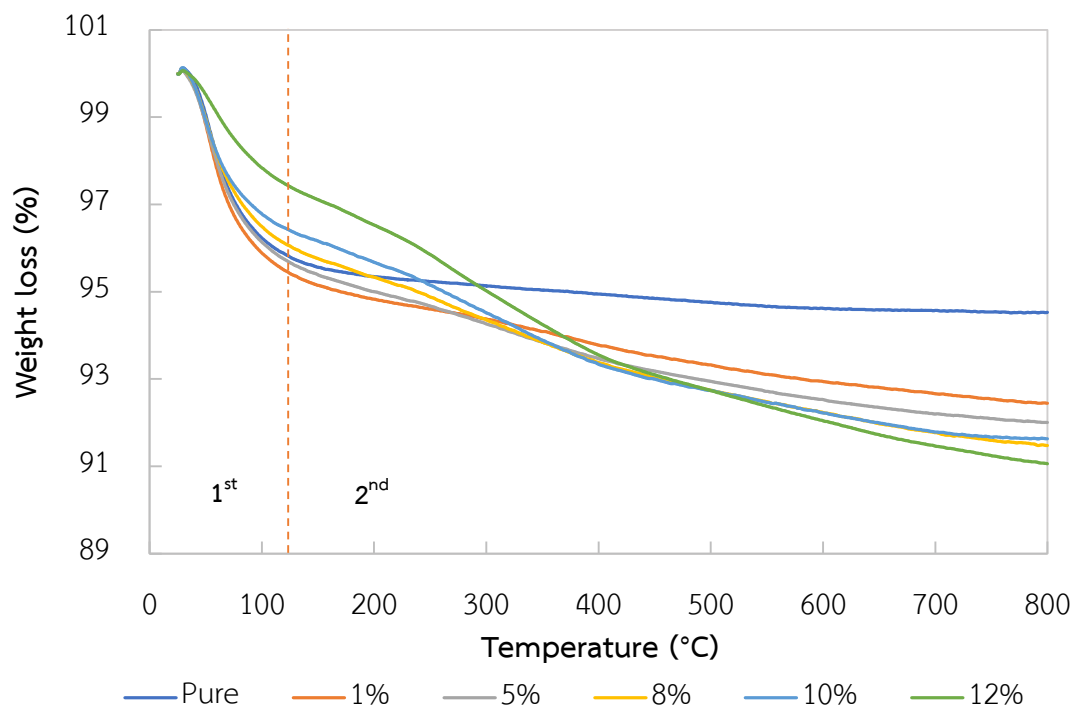


Figure 33 The TGA curve of dried pure silica and modified silica powder with different amount of TESPT.

Table 8 The weight loss in first and second region of dried pure silica and modified silica powder with different amount of TESPT

Weight loss (%)	Pure	1%	5%	8%	10%	12%
1 st region	4.12	4.50	4.25	3.88	3.52	2.51
2 nd region	1.34	3.05	3.74	4.64	4.83	6.42

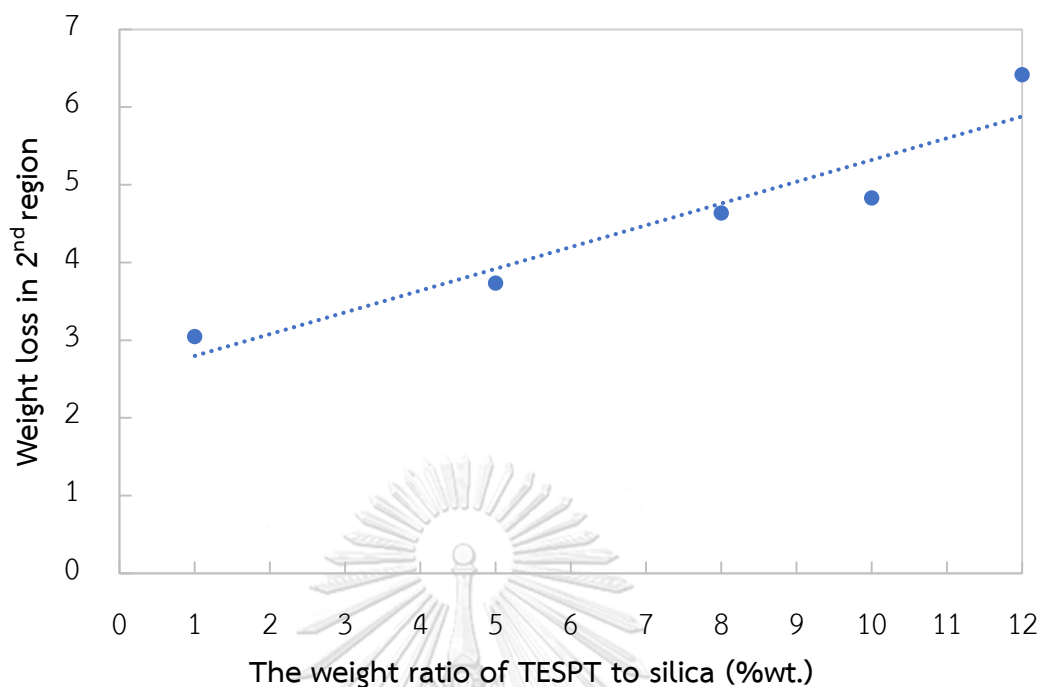


Figure 34 The relationship between the weight loss in the second region and the weight ratio of TESPT to silica.

4.2 The preparation of natural rubber powder

This section is the preparation of natural rubber powder modified with bis(triethoxysilylpropyl)tetrasulfide (TESPT) treated silica by spray drying method, which the effect of TESPT in natural rubber powder and the mass ratio of silica to natural rubber were studied. This experiment was fixed the weight ratio of TESPT to silica at 8% due to this is the best conditions to modified the silica surface from previous step.

4.2.1 The effect of TESPT in natural rubber powder

In this step, we studied the effect of TESPT in natural rubber powder, which the morphology and properties of both before and after dried by spray drying process were characterized via TEM, SEM-EDS, FTIR and TGA analysis. The NRP with TESPT was studied compare to NRP without TESPT, and this experiment studied the NRP with and without TESPT with the mass ratio of silica to natural rubber at 3:1 and 1:1.

4.2.1.1 The morphology of mixture before spray dry

The morphology of natural rubber latex (NRL), NRL particle after mixed with unmodified silica (A) and modified silica colloidal were analyzed by TEM. The NRL particle was fumed with Osmium tetroxide (OsO_4) vapor, which used as staining agent to provide contrast to the TEM image, and OsO_4 can only stain the polyisoprene region via react with double bounds of natural rubber, resulting to the darker color of NRL particle [10]. For another component that not react with OsO_4 can see as lighter color. The TEM image of NRL particle shows in Fig. 35, illustrated that the NRL particle are spherical in shape, and the particle size of was found in the range of 0.1-2.0 μm with good agreement that is in good agreement with the literature [14].

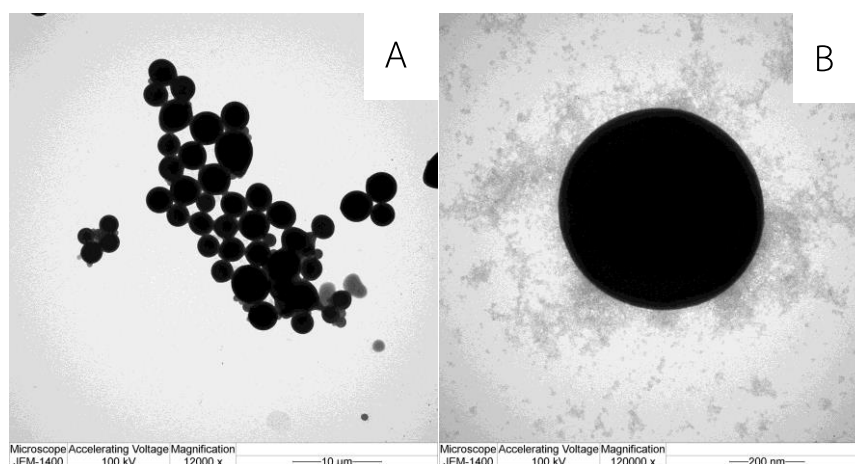


Figure 35 TEM micrographs of NRL particle at A) low magnitude and B) high magnitude

Figure 36 presents TEM micrographs of NRL particle after mixed with (A) modified silica, (B) unmodified silica with the mass ratio of silica to NR at 3:1, (C) modified silica, (D) unmodified silica with the mass ratio of silica to NR at 1:1. From this Fig, resulting that all sample have the same shape and size. No morphological changes were detected in NRL particles before and after mixed with silica. This result indicated that the reaction between silica and NRL via silane coupling agent not occur in this step.

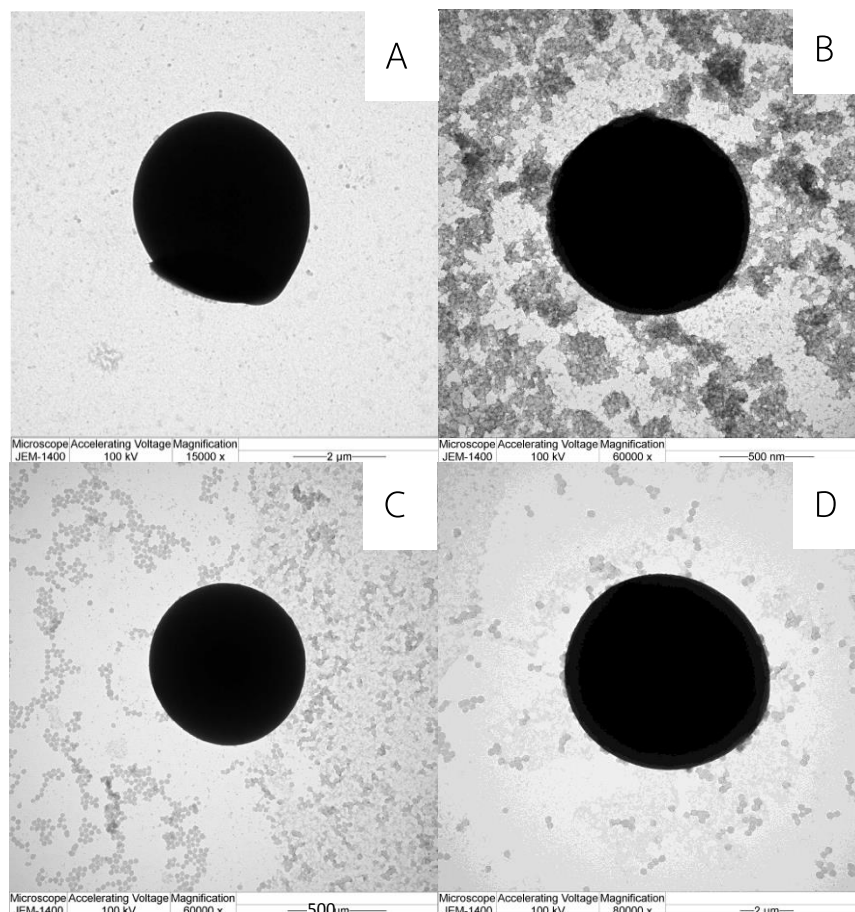
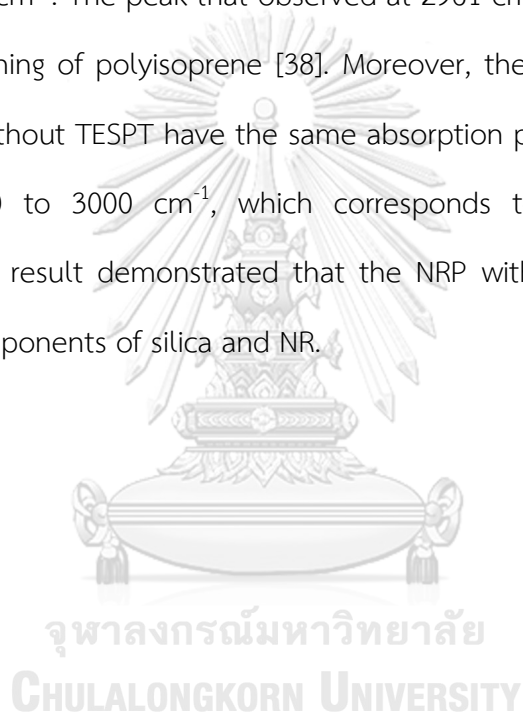


Figure 36 TEM micrographs of NRL particle after mixed with (A) modified silica, (B) unmodified silica with the mass ratio of silica to NR at 3:1, (C) modified silica, (D) unmodified silica with the mass ratio of silica to NR at 1:1.

4.2.1.2 The functional group of NRP

The FTIR spectra of TESPT, NR, pure silica, NRP with TESPT and NRP without TESPT with the mass ratio of silica to NR at 3:1 show in Fig. 37. Both the NRP with TESPT and NRP without TESPT have the same absorption peak at approximately 3400, 1600, 1100, 800 and 480 cm^{-1} , which corresponds to $-\text{OH}$ Stretching, $-\text{OH}$

Bending, -Si-O Asymmetric stretching, -Si-O Symmetric stretching and Si-O-Si Bending respectively. That all absorption peak corresponds to the components of silica. The FTIR spectra of NR found the absorption peak at 835 cm^{-1} corresponding to C=H bending, and the absorption peak at 1375 and 1449 cm^{-1} are characteristics of CH_2 deformation. The absorption peak at 1640 cm^{-1} corresponding to C=C stretching vibration of polyisoprene, and The CH_2 symmetric stretching are found approximately at 2854 and 2927 cm^{-1} . The peak that observed at 2961 cm^{-1} of CH_3 corresponding to asymmetric stretching of polyisoprene [38]. Moreover, the FTIR spectra of NRP with TESPT and NRP without TESPT have the same absorption peak to pristine NR at 1640 and around 2800 to 3000 cm^{-1} , which corresponds to the organic groups of polyisoprene. The result demonstrated that the NRP with TESPT and NRP without consist of the components of silica and NR.



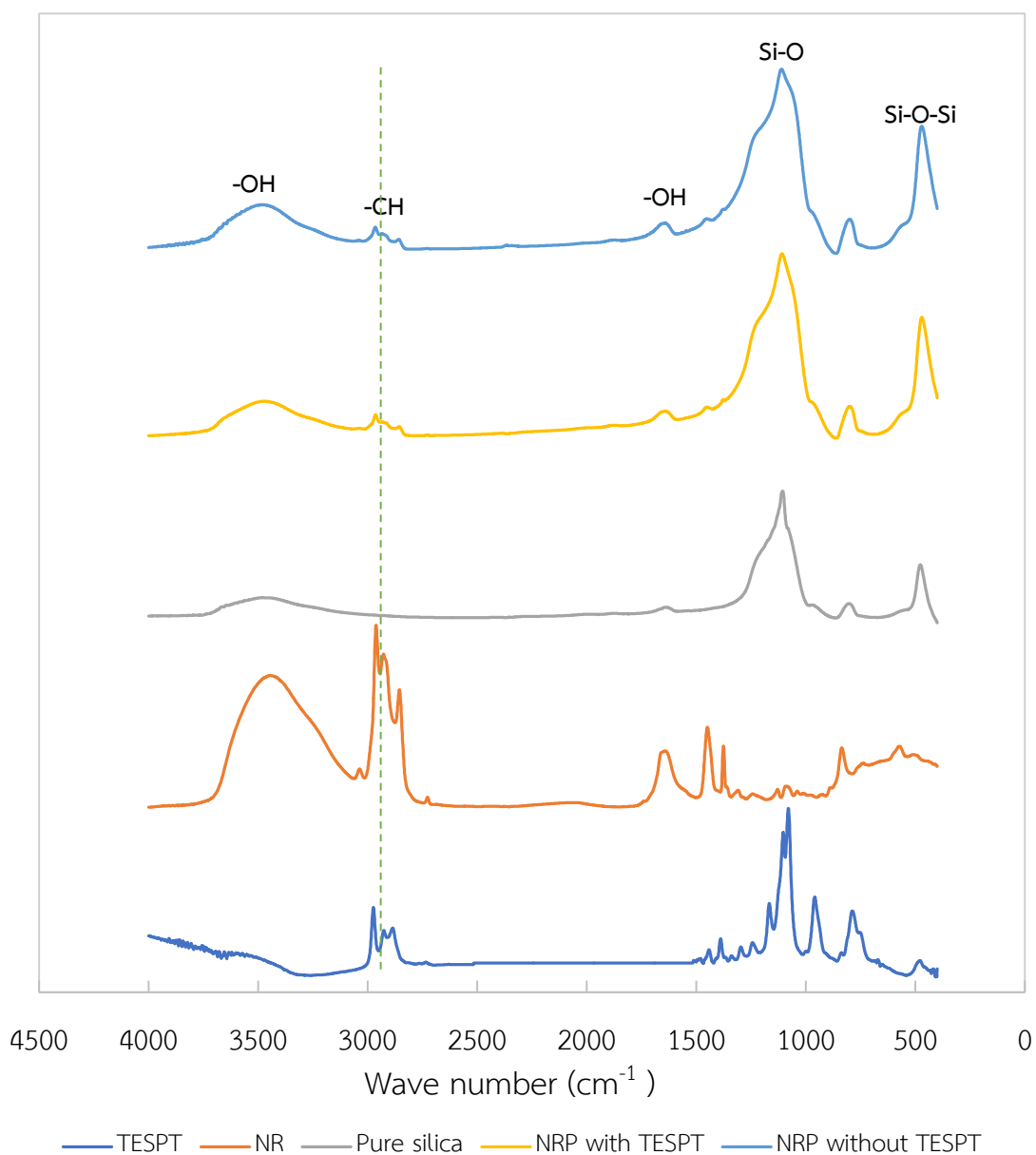


Figure 37 The FTIR spectra of TESPT, NR, pure silica, NRP with TESPT and NRP without TESPT with the mass ratio of silica to NR at 3:1.

4.2.1.3 The morphology of NRP

Figure 38 shows SEM images of A) pure NR and B) modified silica/NR powder obtained by spray drying process. From Figure 38(A), it is obvious that unmodified NR are present in a continuous rubbery sheet state. This is because the NR particles tend to stick and adhere together and partial fusion occurs upon spray drying,

producing agglomerates in sheet form. On contrary, the modified silica/NR powder particles appear to be smooth, spherical with a fairly homogenous distribution, as shown in Figure 38 (B). The SEM analysis suggests that the introduction of silane coating leads to use silica particle to cover or coat the NR particle in preparation of NRP to prevent the adhesion of NR.

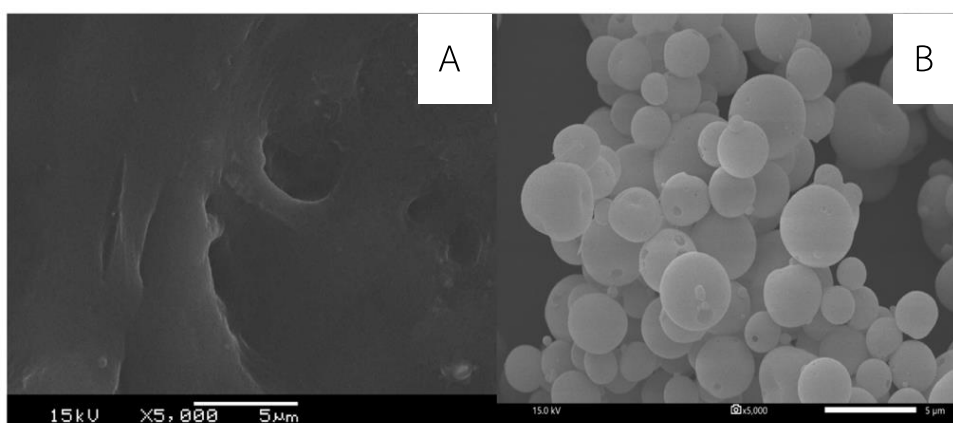


Figure 38 SEM micrographs of A) pristine NR and B) modified silica/NR powder.

The obtained NRP that prepare from spray drying process present in Fig. 39, which observed that the NRP with the mass ratio of silica to NR at 3:1 is a fine powder form, which are less agglomeration than 1:1. Moreover, the NRP with TESPT has a better dispersion of particle than the NRP without TESPT. The morphology of NRP with and without TESPT with the mass ratio of silica to NR at 3:1 and 1:1 show in Fig.40 and 41 respectively. From Fig. 40, indicated that no morphological changes were detected in NRP particle with and without TESPT. On the other hand, the SEM image of NRP 1:1 without TESPT in Fig.41 (B) can observe the residue NR on the surface of microcapsule particle. This result demonstrated that to TESPT can improve the compatibility between silica and NR because TESPT can modified the surface of silica to become hydrophobic silica similar to NR particle, and sulfur atom of TESPT reacts with the unsaturated bonds of the rubber while the spray drying process at high temperature, which the rubber reactive group of silane (tetrasulphane) has strong tendency to form rubber-filler bond [39].

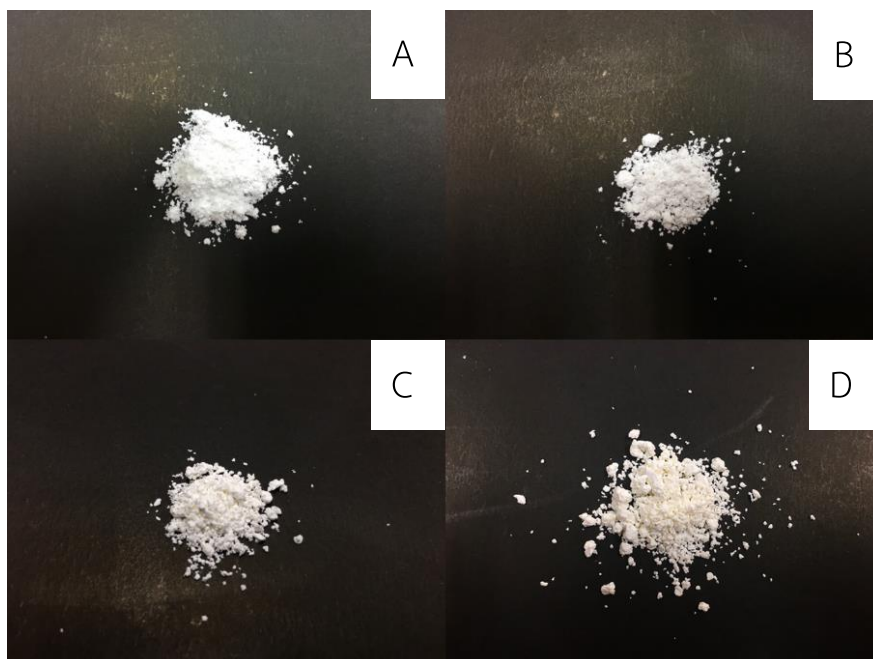


Figure 39 the visible images of A) NRP 3:1 with TESPT, B) NRP 3:1 without TESPT, C) NRP 1:1 with TESPT and D) NRP 1:1 without TESPT.

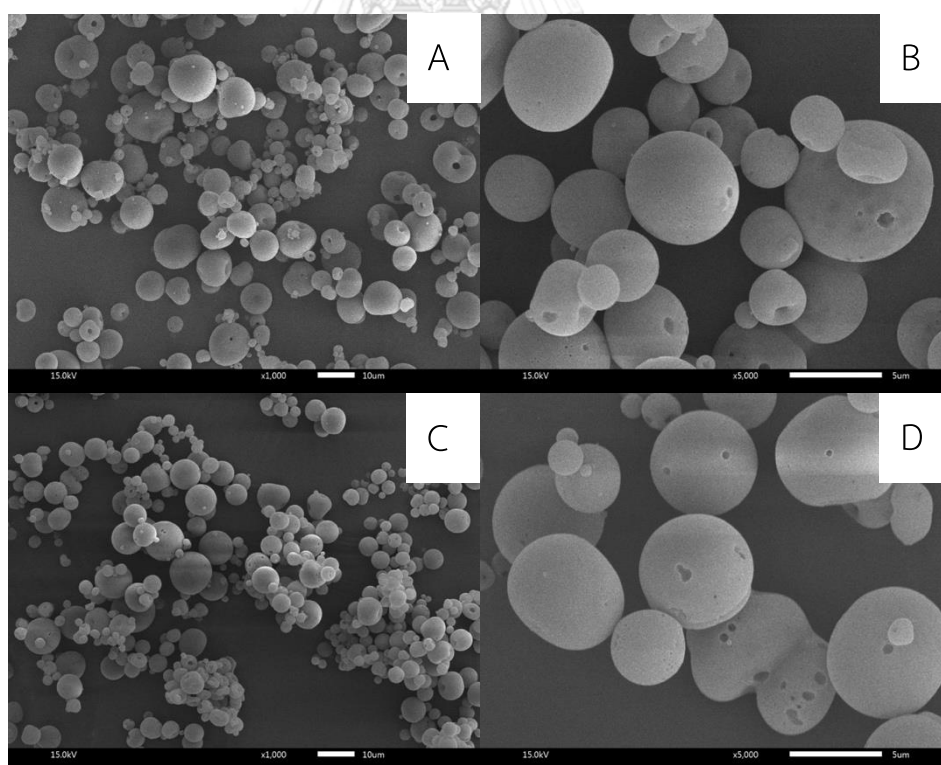


Figure 40 the SEM images of A), B) NRP 3:1 with TESPT and C), D) NRP 3:1 without TESPT.

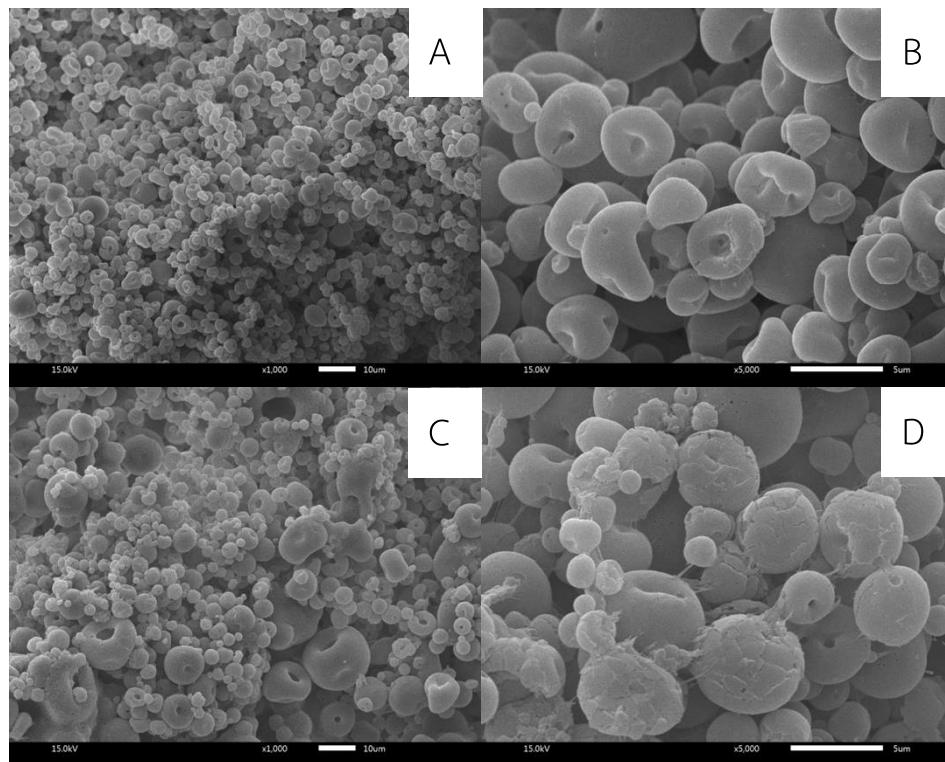


Figure 41 the SEM images of A), B) NRP 1:1 with TESPT and C), D) NRP 1:1 without TESPT.

The morphology of microcapsule NRP was characterized by SEM analysis. Figure 42 shows the cross-section of microcapsule that was molded with epoxy resin and cut the cross-section using a razor as opposed to a microtome. The morphology of microcapsule NRP has a dense particle that is spherical in shape and observed that the NR located inside the particle illustrated in Fig 42 (A) indicating to NR was encapsulated in silica particle. Furthermore, the morphology of microcapsule in Fig. 43 shows a hollow particle that the NR may be located at the edge of particle. The hypothesis of the locating of NR will confirm by EDS analysis in the next topic. From the results in Fig. 42 and 43, indicated that the microcapsule prepared by spray drying method produced the various particles morphologies, which are dense and hollow particles. This result is according to the report of Nandiyanto, A.B.D. and K. Okuyama, which reported that the spray drying method can produce various particle morphologies due to the several parameters, which are the mass and heat transfer of the droplet. For the dense spherical particle, this type is typically created

using the spray method, which can be produced from colloidal solution. The heat transfer from the surface of droplet to the deepest point inside the droplet and the time for drying can produced hollow particle. At high temperature, the solution in the droplet was evaporate to vapor state resulting to high pressure and then forming the hole in the particle [34].The mechanism of the many types of particle formation is shown in Fig. 44.

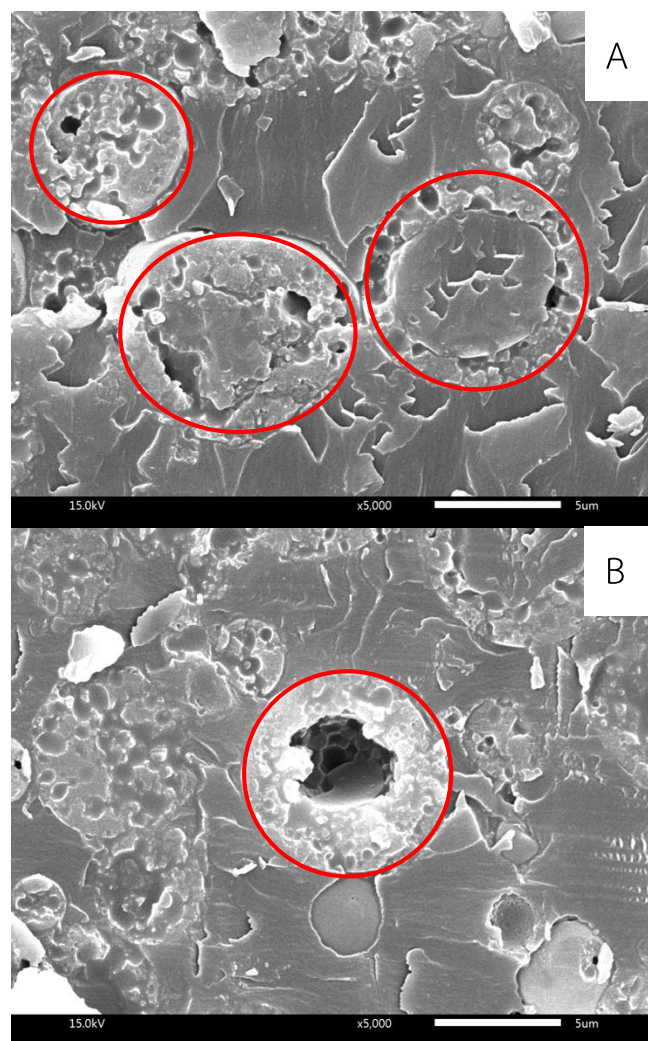


Figure 42 the SEM image of cross-section microcapsule particle of NRP 1:1 with TESPT A) dense and B) hollow particle.

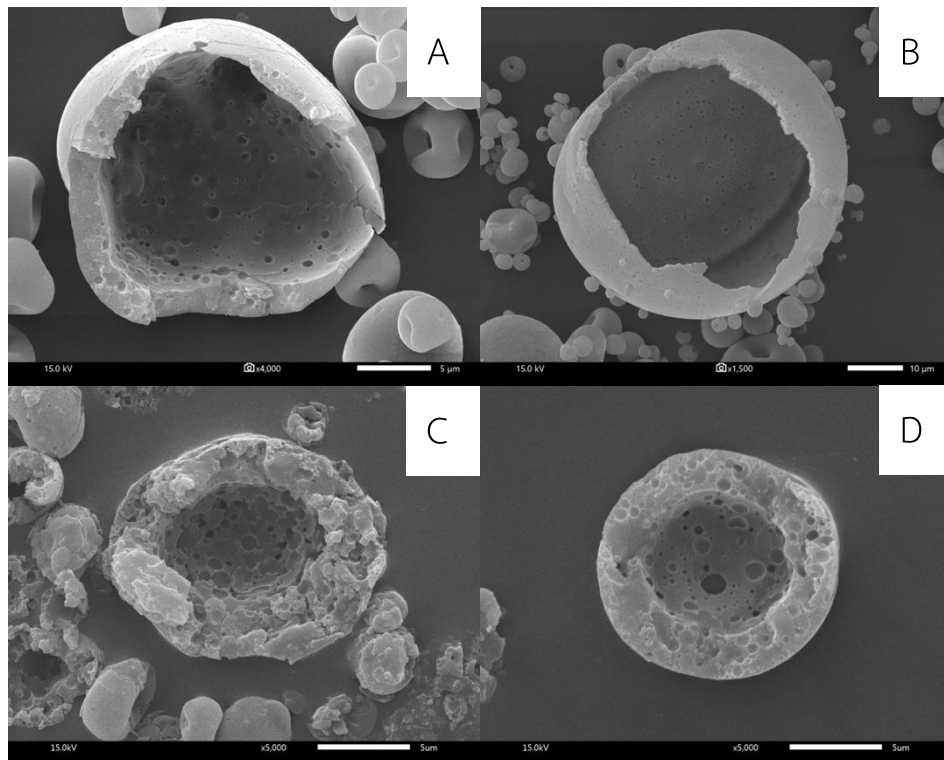


Figure 43 the SEM images of hollow microcapsule particle of A) NRP 3:1 with TESPT, B) NRP 3:1 without TESPT, C) NRP 1:1 with TESPT and D) NRP 1:1 without TESPT.

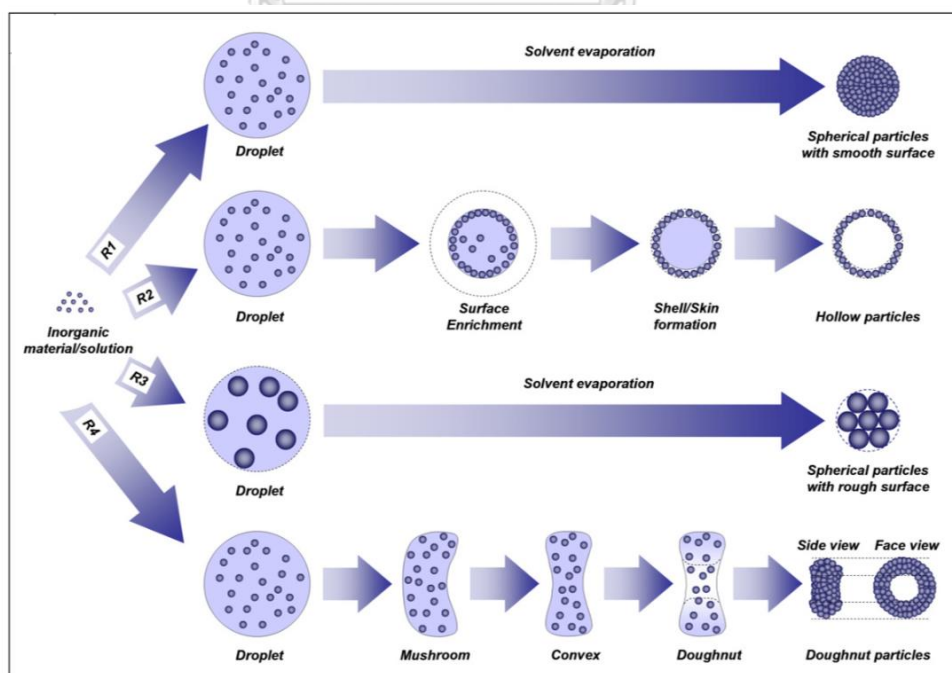


Figure 44 The mechanism of the many types of particle formation[34].

Moreover, the morphology of NRP at the surface of particle were studied using FE-SEM shows in Fig 45. The results presented that the silica particle after spray dry was in spherical shape and the average particle size was approximately 10 nm similar to the morphology of modified silica colloidal before spray dry. No morphological changes were detected in silica particles before and after spray dry. The result indicated that the silica particle is agglomerated to form silica shell to encapsulate the NR particle during spray drying process.

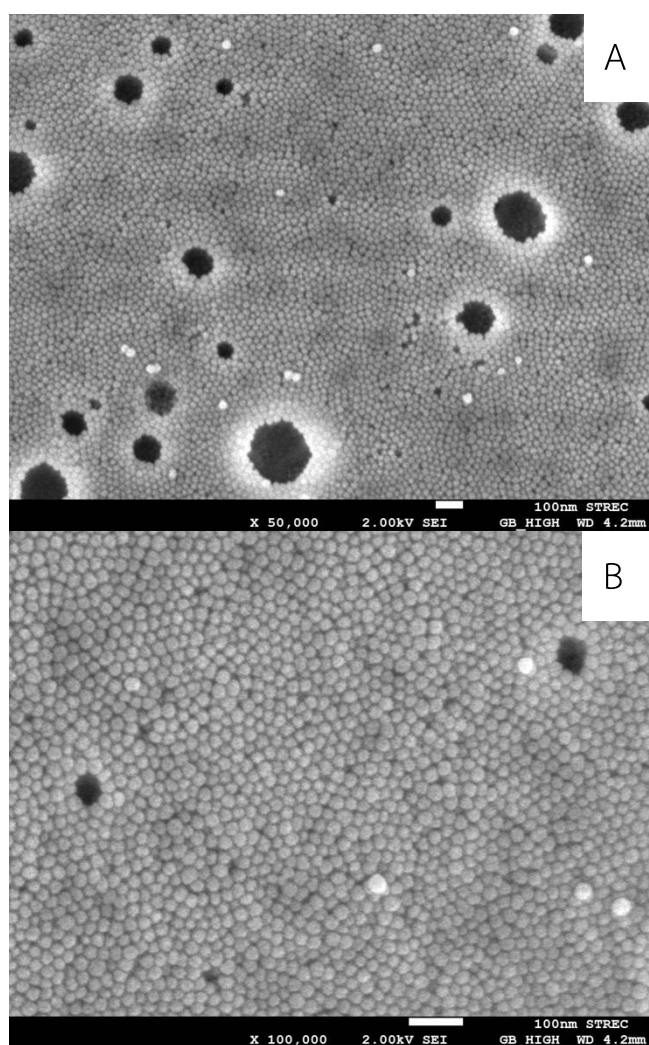


Figure 45 the FE-SEM images at the surface of microcapsule particle of NRP 3:1 with TESPT A) low magnitude and B) high magnitude.

4.2.1.4 The elemental composition of NRP

The elemental mapping was performed using EDS analysis and Fig. 46 shows the elemental distribution maps of modified silica/NR powder. The SEM results illustrated that the composite powders are spherical in shape with diameter of less than 5 μm show in Fig.46 (A) & (B). The EDS maps illustrated that the NR powders are uniformly coated with silica layer, as evidenced by the presence of high density of silicon (orange) on the surface of powder particles. shown in Fig. 46 (D). From Fig. 46 (C) and (E), the results also showed significant presence of oxygen (green) and also small quantities of residue carbon (red). Table 9 provides a summary of the elemental composition of modified silica/NR powder.

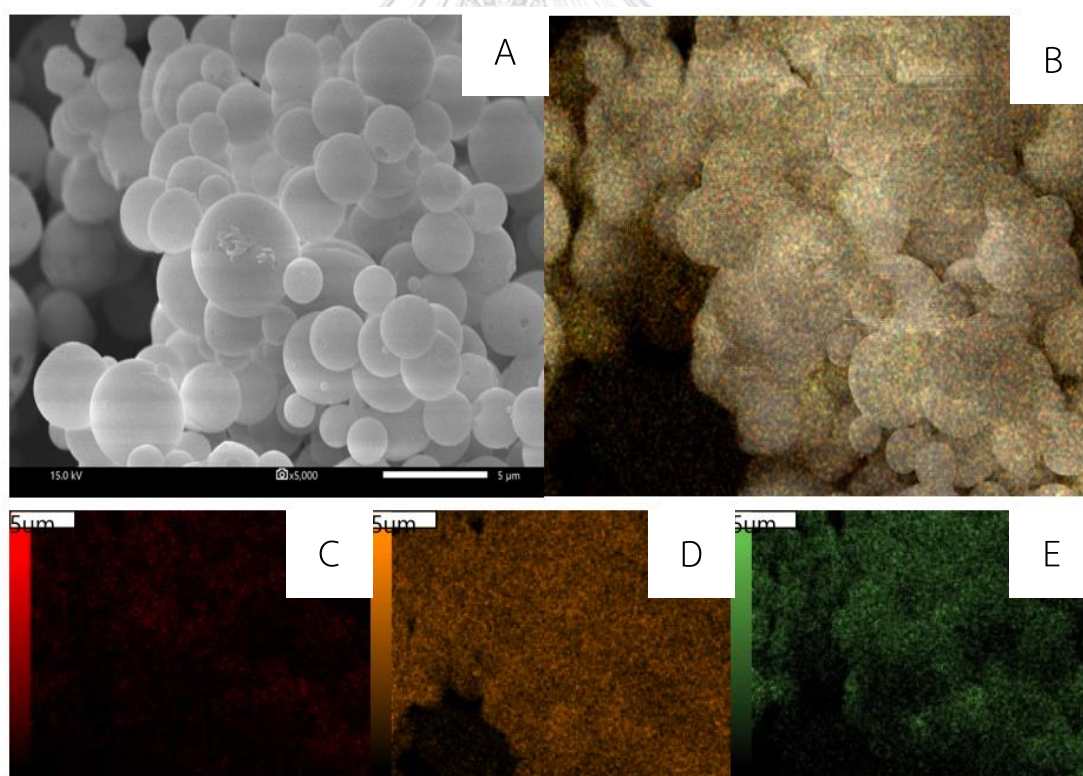


Figure 46 A) and B) SEM images of modified silica/NR powder and EDS mapping of C) carbon D) silicon E) oxygen.

Table 9 Elemental composition of modified silica/NR powder obtained by EDS.

Element	Mass%	Atom%
C	24.62±0.08	34.85±0.11
O	42.72±0.10	45.38±0.11
Si	32.66±0.09	19.77±0.05
Total	100.01	100.00

The elemental composition on surface of NRP

The elemental composition on surface of pure silica and NRP particle were analyzed by EDS analysis. Figure 47 shows the sample position for EDS analysis on the particle surface. The results of elemental composition analysis by EDS are listed in Table 10. The amount of carbon, oxygen and silicon of NRP 3:1 with TESPT and NRP3:1 without TESPT were similar to pure silica, indicating on the surface particle are only silica. The mass ratio of C/S of NRP 3:1 with TESPT and NRP3:1 less than 1, indicating to the NR was completely encapsulated by silica [40]. For the mass ratio of silica to NR at 1:1, The mass ratio of C/S more than 1, indicating to have less residue NR on the surface of particle. The mass ratio of C/S was increase as the sample without TESPT, indicating to TESPT can improve the compatibility between silica and NR resulting to more encapsulation efficiency.

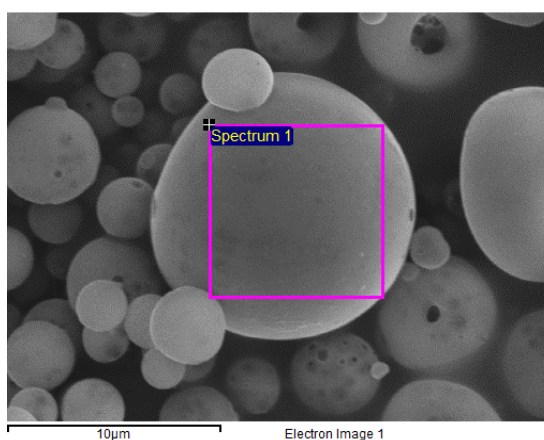
**Figure 47** the sample position for EDS analysis on the particle surface

Table 10 The elemental composition on surface of pure silica and NRP

Sample	The elemental composition			C/Si ratio
	C	O	Si	
Pure silica	22.52	52.46	25.02	0.90
NRP 3:1 with TESPT	20.88	50.22	28.9	0.72
NRP3:1 without TESPT	22.95	47.73	29.32	0.78
NRP1:1 with TESPT	31.87	44.48	23.65	1.35
NRP1:1 without TESPT	41.06	34.85	24.09	1.70

The elemental composition inside the particle of NRP

The elemental composition inside NRP particle were determined by EDS analysis. Figure 48 shows the sample position for EDS inside the particle. The results of elemental composition analysis by EDS are listed in Table 11. The amount of carbon inside the particle more than the surface of particle for all sample, which is confirm that the NR particle was encapsulated in silica particle. For NRP with TESPT, showing the amount of carbon more than without TESPT, indicating to TESPT can improve encapsulation efficiency.

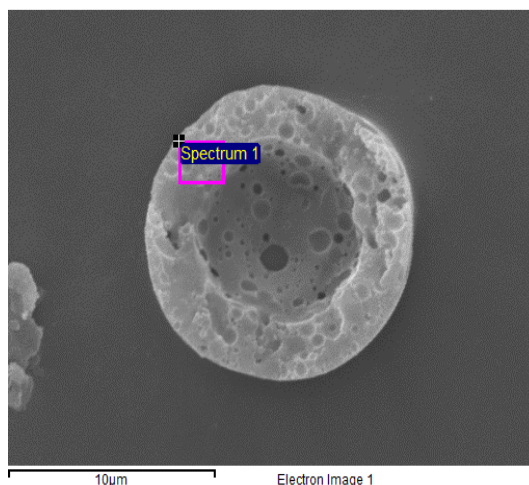


Figure 48 the sample position for EDS analysis inside the particle

Table 11 The elemental composition inside the particle of NRP

Sample	The elemental composition			C/Si
	C	O	Si	
NRP 3:1 with TESPT	41.59	36.88	21.53	1.93
NRP3:1 without TESPT	38.15	45.45	16.41	2.32
NRP1:1 with TESPT	53.10	33.71	13.19	4.02
NRP1:1 without TESPT	45.22	33.11	21.67	1.37

4.2.1.5 The particle size and size distribution of NRP

The spray dried NRP with and without TESPT were measured the mean particle size and size distribution by laser diffraction analyzer. Table 12 shows the mean diameter of NRP with and without TESPT, the result indicating to the smaller particle size as NRP prepared with TESPT. Moreover, the size distribution of NRP without TESPT are broader than NRP with TESPT and the peak shifted to the bigger

size region that shows in Fig.49, indicating to TESPT can prevent the agglomeration of particle due to better encapsulation efficiency.

Table 12 The Mean Diameter of NRP with and without TESPT.

Sample	Mean diameter (μm)
NRP 1:1 with TESPT	4.16
NRP 1:1 without TESPT	4.95

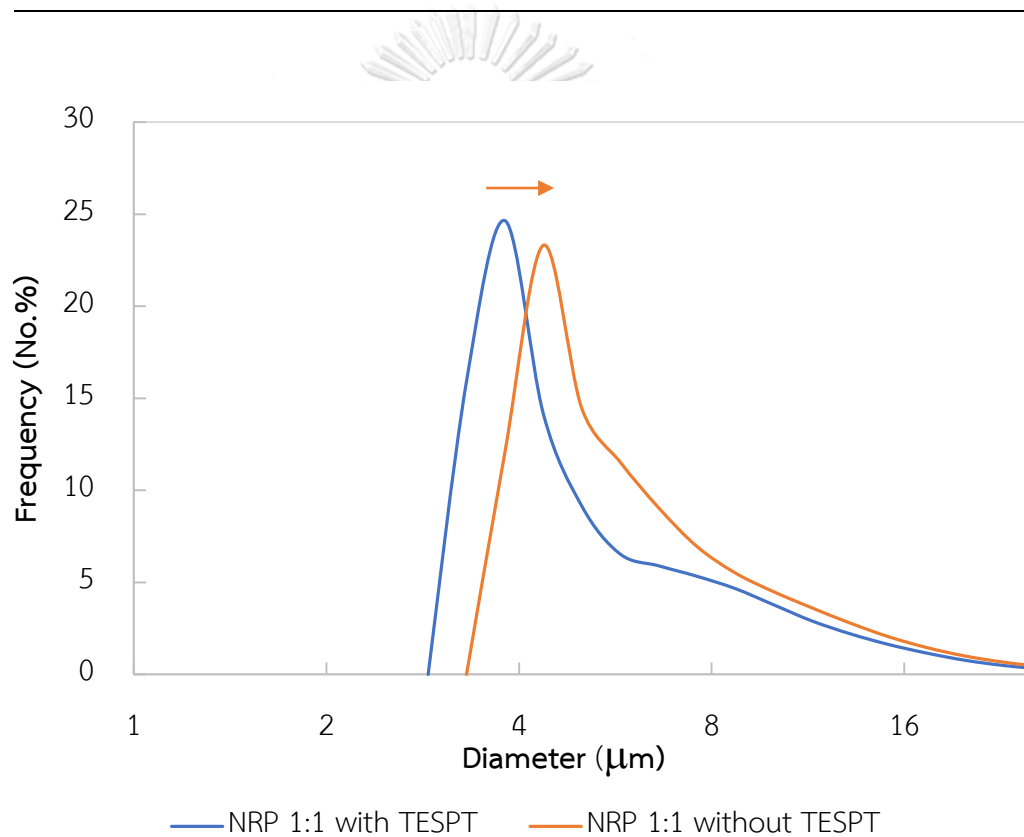


Figure 49 The size distribution curve of NRP with and without TESPT

4.2.1.6 The thermal stability of NRP

Fig.50 represents the TGA curves of samples. As can be seen from Fig. 50, the thermal stability of NR is significantly improved with the incorporation of the modified silica in comparison with that of pristine NR. The major weight loss associated with NR starts around 250°C, which is in good agreement with the literature [41]. However, TESPT exhibits considerable mass loss around 230°C, possibly due to the massive vaporization of water and degradation of silanols. Given its high onset decomposition temperature, there is only a small loss of moisture in pure silica and no degradation is observed.

The mass percentage composition of the modified silica/NR powders determined by TGA analysis is listed in Table 13. The results indicated that the spray dried powder contains 77.84 % modified silica and 22.1% NR, which is in good consistence with the feed composition before spray drying.

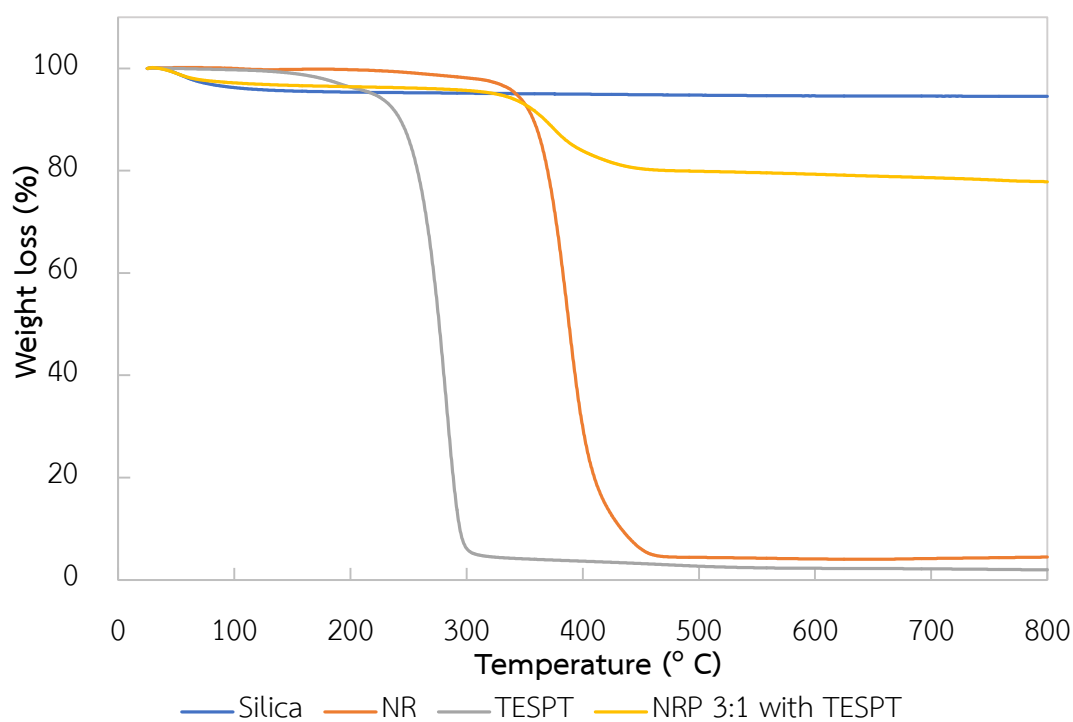


Figure 50 the TGA curves of silica, NR, TESPT and NRP.

Table 13 The composition of NRP 3:1 with TESPT

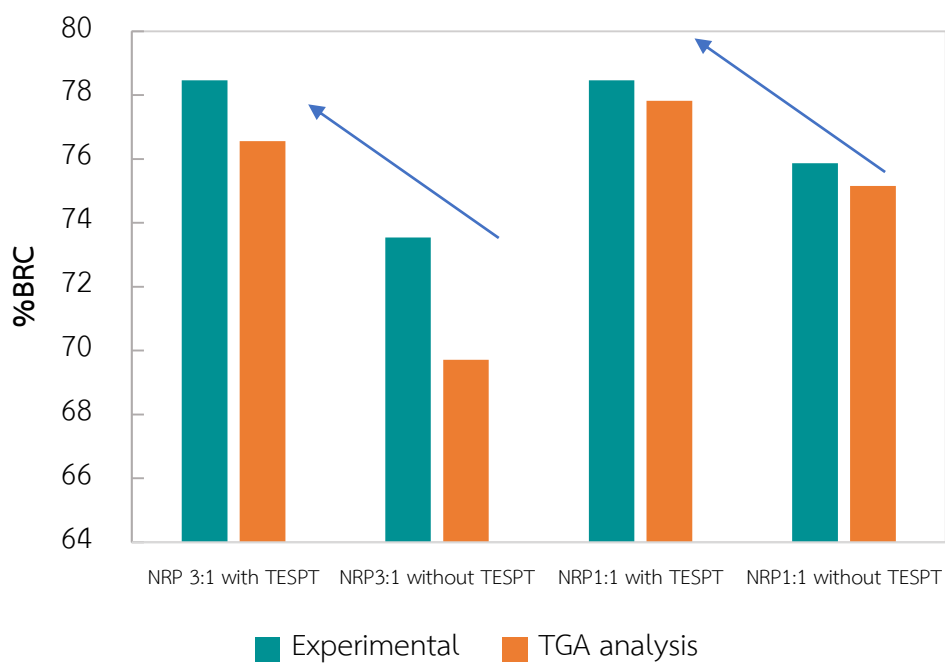
Composition	Solid mass%	
	Theoretical	TGA analysis
Modified silica	75	77.84
NR	25	22.16
Total	100	100

4.2.1.7 The bound rubber content of NRP

The bound rubber content (BRC) of all sample were measured by Immersed the sample in toluene for 7 days and the sample were taken out from the solvent and dried before measured the remain NR. The measurement of remain NR was found by 2 ways: 1) experimental (weighing) and 2) TGA analysis, which to confirm the result. From Fig. 51 show a comparison of BRC between NRP with and without TESPT that show the NRP with TESPT have the higher bound rubber content, which presents stronger interactions between silica and NR [42]. The increasing of BRC resulting to better encapsulation efficiency of NRP, which according to the results from previous analysis. Moreover, it found that the BRC from experimental and TGA analysis are similar. The value of BRC of all sample was listed in Table 14.

Table 14 Bound rubber content of NRP with and without TESPT

Sample	Bound rubber content	
	Experimental	TGA analysis
NRP 3:1 with TESPT	78.46	76.56
NRP3:1 without TESPT	73.54	69.71
NRP1:1 with TESPT	78.46	77.82
NRP1:1 without TESPT	75.87	75.16
Pure Nr	61.96	N/A

**Figure 51** Bound rubber content of NRP with and without TESPT

4.2.2 The effect of the mass ratio of silica to natural rubber

In this step, we studied the effect the mass ratio of silica to natural rubber, which the morphology and properties of both before and after dried by spray drying process were characterized via TEM, SEM-EDS, FTIR and TGA analysis. This section was studied the effect the mass ratio of silica to natural rubber at 3:1, 2:1, 1:1 and 0.5:1.

4.2.2.1 The morphology of mixture before spray dry

Figure 52 presents TEM micrographs of NRL particle after mixed modified silica with the mass ratio of silica to natural rubber at 3:1 (A), 2:1 (B), 1:1 (C) and 0.5:1 (D). All sample have the same shape and size. No morphological changes were detected with different mass ratio of silica to natural rubber. This is because modified silica and NR particle gather in spray drying step to form particle self-assembly, resulting to obtain encapsulate particle [34].

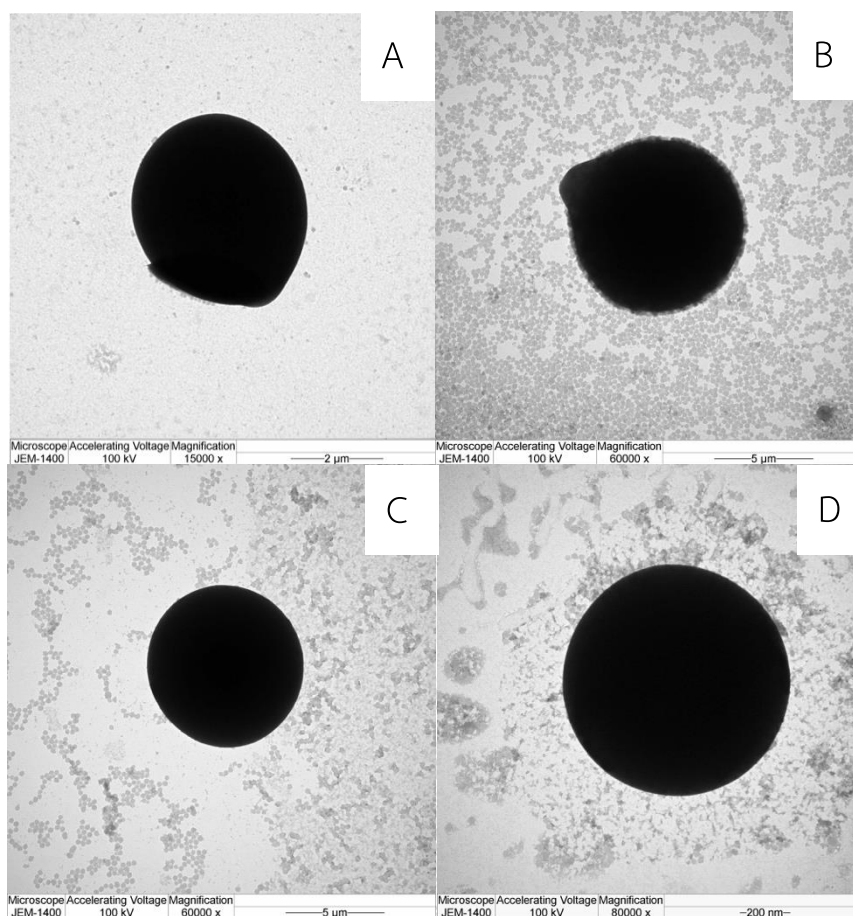


Figure 52 TEM micrographs of natural rubber latex particle after mixed modified silica with the mass ratio of silica to natural rubber at 3:1(A), 2:1(B), 1:1(C) and 0.5:1(D).

4.2.2.2 The functional group of NRP

The FTIR spectra of NRP prepared at different mass ratio of silica to NR show in Fig. 53. All sample have the absorption peak at approximately 1600 cm^{-1} , which corresponds to -Si-O Asymmetric stretching of silica. Nevertheless, The FTIR spectra of NRP 0.5:1 not observe that weak, which indicated the silica/NR mass ratio at 0.5/1 can't provide the NR encapsulated in silica particle due to the amount of silica not enough to cover the NR particle.

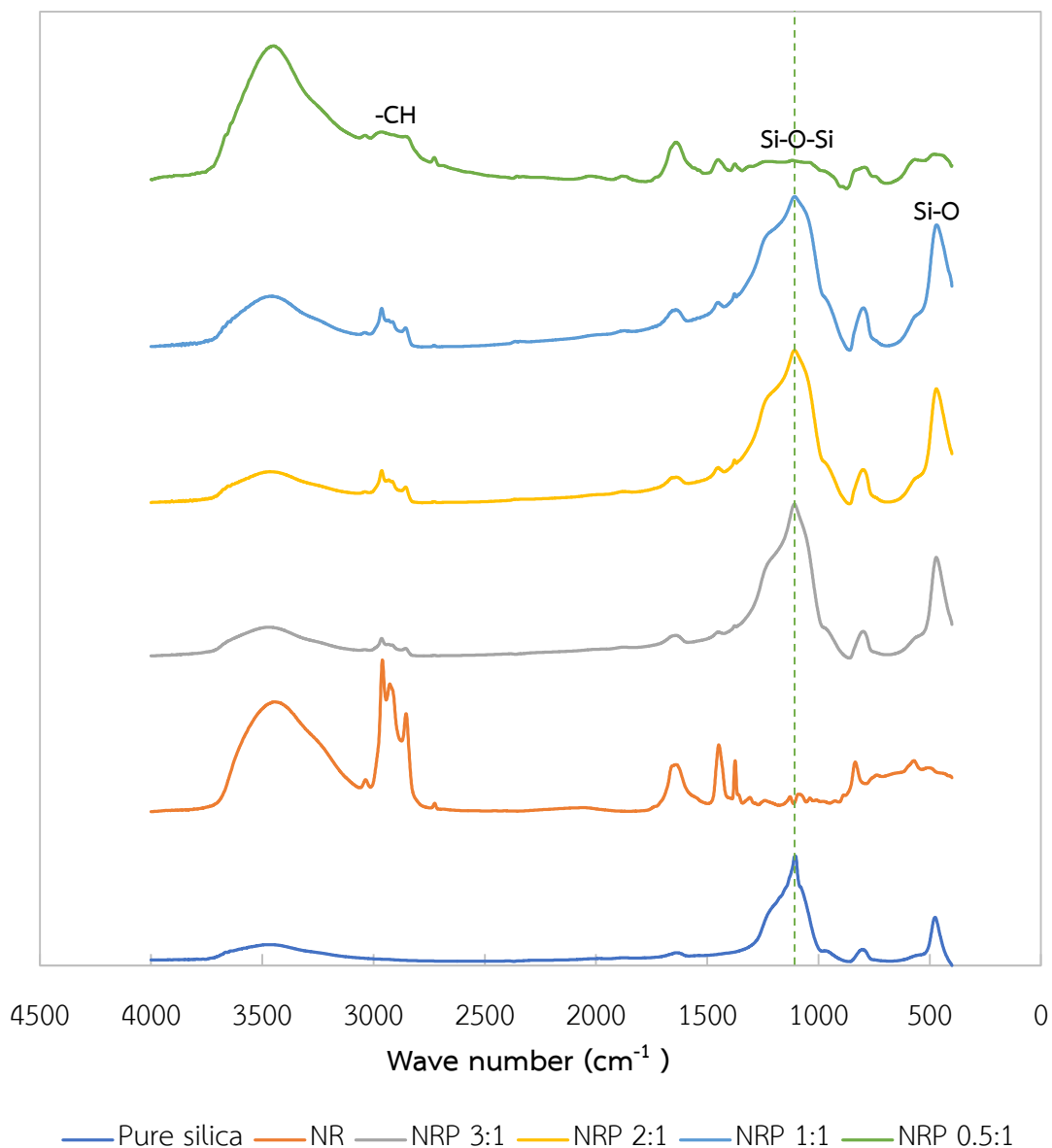


Figure 53 The FTIR spectra of NRP prepared at different mass ratio of silica to NR.

4.2.1.3 The morphology of NRP

The obtained NRP that prepared from spray drying process at different mass ratio of silica to NR present in Fig. 54, which observed that the NRP with the mass ratio of silica to NR at 3:1 to 1:1 are in powder form. On the other hand, the NRP prepared at the mass ratio of silica to NR at 0.5:1 (Fig. 54D) not provided powder

form, which has a severe agglomeration resulting to formation of agglomerated cluster.

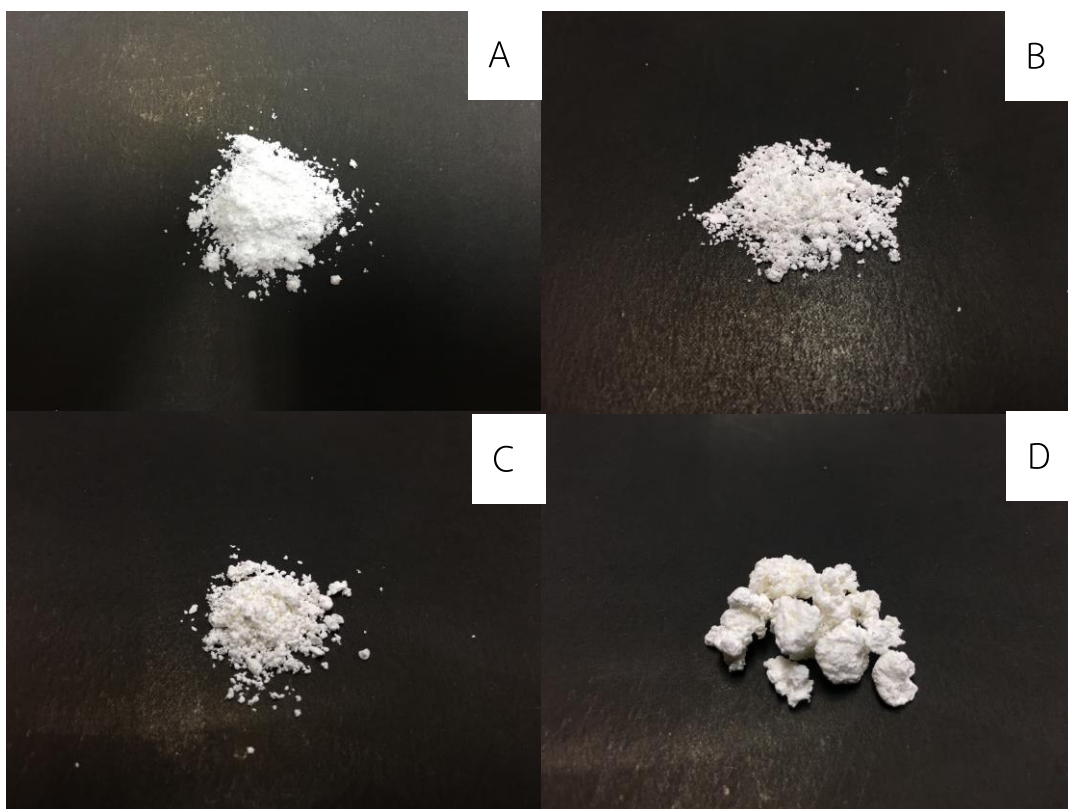


Figure 54 The image of NRP with the mass ratio of silica to natural rubber at 3:1(A), 2:1(B), 1:1(C) and 0.5:1(D).

The morphology of NRP prepared from spray drying process at different mass ratio of silica to NR were determined by SEM show in Fig. 55 and 56 with low and high magnitude respectively. The particle shape of all samples were almost as spherical shape. Although, when decreasing the mass ratio of silica the large agglomeration of particle could observed. For NRP with mass ratio of silica to NR at 3:1 and 2:1, most of particle presented as individual particle. The NRP at mass ratio of silica to NR 1:1 can produced the spherical particle, but the NRP at mass ratio of silica to NR 1:1 cannot formed the spherical particle, which is observed the silica

particle was covered by NR because the amount of silica not enough to encapsulated the NR particle.

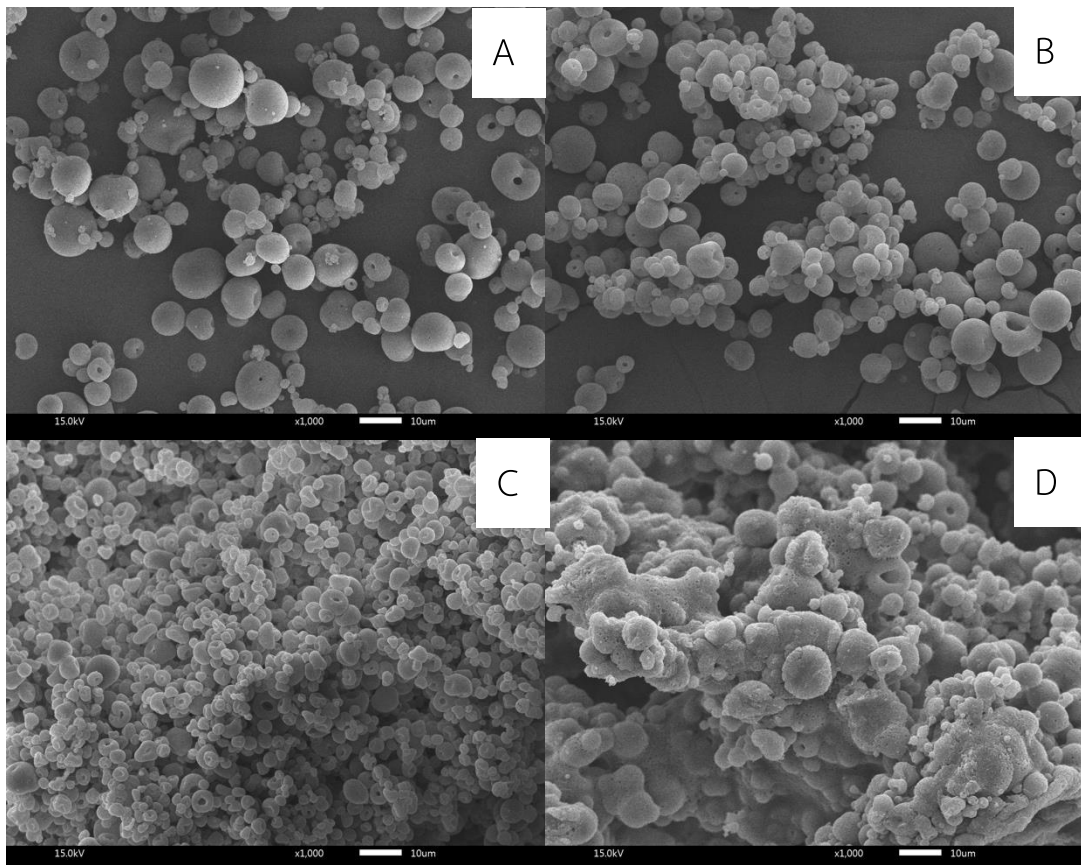


Figure 55 SEM micrographs of NRP with the mass ratio of silica:natural rubber at 3:1(A), 2:1(B), 1:1(C) and 0.5:1(D).

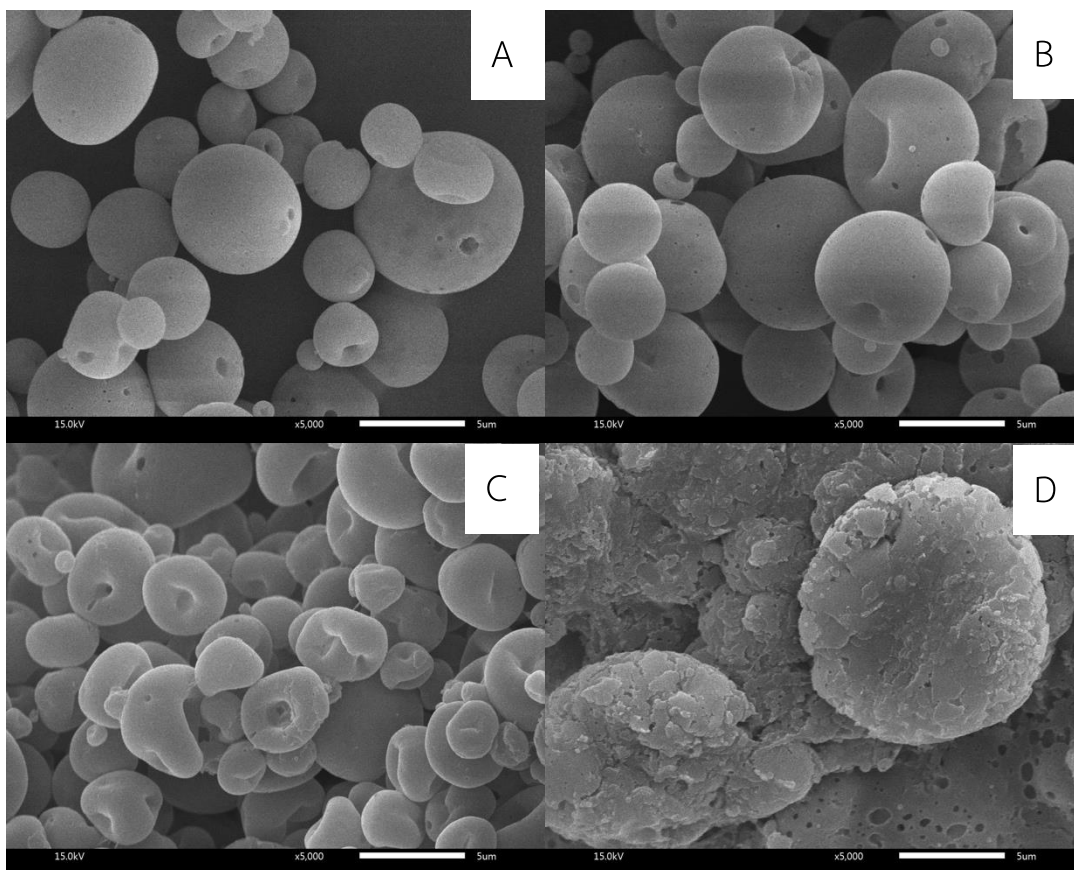


Figure 56 SEM micrographs of NRP with the mass ratio of silica:natural rubber at 3:1(A), 2:1(B), 1:1(C) and 0.5:1(D).

4.2.1.4 The elemental composition of NRP

The elemental composition on surface of NRP particle prepared at different mass ratio of silica to NR were analyzed by EDS analysis. The results of elemental composition analysis by EDS are listed in Table 15. The amount of carbon, oxygen and silicon of NRP 3:1 was similar to NRP 2:1, indicating on the surface of particle are only silica. The mass ratio of C/S of NRP 3:1 and 2:1 less than 1, indicating to the NR was completely encapsulated by silica. For NRP 1:1 and 0.5:1, The mass ratio of C/S more than 1, indicating to the particle has the residue NR on the surface. For the result, implying that at the mass ratio of silica to NR 3:1 to 2:1 the most of NR particle are sufficiently encapsulate in silica particle.

Table 15 the elemental composition on surface of NRP particle

Sample	The elemental composition			C/Si
	C	O	Si	
NRP 3:1	20.88	50.22	28.90	0.72
NRP 2:1	22.00	45.08	32.92	0.67
NRP 1:1	31.87	44.48	23.65	1.35
NRP 0.5:1	52.12	29.6	18.29	2.85

The elemental composition inside NRP particle prepared at different mass ratio of silica to NR were determined by EDS analysis. The results of elemental composition analysis by EDS are listed in Table 15. The amount of carbon inside the particle more than the surface of particle for all sample, which is confirm that the NR particle was encapsulated in silica particle. Moreover, the amount of carbon inside the particle increase when increasing the amount of NR in the sample, which resulting to increasing NR were encapsulated in silica particle. The mass ratio of C/S of NRP increasing when increasing amount of NR in sample, indicating to the amount of NR particle encapsulated by silica were increased.

Table 16 the elemental composition inside the NRP particle

Sample	The elemental composition			C/Si
	C	O	Si	
NRP 3:1	41.59	36.88	21.53	1.93
NRP 2:1	46.86	37.14	16.00	2.93
NRP 1:1	53.10	33.71	13.19	4.02
NRP 0.5:1		N/A		

4.2.1.5 The particle size and size distribution of NRP

The spray dried NRP at different mass ratio of silica to NR were measured the mean particle size and size distribution by laser diffraction analyzer. Table 16 shows the mean diameter of NRP with different mass ratio of silica to NR at 3:1, 2:1 and 1:1 are 2.5, 2.16 and 4.16 μm respectively. The size distribution curve of NRP 1:1 is broader than the others and the peak shifted to the bigger size region that shows in Fig.57. This result because of the residue NR of the surface of particle lead to the agglomeration.

Table 17 The Mean Diameter of NRP prepared at different mass ratio of silica to NR

Ratio of silica:NR	Mean diameter(μm)
NRP 3:1	2.50
NRP 2:1	2.16
NRP 1:1	4.16
NRP 0.5:1	N/A

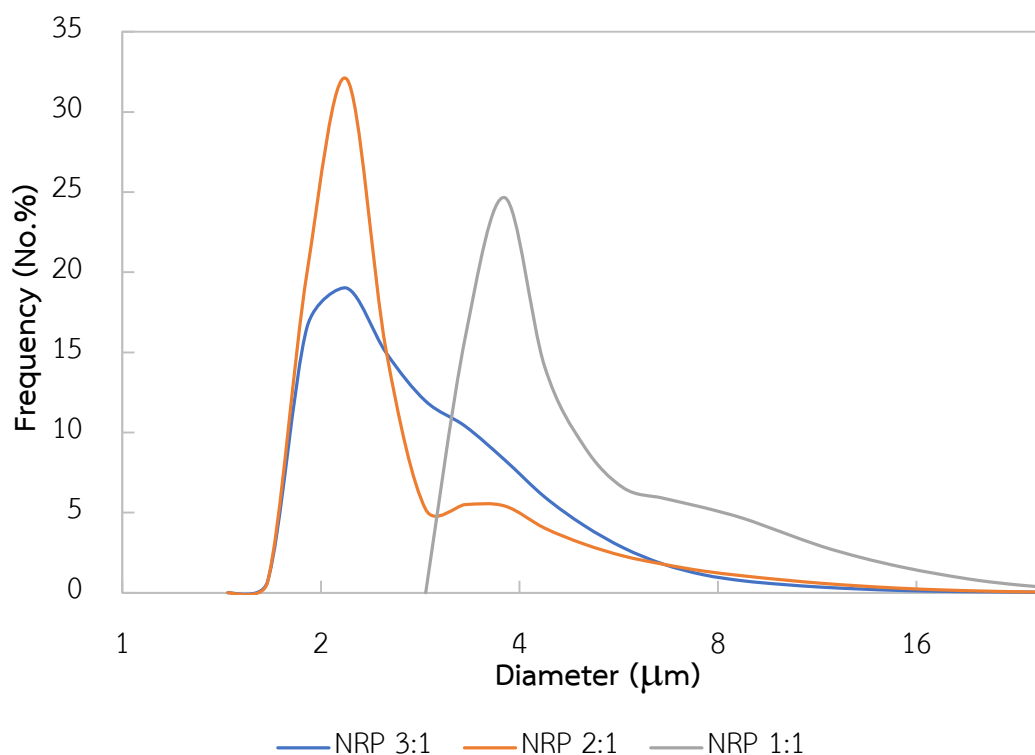
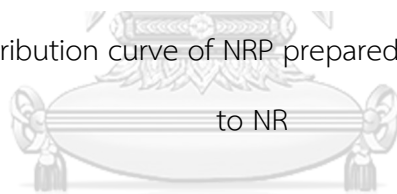


Figure 57 The size distribution curve of NRP prepared at different mass ratio of silica



4.2.1.6 The thermal stability of NRP

CHULALONGKORN UNIVERSITY

The TGA curves of NRP prepared at different mass ratio of silica to NR present in Fig. 58. As can be seen from Fig. 58, the thermal stability of NR is significantly improved with increasing mass ratio of silica to NR present. The major weight loss associated with NR starts around 250°C, which is in good agreement with the literature [41]. The percent weight loss in the temperature region at 120-800°C, corresponding to the percent weight of NR in the sample, which listed in table 17. The results can confirm the composition of NR and silica in the NRP prepared by spray drying process.

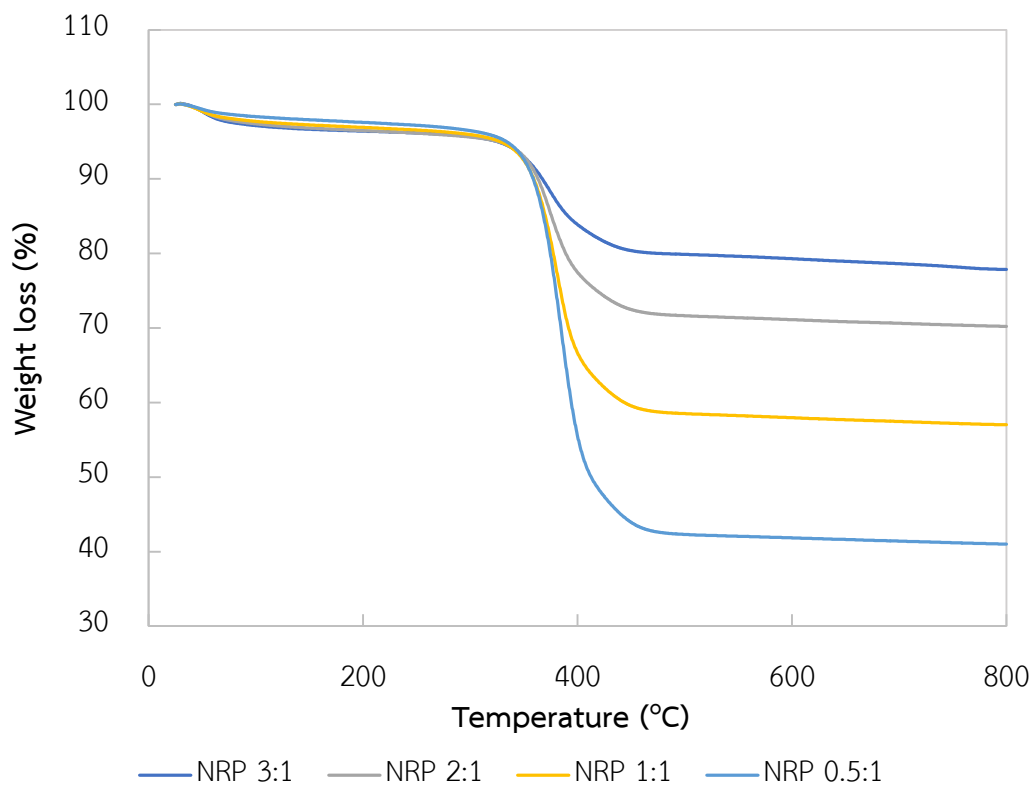


Figure 58 The TGA curve of NRP prepared at different mass ratio of silica to NR

Table 18 The Compositions and weight loss of NRP prepared at different mass ratio of silica to NR

Sample	Compositions (wt%)		Weight loss (wt%) At 120-800°C
	m-silica	NR	
3:1	75.00	25.00	22.16
2:1	66.67	33.33	29.79
1:1	50.00	50.00	42.99
0.5:1	33.33	66.67	59.00

CHAPTER 5

CONCLUSION

5.1 Conclusion

In this work, we have successfully produced the NRP via spray drying process. Our FTIR analysis confirmed that the silane coupling agent, TESPT were successfully grafted on the surface of silica particles. FTIR results shown that the hydrolysed silanol groups from TESPT were chemically bonded to the hydroxyl groups of silica particles. It was found that modified silica powders prepared at 8% of TESPT exhibited the highest grafting efficiencies.

The SEM study revealed that the NRP particles were smooth and spherical in morphology. Our findings confirmed that the NR particle was encapsulated within silica shell and indicating that TESPT can improve the compatibility between NR and silica, resulting in the better encapsulation efficiency as evidenced by its higher bound rubber content. Moreover, the results shown that the mass ratio of silica to NR ranging from 3:1 to 2:1 most of NR was sufficiency encapsulated in silica particle.

5.2 Recommendation

5.2.1 Change the type of silane coupling agent to compare the effect of silane to NRP.

5.2.2 Varying the size of silica to evaluate the encapsulation efficiency to find the most suitable size of silica to encapsulate the NR particle.

5.2.1 Investigate the optimum mass ratio of silica to NR between 2:1 to 1:1 to find the most suitable ratio that use the least amount of silica to was sufficiency NR particle.

REFERENCES

1. Rubber information 2020; Available from: <http://www.industrialrubbergoods.com/natural-rubber.html>.
2. A Z Abidin, N.R.W., I Rahardi, D A Tirahayu, *Natural Rubber Powder Production from Latex*, in *1st International Symposium of Indonesian Chemical Engineering (ISIChem) 2018*. 2019: Indonesian.
3. Jaiphuephae, T., K. Poochinda, and S. Poompradub, *Yield Optimization of Spray-Dried Natural Rubber and Properties of Its Silica-Filled Composite*. *Advances in Polymer Technology*, 2014. 33(4): p. n/a-n/a.
4. Paiva, L.B.d., A.M.d. Oliveira, and R.R. Gavioli, *Preparation and properties of rubber powder from modified-SBR latex by spray drying process*. *Powder Technology*, 2014. 264: p. 507-513.
5. Bitinis, N., et al., *Structure and properties of polylactide/natural rubber blends*. *Materials Chemistry and Physics*, 2011. 129(3): p. 823-831.
6. Li, D., et al., *Radiation preparation of nano-powdered styrene-butadiene rubber (SBR) and its toughening effect for polystyrene and high-impact polystyrene*. *Radiation Physics and Chemistry*, 2007. 76(11-12): p. 1732-1735.
7. Sae-Oui, P., et al., *Properties and recyclability of thermoplastic elastomer prepared from natural rubber powder (NRP) and high density polyethylene (HDPE)*. *Polymer Testing*, 2010. 29(3): p. 346-351.
8. Jaiphuephae, T., *Production of powder natural rubber by spray dryer*, in *Chemical Technology*. 2010, Chulalongkorn: Bangkok.
9. Sopanon, P., *PREPARATION OF NATURAL RUBBER/SILICA COMPOSITE POWDER BY SPRAY DRYING*, in *Chemical Engineering*. 2011, Chulalongkorn: Bangkok.
10. Sangthongyingdee, N., *Preparation of graft copolymer natural rubber/polymethyl methacrylate powder by spray drying*, in *chemical engineering*. 2015, Chulalongkorn: Bangkok.
11. Sae-Oui, P. *Types and usage of rubber*. 2020; Available from: <http://www.rubbercenter.org/files/technologys.pdf>

12. stocker, N. *Rubber Latex extracted from rubber tree*. 2010; Available from: <https://www.shutterstock.com/image-photo/rubber-latex-extracted-tree-hevea-brasiliensis-546240769>.
13. Atieh, M.A., et al., *Radiation Vulcanization of Natural Rubber Latex Loaded with Carbon Nanotubes*. Fullerenes, Nanotubes and Carbon Nanostructures, 2010. 18(1): p. 56-71.
14. Nawamawat, K., et al., *Surface nanostructure of Hevea brasiliensis natural rubber latex particles*. Colloids and Surfaces A: Physicochemical and Engineering Aspects, 2011. 390(1-3): p. 157-166.
15. Chemistry, S. *Natural rubber*. 2020; Available from: <http://spmchemistry.blog.onlinetuition.com.my/2019/08/natural-rubber.html>.
16. O Aguele, F. and C. I. Madufor, *Effects of Carbonised Coir on Physical Properties of Natural Rubber Composites*. American Journal of Polymer Science, 2012. 2(3): p. 28-34.
17. *Silicon Dioxide Properties*. 2020; Available from: <https://www.iue.tuwien.ac.at/phd/filipovic/node26.html>.
18. *Silane Coupling Agents*. 2020; Available from: https://www.shinetsusilicone-global.com/catalog/pdf/SilaneCouplingAgents_e.pdf.
19. Xiao, Y., et al., *Surface modification of silica nanoparticles by a polyoxyethylene sorbitan and silane coupling agent to prepare high-performance rubber composites*. Polymer Testing, 2020. 81.
20. Li, Y., et al., *Surface modification of silica by two-step method and properties of solution styrene butadiene rubber (SSBR) nanocomposites filled with modified silica*. Composites Science and Technology, 2013. 88: p. 69-75.
21. Sarkawi, S.S., W.K. Dierkes, and J.W.M. Noordermeer, *The influence of non-rubber constituents on performance of silica reinforced natural rubber compounds*. European Polymer Journal, 2013. 49(10): p. 3199-3209.
22. Zhang, C., et al., *Significantly improved rubber-silica interface via subtly controlling surface chemistry of silica*. Composites Science and Technology, 2018. 156: p. 70-77.
23. KUNA, A.P.a.A., *Microencapsulation technology: A review*. 2010: p. 86-102.

24. AG, B.L. *Microencapsulation: Generate added value*. 2020; Available from: <https://www.buchi.com/en/products-solutions/spray-drying-encapsulation/solutions/microencapsulation>.
25. Bakry, A.M., et al., *Microencapsulation of Oils: A Comprehensive Review of Benefits, Techniques, and Applications*. *Comprehensive Reviews in Food Science and Food Safety*, 2016. 15(1): p. 143-182.
26. Ozkan, G., et al., *A review of microencapsulation methods for food antioxidants: Principles, advantages, drawbacks and applications*. *Food Chem*, 2019. 272: p. 494-506.
27. Arpagaus, C., et al., *Nanocapsules formation by nano spray drying, in Nanoencapsulation Technologies for the Food and Nutraceutical Industries*. 2017. p. 346-401.
28. Arpagaus, C., et al., *Nano spray drying for encapsulation of pharmaceuticals*. *Int J Pharm*, 2018. 546(1-2): p. 194-214.
29. Li, Y., et al., *Effect of the temperature on surface modification of silica and properties of modified silica filled rubber composites*. *Composites Part A: Applied Science and Manufacturing*, 2014. 62: p. 52-59.
30. Sae-oui, P., et al., *Roles of silane coupling agents on properties of silica-filled polychloroprene*. *European Polymer Journal*, 2006. 42(3): p. 479-486.
31. Tian, Q., et al., *Effect of nano-silica surface-capped by bis[3-(triethoxysilyl)propyl] tetrasulfide on the mechanical properties of styrene-butadiene rubber/butadiene rubber nanocomposites*. *Composites Communications*, 2018. 10: p. 190-193.
32. Rezaei Abadchi, M. and A. Jalali-Arani, *The use of gamma irradiation in preparation of polybutadiene rubber nanopowder; Its effect on particle size, morphology and crosslink structure of the powder*. *Nuclear Instruments and Methods in Physics Research Section B: Beam Interactions with Materials and Atoms*, 2014. 320: p. 1-5.
33. Siriwong, C., P. Sae-Oui, and C. Sirisinha, *Comparison of coupling effectiveness among amino-, chloro-, and mercapto silanes in chloroprene rubber*. *Polymer Testing*, 2014. 38: p. 64-72.

34. Nandiyanto, A.B.D. and K. Okuyama, *Progress in developing spray-drying methods for the production of controlled morphology particles: From the nanometer to submicrometer size ranges*. *Advanced Powder Technology*, 2011. 22(1): p. 1-19.
35. Zheng, J., et al., *Chemical and physical interaction between silane coupling agent with long arms and silica and its effect on silica/natural rubber composites*. *Polymer*, 2018. 135: p. 200-210.
36. Jaslin Ikhsan, S.F., *An Isotherm Model of The Adsorption of Nitrate Ions on The Surface of Silica From Sugarcane Bagasse*. *Chemical technology and metallurgy*, 2019. 54: p. 702-708.
37. Vilmin, F., et al., *Reactivity of Bis[3-(triethoxysilyl)propyl] Tetrasulfide (TESPT) Silane Coupling Agent over Hydrated Silica: Operando IR Spectroscopy and Chemometrics Study*. *The Journal of Physical Chemistry C*, 2014. 118(8): p. 4056-4071.
38. Aiello, P.B., et al., *Evaluation of sodium diclofenac release using natural rubber latex as carrier*. *Materials Research*, 2014. 17(suppl 1): p. 146-152.
39. S. SALINA SARKAWI, W.K., K. SAHAKARO, W.K. DIERKES AND J.W.M. NOORDERMEER, *A Review on Reinforcement of Natural Rubber by Silica Fillers for Use in Low-Rolling Resistance Tyres*. *Journal of Rubber Research*, 2015. 18: p. 203-233.
40. Tang, S.Y., et al., *Preparation and Properties of Spherical Natural Rubber/Silica Composite Powders via Spray Drying*. *KONA Powder and Particle Journal*, 2020. 37(0): p. 214-223.
41. Lamond, A.K.S.a.T.G., *Identification of Elastomers by Thermal Analysis*. *Rubber Chemistry and Technology*, 1972. 45: p. 329-345.
42. Hassan, A.A., K. Formela, and S. Wang, *Enhanced interfacial and mechanical performance of styrene-butadiene rubber/silica composites compatibilized by soybean oil derived silanized plasticization*. *Composites Science and Technology*, 2020. 197.



จุฬาลงกรณ์มหาวิทยาลัย
CHULALONGKORN UNIVERSITY

VITA

NAME Intira Boonvisood

DATE OF BIRTH 29 January 1995

PLACE OF BIRTH Phatthalung, Thailand

INSTITUTIONS ATTENDED B.Eng Chemical Engineering Faculty of Engineering,
Thammasat Univerity

HOME ADDRESS 50/1 Moo.1, Nathom subdistrict, Mueng district,
Phatthalung province, 93000



จุฬาลงกรณ์มหาวิทยาลัย
CHULALONGKORN UNIVERSITY